TECHNISCHE UNIVERSITÄT MÜNCHEN

Lehrstuhl für Raumfahrttechnik

Synthetic Gear Wheels for Space Mechanisms

Dipl.-Ing. Univ. Ralf Purschke

Vollständiger Abdruck der von der Fakultät für Maschinenwesen der Technischen Universität München zur Erlangung des akademischen Grades eines

Doktor-Ingenieurs (Dr.-Ing.)

genehmigten Dissertation.

Vorsitzender:	Univ.-Prof. Dr.-Ing. Horst Baier
Prüfer der Dissertation:	1. Univ.-Prof. Dr. rer. nat., Dr. h.c. Ulrich Walter
	2. Univ.-Prof. Dr.-Ing. Enrico Stoll (Technische Universität Braunschweig)

Die Dissertation wurde am 20.04.2015 bei der Technischen Universität München eingereicht und durch die Fakultät für Maschinenwesen am 18.11.2015 angenommen.

Technische Universität München
Fakultät für Maschinenwesen

Synthetic Gear Wheels for Space Mechanisms

Dipl.-Ing. (univ.) Ralf Purschke
Lehrstuhl für Raumfahrttechnik

Abstract

Gear wheels are not only widely used in Earth applications but also in space mechanisms on board of spacecraft. There, the demands on the gear wheels change fundamentally. For the application in vacuum, at extreme temperatures, and the required maintenance-free operation over several years, gear wheels have to meet most demanding requirements. Since the beginning of spaceflight mainly gear wheels made out of metallic materials such as steel have been used. They have the advantage of high strength at good vacuum and temperature compatibility. Furthermore, with all the Earth applications, a lot of experience is already available. However, problems also occurred during the operation of established metallic gear wheels in the extreme environment of spaceflight, especially regarding the lubrication. For a reliable and maintenance-free operation over many years, metallic gear wheels have to be lubricated. And this is everything but easy in the reduced-gravity and vacuum environment of space. Often complex reservoirs have to be designed for the lubricant and also lubricating the wheels requires a lot of experience. Consequently it is definitely worthwhile also to consider alternatives to metallic gear wheels.

Synthetics might be one of the possible alternatives. With the development of new high performance polymers in recent decades, synthetic materials can be used nowadays also for highly demanding applications, such as, for example, as gear wheels. In Earth applications, synthetic gear wheels have already been commonly used. In particular in areas where mass savings or a corrosion free operation has to be realized (examples: automotive, life sciences or medicine). Synthetic material gear wheels might also be an option for space applications. Besides the obvious advantages such as potential mass savings or avoiding corrosion, the main benefit for space mechanisms would be the potential lubrication-free operation. Furthermore, due to the lower stiffness, polymers have vibration damping properties which is an important characteristic for high accuracy mechanisms. But gear wheels made of polymers also bring disadvantages. Particularly the larger coefficient of thermal expansion has to be addressed, since temperature difference in excess of ±100°C can easily occur during space missions. Also the suboptimal wear behavior and a possible outgassing in vacuum, as well as temperature extremes have to be considered. Generally, not much is known yet about the influence of vacuum and extreme temperatures on the behavior of synthetic gear wheels.

Consequently it is the goal of this work to evaluate different polymers regarding their applicability as gear wheel materials in space, to choose promising candidates, and to test the influence of space environment on the performance of the selected gear wheels. Many popular low cost polymers like Polyethylene (PE) or Polyvinylchloride (PVC) cannot be considered due to their poor mechanical properties. Others, do not fulfill the spaceflight-imposed outgassing or flammability requirements coming from the European Space Agency (ESA) or NASA. However, the high performance synthetics Polyetheretherketone (PEEK)

und Polyoxymethylene (POM) promise to satisfy spaceflight constraints and were chosen as possible materials for space gear wheels. Both polymers exhibit excellent mechanical properties, show good behavior in a wide temperature range and under vacuum, and have already been utilized in spacecraft. PEEK even exceeds the mechanical properties of POM, but is also more expensive. Both materials fulfil the critical offgas requirement for the application in spaceflight and meet the ESA standard for vacuum behavior of materials.

In order to evaluate the actual behavior of the PEEK and POM gear wheels in space, different tests have to be conducted under relevant simulated spaceflight conditions. The required tests are specified by VDI standards. Since these standards consider the evaluation of synthetic gear wheels in Earth applications, not all recommended tests are relevant for spaceflight applications. The required tests have to be conducted as close as possible to real spaceflight conditions in order to evaluate the influence of vacuum and temperature exposure on the behavior of the polymers for the gear application. In the context of this work, the characteristics of wear, tooth root carrying capacity, environmental influence on geometry, and tooth temperature were to be tested. Methods and test rigs were developed to adapt these tests and to conduct experimental characterization of candidate materials under spaceflight-similar conditions.

The results show in particular for wear and load carrying capacity a significant influence of the test condition on the behavior of the gear wheels. The wear results indicate the mechanical advantage of PEEK compared to POM through a lower wear coefficient at all tested environments. PEEK performs in vacuum even better than in air. For POM, especially at higher temperatures, a significant increase in wear is observed. The tooth temperature is rather unaffected by the test environment, and the geometry of the gear wheels changes corresponding to the coefficient of thermal expansion.

From the obtained results one can draw conclusions on the suitability of the materials for space gear wheel applications. However it is not possible to make an absolute statement because depending on requirements and environment the application potentials of synthetic gear wheels change. Results for POM show that it is only suitable in high temperature differences as long as accuracy requirements do not have to be better than 1°. POM also has disadvantages when large cycle numbers of more than 1 000 000 cycles are required or large applied torques of more than 1 N·m are required. Consequently, POM gear wheels would mainly be suitable for deployment mechanisms with typically very low revolutions and rather low accuracy requirements.

For PEEK, however, the field of possible applications is much larger. PEEK gear wheels can also be used for high accuracy applications up to around 0.01° accuracy as long as temperature differences are in the range of ±30°C. In that case, cycle life of 200000 cycles and a load torque of 0.3 N·m are definitely possible. These obtainable performance

characteristics are quite realistic numbers for pointing mechanism requirements. Because of their higher coefficient of thermal expansion, synthetic gear wheels generally have problems to meet high accuracy requirements.

In contrast to wear, strength of synthetic gear wheels does not cause any problems during the application in space mechanisms. For loads of 0.3 N·m, PEEK as well as POM gear wheels are appropriate. Despite their dependence on the thermal-vacuum environment, they provide enough margin for a safe application in space mechanisms.

Zusammenfassung

Zahnräder sind nicht nur in Erdanwendungen weit verbreitet, sondern werden auch in Weltraummechanismen in nahezu allen Raumfahrtzeugen eingesetzt. Die Anforderungen an die Zahnräder beim Einsatz im Weltall ändern sich dabei jedoch grundlegend. Die Verwendung im Vakuum, bei extremen Temperaturen und der wartungsfreie Betrieb über mehrere Jahre stellen höchste Ansprüche an die Zahnräder. Seit Beginn der Raumfahrt werden hauptsächlich Zahnräder aus metallischen Materialien wie Stahl verwendet. Metallische Materialien haben den Vorteil einer hohen Festigkeit und guter Vakuum- sowie Temperaturbeständigkeit. Außerdem hat man durch Erdanwendungen bereits sehr viel Erfahrung über deren Verhalten gesammelt. Jedoch ist auch der Einsatz von Metallzahnrädern im Weltall problematisch. Die größte Schwierigkeit stellt die Schmierung metallischer Zahnräder dar, die in der schwerelosen Umgebung über mehrere Jahre hinweg zuverlässig und wartungsfrei sein soll. Dafür müssen oft aufwendige Reservoirs für den Schmierstoff konstruiert werden und auch das Aufbringen der Schmierung selbst erfordert viel Erfahrung. Folglich lohnt es sich durchaus, Alternativen zu metallischen Zahnrädern zu erforschen.

Kunststoffe könnten dabei eine entscheidende Rolle spielen. In den letzten Jahrzehnten wurden neuartige Hochleistungskunststoffe entwickelt, die in mechanisch anspruchsvollen Anwendungen eingesetzt werden können, wie zum Beispiel als Werkstoff für Zahnräder. In Erdanwendungen ist der Einsatz von Kunststoffzahnrädern bereits weit verbreitet, vor allem in Bereichen, in denen Gewicht gespart werden soll oder wo ein korrosionsfreier Betrieb gewährleistet sein muss. Dies sind zum Beispiel Anwendungen im Automobilbau oder in der Medizin. Aber auch für die Anwendung im Weltall könnten Kunststoffzahnräder in Frage kommen. Neben den Vorteilen der Gewichtsersparnis und der Vermeidung von Korrosion ist es vor allem der schmierungsfreie Betrieb von Kunststoffzahnrädern, der in der Raumfahrt von großem Nutzen wäre. Des Weiteren haben Kunststoffe, durch ihre geringere Steifigkeit, dämpfende Eigenschaften, die vor allem beim Einsatz in präzisen Mechanismen zum Tragen kommen würden. Jedoch bringen Zahnräder aus Kunststoffen auch Nachteile mit sich. Problematisch ist vor allem deren höherer Wärmeausdehnungskoeffizient, da im Weltall durchaus Temperaturunterschiede von ±100°C auftreten können. Auch das schlechtere Verschleißverhalten und ein mögliches Ausgasen im Vakuum müssen berücksichtigt werden. Grundsätzlich ist noch wenig über den Einfluss von Vakuum und extremen Temperaturen auf das Verhalten von Kunststoffzahnrädern bekannt.

Es ist das Ziel dieser Arbeit, verschiedene Kunststoffe als Material für Zahnräder im Weltraumeinsatz zu erproben, geeignete Polymere auszuwählen und den Einfluss der Weltraumumgebung auf verschiedene Parameter wie Verschleiß und Festigkeit zu untersuchen. Viele gängige Kunststoffe wie Polyethylen (PE) oder Polyvinylchlorid (PVC) kommen auf Grund ihrer schlechten mechanischen Eigenschaften nicht in Frage. Andere

wiederum überschreiten die von der Europäischen Raumfahrtagentur (ESA) gestellten Anforderungen bezüglich Ausgasraten im Vakuum. Somit wurden letztendlich die Kunststoffe Polyetheretherketon (PEEK) und Polyoxymethylen (POM) als mögliche Zahnradmaterialien ausgewählt. Beide Polymere bieten hervorragende mechanische Eigenschaften, sind temperatur- und vakuumbeständig und wurden auch schon in Raumfahrtanwendungen eingesetzt. Dabei ist PEEK vor allem in den mechanischen Eigenschaften POM noch überlegen, allerdings ist PEEK dadurch auch deutlich teurer. Beide Materialien sind vakuum-kompatibel und erfüllen damit eine Grundvoraussetzung für den Einsatz im Weltall und entsprechen den ESA Richtlinien zum Verhalten von Materialien im Vakuum.

Um das tatsächliche Verhalten der Zahnräder aus PEEK und POM im Weltall beurteilen zu können müssen verschiedene Tests unter simulierten Raumfahrtbedingungen entwickelt und durchgeführt werden. Die notwenigen Untersuchungen sind unter anderem durch VDI Richtlinien vorgegeben. Da sich diese Richtlinien auf die Untersuchung von Kunststoffzahnrädern in Erdanwendungen beziehen, sind nicht alle empfohlenen Tests auch für Raumfahrtanwendungen relevant. Die zur Weltraumqualifizierung benötigten Tests unter simulierten Weltraumbedingungen müssen jedoch so realistisch wie möglich durchgeführt werden um den Einfluss von Vakuum und Temperatur auf das Verhalten der Kunststoffe evaluieren zu können.

Im Rahmen dieser Arbeit wurden Tests und Testprozeduren bezüglich Verschleiß, Zahnfußtragfähigkeit, Umwelteinfluss auf die Zahnradgeometrie sowie Zahntemperatur entwickelt und durchgeführt. Dafür wurden Testmethoden und Teststände entwickelt, die den Ablauf der Experimente unter Raumfahrtbedingungen erlauben. Die Testergebnisse zeigen vor allem bei Verschleiß und Zahnfußtragfähigkeit einen deutlichen Einfluss der Testumgebung auf das Verhalten der Kunststoffzahnräder. Beim Verschleiß offenbart sich die mechanische Überlegenheit von PEEK gegenüber POM durch einen niedrigeren Verschleißkoeffizienten bei allen getesteten Umweltbedingungen. Das Verschleißverhalten von PEEK im Vakuum ist jenem in Luft sogar überlegen. Bei POM ist vor allem bei hohen Temperaturen ein deutlich erhöhter Verschleißkoeffizient zu erkennen. Die Zahntemperatur bleibt relativ unbeeinflusst von der Testumgebung und die Geometrie ändert sich gemäß den Wärmeausdehnungskoeffizienten.

Aus den Ergebnissen lassen sich nun Rückschlüsse auf die Anwendbarkeit der Materialien für Weltraumzahnräder ziehen. Dabei lässt sich jedoch keine absolute Aussage treffen, denn je nach Anforderungen und Umweltbedingungen ändern sich das Einsatzpotential der Kunststoffzahnräder. Es zeigt sich, dass POM bei hohen Temperatur Unterschieden nur einsetzbar ist, wenn die Anforderung an die Genauigkeit nicht besser als 1° sein soll. POM zeigt auch Schwächen bei hohen Umlaufwiederholungen (>1 000 000) und hohen Drehmomenten (>1 N·m). Damit kommen POM Zahnräder hauptsächlich in Anwendungen

für Deployment Mechanismen in Frage, wo sehr geringe Umdrehungszahlen benötigt werden, und auch die Anforderung an die Genauigkeit eher gering ist. Für PEEK dagegen bietet sich schon ein größeres Anwendungsgebiet. Auch für hochgenaue Anforderungen um 0.01° Genauigkeit können PEEK Zahnräder verwendet werden, solange Temperaturänderungen im Bereich von ±30°C bleiben. Dann sind auch 200 000 Umdrehungen bei 0.3 N·m möglich, was durchaus realistische Werte für die Anforderungen eines Pointing Mechanismus wären. Auf Grund ihres hohen Wärmeausdehnungskoeffizienten haben Kunststoffzahnräder grundsätzlich bei hohen Temperaturunterschiede Probleme, die geforderte Genauigkeit einzuhalten.

Im Gegensatz zum Verschleiß stellt die Festigkeit der Kunststoffzahnräder keine Probleme beim Einsatz in Weltraummechanismen dar. Bei Lasten von 0.3 N·m sind sowohl PEEK als auch POM Zahnräder geeignet. Sie verfügen trotz einer Abhängigkeit von der thermal-vakuum Umgebung über genügend Reserven für einen sicheren Einsatz in Raumfahrtmechanismen.

Acknowledgements

During my time at the Institute of Astronautics (LRT) I got to know many different people. With some I spent only a couple of months, others became friends over the years. Because of all these people I (almost) always was happy to go to work in the morning. And that is why I want to thank at first all the students, colleagues, and staff at the LRT for the great time I had in the last years. When considering the first Semesterarbeit I wrote at the LRT in 2006, I spent almost nine years at the Institute. During these nine years Jan Harder and Claas Olthoff have been constant companions, partners for discussions, and friends. I hope we will stay in touch! With Markus Pietras I found someone at the LRT who shared my enthusiasm for the mountains and it was always fun to discuss previous and plan new tours with him. I hope many more will follow in the future.

I want to thank Dr. Martin Rott for all the support in the different organization and financial issues. It was good to know during all the years to be sure that he would always find a solution for any possible problem. Dr. Alex Hoehn made a big contribution to this work. He always asked annoying questions at the wrong time. But these questions are so important for the progress of a work. They make you think outside the box and make sure you are not getting lost in details. Thank you! I am also grateful to our secretary Petra Lochner. She handled all the little things which made life at the Institute easier.

I am very thankful to all of the students who supported this work in different ways. Sebastian Rieger, Alexander Schmidt, and Jonis Kiesby did a great work in programming control software for the test setups and the vacuum chamber as well as the evaluation software. The manufacturing and implementation of the test setups was supported by our machine shop and electronic laboratory. Tobias Abstreiter manufactured many critical components of the test setup and he was always an important partner for discussing the experiments. Leonhard Röpfl contributed to the electronic design of the experiments. Often with short notice, he always found an easy way to make the electric of the test setup work. I also want to thank Matthias Tebbe and Philipp Reiß who built up the thermal-vacuum chamber and often rescheduled their own tests in order to provide testing time for my experiments.

Prof. Walter, thank you for the opportunity to do my PhD work at your Institute. For giving me the freedom to find a topic of my interest and skills and to pursuit the goals which were important to me. This allowed me to find my individual way which will be very helpful in my professional future.

A special thank goes to the Institute of Machine Elements (FZG) at the Technische Universität München (TUM) where some of my experiments were conducted. Marco

Breidinger did all of the gear wheel contour scans which were essential for the wear calculation. Florian Dobler did not only run the Pulsator tests, he also discussed the results with me and supported me with his knowledge about gear wheels in general. The cooperation with the FZG was exemplary and showed how productive people from different institutes at the TUM can work together.

But above all I am grateful to my family and friends. During all the years at the University I knew that my parents would support me in all I was doing. And that was not only the fundament for my PhD work but also for my time in school and my studies. Also my old friends from school contributed in an own way to this thesis. When I spent time with them, I did not think about all the problems of my work anymore, which is extremely important from time to time. Especially I want to thank my wife Hannah. She had to live with all my doubts about the work, and she agreed to a weekend-relationship during the last one and half years of my work.

Table of Contents

Nomenclature

Symbol	Unit	Description
$A_{tooth,new}$	mm^2	Tooth area before operation
$A_{tooth,op}$	mm^2	Tooth area after operation
a	mm	Axis distance
a_d	mm	Reference center distance
b	mm	Tooth thickness
c	mm	Bottom clearance
d	mm	Reference diamete
d_a	mm	Tip circle diameter
d_b	mm	Base circle diameter
d_f	mm	Root diameter
d_w	mm	Pitch diameter
E	N/mm^2	Young's modulus
F_0	N	Pulsator preload
F_a	N	Axial force
F_r	N	Radial force
F_t	N	Tangential force
F_P	µm	Total pitch variation
F_{rl}	µm	Concentricity variation
ΔF_1	N	Pulsator load level 1
ΔF_2	N	Pulsator load level 2
f	Hz	Frequency
f_P	µm	Individual pitch variation
f_u	µm	Pitch error
g_α	mm	Length of path of contact
H_V	-	Tooth loss factor
h	mm	Tooth depth
i	-	Gear ratio
j_n	mm	Normal backlash
j_t	mm	Circumferential backlash
K_A	-	Application factor
$K_{F\alpha}$	-	Transverse factor
$K_{F\beta}$	-	Face load coefficient
K_V	-	Dynamic factor
l	mm	Distance between two axis

l_{Fl}	mm	Profile length
M_T	N·m	Torque
M_W	g	Mass wear
M_{WN}	10^{-6}·g	Mass wear rate
m_n	mm	Module
N	-	Cycle number
n	1/min	Revolutions per minute
P	W	Power
P_d	mm	Diametral pitch
p_b	mm	Base circle pitch
p_e	mm	Normal base pitch
p_t	mm	Circular pitch
R_p	µm	Pitch fluctuation
S_E	mm	Required backlash
S_{Fmin}	-	Safety factor
s	-	Standard deviation
v_g	m/s	Sliding speed
x	-	Addendum modification coefficient
Y_ε	-	Coverage factor
Y_{Fa}	-	Form factor
Y_{Sa}	-	Stress correction factor
z	-	Number of teeth
α	°	Normal pressure angle
α_t	°	Transverse normal base angle
α_w	°	Operating pressure angle
α_{th}	1/K	Thermal expansion coefficient
β	°	Helix angle
$\Delta\vartheta$	°	Temperature difference
ε_α	-	Trans-verse contact ratio
ε_f	-	Humidity factor
λ	mm	Deformation of tooth
λ_{max}	mm	Acceptable maximum deformation
ρ	g/cm³	Material density
σ_F	N/mm²	Tooth root stress
σ_{FG}	N/mm²	Load capacity
σ_{FlimN}	N/mm²	Fatigue stress under fluctuating stress

ω	°/s	Angular velocity

Abbreviations

AC	Alternating current
APM	Antenna pointing mechanism
BAPS	Bearing Active Preload System
CNC	Computer numerical control
CTE	Coefficient of thermal expansion
CVCM	Collected volatile condensed material
DC	Direct current
DIN	Deutsches Institut für Normung
ESA	European Space Agency
GEO	Geostationary
HD	Harmonic Drive
LEO	Low Earth orbit
MLI	Multi-layer-insulation
MoS_s	Molybdenum disulfide
NASA	National Aeronautic and Space Administration
NI	National Instruments
PA	Polyamide
PCB	Polychlorierte Biphenyle
PEEK	Polyetheretherketone
PI	Polyimide
POM	Polyoxymethylene
PTFE	Polytetrafluoroethylene
PUT	Pinion under test
PVC	Polyvinylchloride
RF	Radio frequency
RJ	Rotary joint
rpm	Rounds per minute
RTG	Radioisotope thermoelectric generator
SLS	Selective laser sintering
TML	Total mass loss
TV	Thermal-vacuum
UHMWPE	Ultra-high molecular weight polyethylenes
VDI	Verein Deutscher Ingenieure

Tables

Figures

1 Introduction

1.1 Overview

Spaceflight mechanisms are mechanically moving components built for applications under the harsh conditions of spaceflight, such as vacuum and temperature extremes. In recent years the accuracy requirements on spaceflight mechanisms, and thus on its components, have been rising continuously. For example with the desire for high data rate downlink, high frequency communication bands are becoming state of the art [1]. This results in more challenging requirements in pointing accuracy. A 40 cm Ka-band antenna, for example, requires a pointing accuracy of typically better than 0.16° [2]. These required pointing accuracies and the requirement for faster and backlash-free mechanisms are becoming even more demanding with increasingly higher communication frequencies up to laser light frequencies in optical instruments.

Consequently new ideas, concepts or materials should be considered for the design of future space components. Using synthetics could be a possible choice. Synthetics have not been very popular in spaceflight to date, mainly because of originally low strength, undesired behavior at extreme temperatures, and outgassing in vacuum. However, novel high-performance polymers have been developed in recent years and are already successfully applied in many Earth applications, such as gear wheels. For example in the field of medical equipment, synthetic gear wheels score with their low mass and the ability of dry-running.

Metallic gear wheels have been used and optimized for space applications for many years and can be considered state of the art, but they also have disadvantages. Metal gear wheels transmit micro vibration, suffer from corrosion, and need lubrication. Especially lubricating the gear wheels for unserviced operating times of up to 15 years in space pose challenges in today's space mechanism design, and the exact performance in microgravity often cannot be tested on ground. For example, during the design of the Beagle2 Mars lander mechanisms, the wet lubrication of the planetary gearbox and the spur gear was seen to be a critical part of the mechanism design. Therefore, a dedicated research program with a series of specialized tests was carried out to find the proper lubrication [3]. Also, the antenna pointing mechanism of the BepiColombo mission to planet Mercury showed problems with lubrication above 200°C [4]. Dry lubrication, designed to avoid the issues of wet lubrication in microgravity and vacuum environments, has its own challenges. MoS_s particles, the standard dry lubricant employed in space mechanisms, can peel off from the gear and contaminate slip rings or other electronic devices [5] in the vicinity.

The dry-running ability of synthetic gear wheels, meaning the absence of lubrication, is an advantage compared to metallic wheels and makes gear wheels made out of polymer

material very interesting for spaceflight. In addition to their dry-running ability, synthetic gear wheels have additional beneficial properties such as: damping of micro-vibration, no risk of corrosion, and low mass.

The motivation of this work is to find alternative gear wheel materials for space mechanisms and to characterize their performance in simulated spaceflight environments. Specifically, this work tests if polymer gear wheels are a suitable choice for applications in space. The relevance of this work is supported by statements in different industry standard books on space mechanisms. For example, the Handbook for Spacecraft Structures and Mechanisms [6] points out that in particular corrosion and lubrication have to be considered during bearing and gear wheel design and that lubrication is a design driver for many space mechanisms. Especially corrosion and lubrication are two factors which can be avoided with the choice of polymer materials. The design of Surrey Satellite Technology Ltd's antenna pointing mechanism [7] uses a Delrin spur gear in combination with a stainless-steel worm gear, where the Delrin gear was chosen to operate the system without lubrication. Handling of the manufactured component is becoming easier and less expensive in some ways with synthetics since the effect of corrosion does not have to be considered for polymers. The Space Tribology Handbook [8] indicates that polymer gears often would be the better solution. For example steel gears have to be hardened to meet wear and efficiency requirements. When hardening is not possible (for example for high precision low module gears) the load on the gear has to be reduced. And in reduced load applications, where the strength of the gear wheel is secondary, it is preferable to use polymer gears because of their lighter mass. In [9], the author reports that published literature about synthetic gear wheels only exists for air environment, and points out that more work needs to be done to evaluate polymer materials in vacuum environments.

The use of polymers for gear applications imposes challenges for their successful use in spaceflight. Potential issues to be addressed include excessive wear, lower strength, or larger coefficient of thermal expansion when compared to metal gears. Furthermore, the behavior of polymers in space environments has not been tested extensively. In one study [10], friction and wear performed unexpected in vacuum conditions. An unexplainable fall-off in performance was observed. A change in friction between a Polyetheretherketone (PEEK) guiding element and the shaft, was assumed to be responsible for the changes between tests conducted under vacuum and air. In another study friction and wear behavior of PEEK filled with graphite or MoS_2 was investigated in vacuum at temperatures from -80°C to +20°C. A change in performance was observed as a function of temperature [10].

The opinions about the potential use of synthetic gear wheels for space mechanism applications varies widely with many pro and cons, advantages and disadvantages, prejudgments and opinions, experiences and know-how. This work aims at providing further data on the suitability of state-of-the art polymers in spaceflight gear mechanisms.

Therefore extensive testing of synthetic gear wheels in simulated spaceflight environments is the main focus of this thesis.

This experimental thesis is divided into three sections. First the theoretical and analytical background of the work, next the description of the conducted experiments, and finally the concluding discussion and summary. The first section (chapter 1) starts with the motivation of the work and leads to the research hypothesis, followed by a review of the state of the art for the main elements of the thesis. This includes space mechanisms, gear wheels in space application, synthetic gear wheels with an overview of current polymers, and synthetic gear wheels in space or vacuum application. On the basis of this literature review, a knowledge gap analysis is conducted and finally the objectives of the thesis are derived.

The second section (chapters 2 to 7) describes the various characterization tests. It starts in chapter 2 with the test preparation where the background and rationale for each test is given. Furthermore a detailed description of the test devices and reasons for the material selection are presented. All the test setups and equipment are explained as well as the test environment. Finally the functional verification tests are described which were conducted in advance of the actual tests in order to verify the test setup. Chapters 3 to 6 describe the four main tests of the thesis: 1) wear, 2) carrying capacity, 3) environmental impact on geometry, and 4) tooth temperature. Each chapter shows the test objective of the particular test, the test method, the operation of the tests, the results, and a short discussion. In chapters 7 the gear wheel quality is described. Chapter 8 presents the result discussion and conclusion, summarizes the tests, and gives an outlook to future work. An overview of the structure of this thesis is given on the next two pages.

Introduction

Research Hypothesis

Gear wheels made out of the polymers PEEK and POM are appropriate for the application in space mechanisms

State of the Art

Space mechanisms | **Gear wheel basics** | **Gear wheels in space** | **Synthetic gear wheel** | **Synthetic gear wheels in space**

Gap Analysis

No experimental data is available about the behavior of synthetic gear wheels in space environment

Research Question

How does the spaceflight environment influence the performance of PEEK and POM gear wheels as selected representatives of high performance synthetic materials, and do the wheels made of PEEK and POM fulfill the requirements for space mechanisms?

Thesis Objective

Evaluation of the behavior of PEEK and POM gear wheels in a siulated space environment and their applicability in space mechanisms

1. Study of space mechanism requirements as applicable for gear wheels

2. Preselecting promising polymers for space and gear wheel application

3. Wear characterization of PEEK and POM gear wheels in a simulated space environment

Development of a test method to study the wear of the gear wheels under space environment.

Determine the wear of the gear wheels in space environment.

4. Strength characterization of PEEK and POM gear wheels in a simulated space environment

Development of a test method to study the influence of the space environments on the strength of the gear wheels.

Determine the strength of the gear wheels depending on space environment.

5. Characterization of the environmental impact on the geometry of PEEK and POM gear wheels

Development of a test method to study the influence of the space environments on the geometry of the gear wheels.

Determine the geometry change of the gear wheels depending on space environment.

6. Temperature characterization of PEEK and POM gear wheels in a simulated space environment

Development of a test method to study the influence of the space environments on the temperature of the gear wheels during operation.

Determine the temperature of the gear wheels during operation depending on space environment.

7. Evaluation of the applicability of PEEK and POM gear wheels in space mechanisms

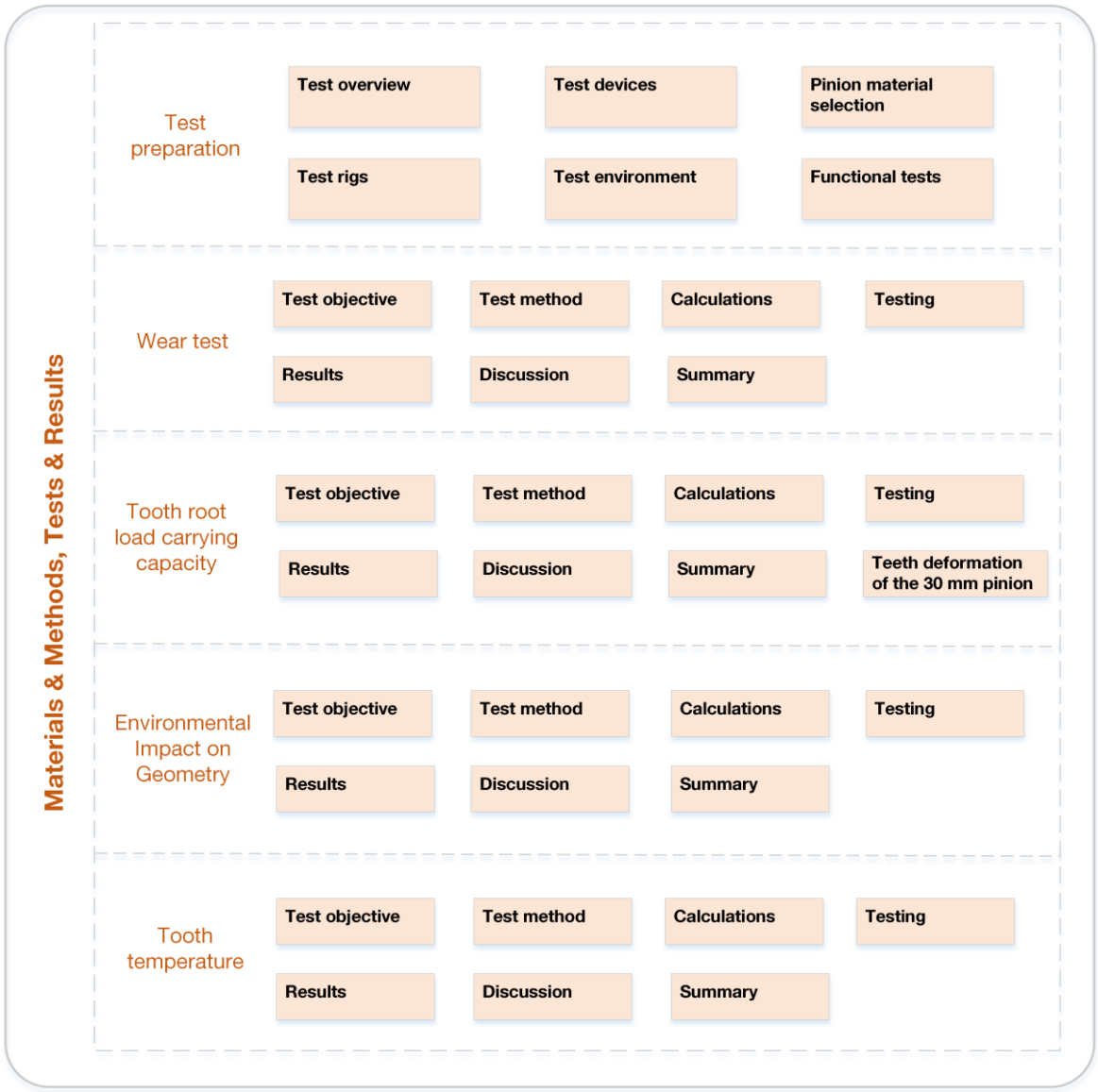
Materials & Methods, Tests & Results
Test preparation
Test overview
Test devices
Pinion material selection
Test rigs
Test environment
Functional tests
Wear test
Test objective
Test method
Calculations
Testing
Results
Discussion
Summary
Tooth root load carrying capacity
Test objective
Test method
Calculations
Testing
Results
Discussion
Summary
Teeth deformation of the 30 mm pinion
Environmental Impact on Geometry
Test objective
Test method
Calculations
Testing
Results
Discussion
Summary
Tooth temperature
Test objective
Test method
Calculations
Testing
Results
Discussion
Summary

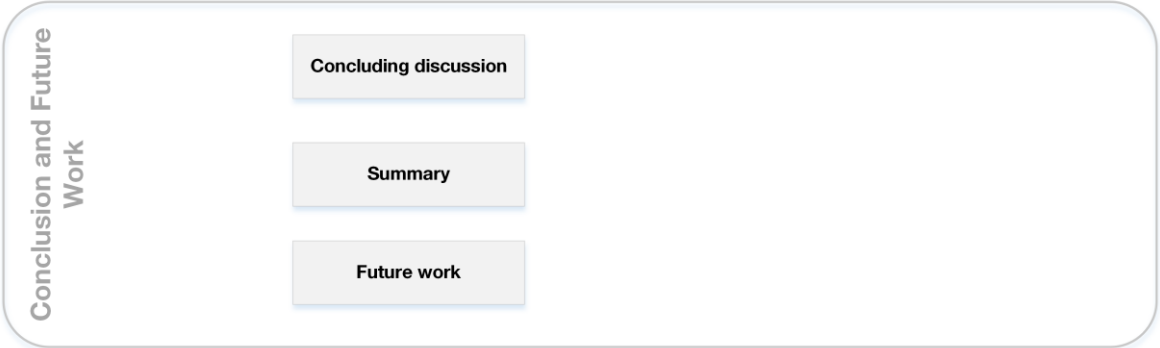
Conclusion and Future Work
Concluding discussion
Summary
Future work

1.2 Research Hypothesis

Metallic gear wheels have been used in space mechanisms since the 1960s. But with rising demands on mechanisms and with the development of high performance polymers in the last decades, synthetic gear wheels are becoming an interesting alternative. Especially because they are already used in many different ambitious applications on Earth. Thus, the hypothesis of this work is:

Gear wheels made out of the polymers PEEK and POM are appropriate for the application in space mechanisms.

The constraints of the thesis are as follows:

(1) The polymers shall be available off-the-shelf without any expensive and complex modifications.

(2) As far as possible, the design, size, and geometry of the gear wheels shall be comparable to real applications.

(3) The operational parameters like velocities, cycles, and loads shall be comparable to current pointing mechanisms.

(4) The test environment shall simulate relevant aspects of the typical spaceflight environment in Low-Earth orbit.

1.3 State of the Art

1.3.1 Space Mechanisms

Mechanisms can be found in almost all spacecraft. They point, rotate, or deploy components or instruments. Over many decades industry has already the ability to design moving machinery that can operate in Earth orbit, planetary orbit, or on extraterrestrial surfaces. They always aim for better design which means more reliable, lighter, and less costly mechanisms [11]. Spaceflight mechanisms consist of motors, bearings, gears, springs, dampers, and other moving subcomponents. Compared to mechanisms used on land-based applications, space mechanisms must have high reliability and be very light. High reliability is required, because once they are launched, the mechanism can usually not be repaired or serviced anymore [6]. Thus, mechanism failure usually means mission failure [12]. Mechanisms have to operate reliably in space environment, which means wide temperature ranges, thermal gradients, and rapid changes in temperature. Furthermore, ultraviolet radiation and vacuum can cause the properties of some materials to degrade. Also the lack of gravity in space has to be considered during mechanism design since mechanisms may show different behavior in the weightlessness of space than on ground. Although this can be simulated in some degree other effects like the mitigation of lubricant cannot be tested but is critical for the mechanism [12].

Beside the environment, space mechanisms also have to fulfill many performance requirements. These are for example applied torque, operating speed, accuracy, operating cycles, or structural demands like strength and stiffness. The most challenging requirements are precision and a long operating life [13]. Depending on the number of operating cycles, space mechanisms can be divided into high-cycle and low-cycle mechanisms. High-cycle applications are antenna gimbals or solar array drives. They are frequently or constantly in motion. Low-cycle applications are mechanisms to restrain or retrieve payloads at launch or to deploy or store instruments [13].

High cycle mechanisms:

- Antenna pointing and tracking
- Solar array tracking and pointing
- Attitude control reaction wheels

Low-cycle mechanisms:

- Antenna launch retention
- Antenna deployment
- Solar array retention
- Solar array deployment
- Contamination cover removal
- Spacecraft/launch vehicle separation

1.3.1.1 Different types of Space Mechanisms

Deployment Mechanisms (single shot)

Often spacecraft components are too large to fit within the payload fairing of the launch vehicle or are too fragile to withstand the loads during launch. These components are folded and stowed compactly during launch and are deployed after reaching orbit. Therefore deployment mechanisms are required to move these stowed components from launch to in-orbit configuration. Solar arrays and antennas are the most common deployables because these structures are large and are required for basically all spacecraft. But also booms or covers often have to be deployed. Deployment mechanisms normally operate only once as soon as they are in orbit [12].

Solar array panels often are stacked during launch and are opened once in orbit. To deploy them one or more rotations are required to move them away from the spacecraft. Sometimes a boom is used to increase the distance between spacecraft and panel. Also antennas often are stowed during launch because they are too large to fit within the fairing. Once in orbit, some antennas are unfurled in an umbrella-like fashion others have a rigid structure and are just moved away from the spacecraft. Covers and lids can have many different purposes: to protect sensitive devices, to keep out contamination, or to maintain vacuum within a canister. But they have in common to be opened as soon as the spacecraft is in orbit. The designated mechanism usually has to operate one-time although there are applications where a repetitive operation is required. For example when a star tracker is protected from directly viewing the Sun. Deployable booms consist of a hinge and a drive mechanism. Their purpose often is to place a component away from the spacecraft in order to reduce interferences.

A deployment mechanism system usually is built up of three sub-mechanisms: a restraint and release mechanism, a drive mechanism, and a latch mechanism. The restraint and release mechanism holds the deployable in the stowed configuration during launch. They are activated in orbit to initiate release. Often this mechanisms consist of two elements. One to hold the deployable and another one to release the holding. Therefore most commonly,

pin pullers, separation nuts, and explosive bolts are used. The activation usually is done by pyrotechnic devices. Drive mechanisms provide the motion of the deployable. Either rotational or axial. Typically electric motors are used to move the component or instrument to the desired position. Then a latch mechanism locks the deployed element. Therefore the simplest solution is a spring-loaded pin that drops into a hole to fix the component. Usually the latch mechanism only has to work once.
Deployment mechanisms are for example required for the two deployable booms of the ROSETTA spacecraft. The function of the boom is to place sensors far from the spacecraft to minimize the disturbance created by the spacecraft electromagnetic field. During launch phase the booms are stowed and hold with a hold down and release mechanism. As soon as the spacecraft is in orbit the booms are released and deployed in an early stage of the mission. Each deployable boom is composed by the boom structure, the deployment mechanism, the hold down and release mechanism, the harness and accessories, and the thermal hardware. The booms have a length of 1345 mm and 2295 mm. The deployment mechanism is integrated by an actuator, a hinge, a flexible coupling, a latching system, and position switches. The actuator consists of a brush motor, planetary gears, and a worm reduction gear [14].

For the Total and Spectral Solar Irradiance Sensor which has the goal to measure total solar irradiance, a deployment mechanism is integrated in the thermal pointing system [15]. The deployment mechanism has to bring the thermal pointing system from the launch locked position to the on-orbit operational position. The mechanism comprises many different mechanical components. A stepper motor drives the mechanism which includes a ball screw, gears, bearings, flexures, and position sensors. The mechanism has a 75° range of motion between the stowed and deployed position. The maximum backlash was measured as <0.2°. But backlash is not an issue because in the deployed state, the preload from the compression spring removes all the play in the system.

For the Solar Dynamics Observatory [16] a cover mechanism is required to protect the extremely sensitive optics from contamination during ground assembly, launch, and initial spacecraft outgassing. The mechanism consists of an actuator and a latch and is operated in space to remove the cover.

Although this work focus of applications in zero-gravity applications, it is also worth to have a look at planetary missions. Different deployment mechanisms were for example integrated in the Beagle2 Mars lander. The main hinge has to open the lander once it landed on the surface of Mars. It has an essential role because the solar arrays cannot be deployed until the lid has been opened. And without deployed solar arrays no power can be generated which would result in freeze of Beagle2 in the first night. The hinge mechanism is equipped with a Maxon motor, a planetary gearbox, a spur gear, as well as a Harmonic Drive gearbox. This gives a total gear ratio of 201420:1 and a deployment time of about 10 minutes for

180° rotation. Another spur gear is used to drive a potentiometer which gives information about the position of the lid during opening [3]. To deploy the mentioned four solar arrays, they are equipped with four essentially equal mechanisms. They deploy the solar arrays as soon as the lid of the lander is opened. The mechanisms are driven by a Maxon motor which drives a planetary gearbox and a spur gear. The total gear ration is 3729:1 which results in a deployment time of 12 seconds for 180° rotation [3].

Rotating Mechanisms

Rotating mechanisms are used where a continuously rotation is required. For example in attitude control systems like gyroscopes, momentum wheels, or reaction wheels. The wheels of these components are turning with up to 8000 rounds per minute (rpm) to generate a large angular momentum in order to provide spacecraft stability. Also solar array drives require rotating mechanisms to provide a constant orientation of the arrays to the sun. For a continuously scanning also sensors often are equipped with a rotating mechanism.

An example for rotating mechanisms is the Spin Mechanism Assembly for the Global Microwave Imager (GMI). The GMI is part of the Global Precipitation Measurement (GPM) spacecraft and will be used to make calibrated radiometric measurements at multiple microwave frequencies and polarizations. The GMP mission is managed by NASA and has the goal to improve climate and weather prediction through more accurate and frequent precipitation measurements [17]. The GMI Spin Mechanism Assembly supports and spins the GMI at a constant rate of 32 rpm for a duration of three years. The PACS instrument designed for the Herschel mission requires a rotating mechanism to switch between filters in order to select spectral bands [18]. PACS is a Photodetector Array Camera & Spectrometer which operates over a spectral band from 57 to 210 µm. The rotating system was chosen in order to reduce the amount of sliding and rolling of flexible parts and due to envelope reasons. Also scanning mechanisms are part of the rotating mechanism category. For the Millimeter Wave Radiometer Instrument (MWRI) a scanning mechanism is required for a continuously operation of the instrument [19]. It has to operate for 5 years which corresponds to 90 million revolutions of the mechanism. It is equipped with two pairs of ball bearings, a redundant brushless DC motor, a redundant optical encoder for velocity control, and a slip ring for power and signal transfer. Drive mechanisms are another type of rotating mechanisms. Surrey Satellite Technology Ltd (SSTL) built the Bi-Axial Solar Array Drive Mechanism [20]. It is designed to orient a solar panel to the sun, track the sun, and compensate satellite attitude changes to maintain the proper orientation. The mechanism is equipped with a stepper motor to generate the required torque for the rotation of the solar panels. A planetary gear box and a spur gear provide amplification of the motor torque. Furthermore angular contact bearings lubricated with Maplub pf 101A are used. A classical rotation mechanism is the rotary mechanism assembly designed by [21] for an Earth

monitoring mission. It enables the rotation of six RF beams integrated on an antenna structure. The mechanism provides continuous rotation at 5.6 rounds per minute while transmitting high power RF signals.

Pointing Mechanisms

Compared to rotating mechanisms, pointing mechanisms have to manage more complex tasks. Pointing mechanisms not only rotate components continuously but they have to move a device rapidly and have to stop at a specific position with high accuracy. Pointing mechanisms are used to slew antennas, telescopes, or scanning mirrors. Antenna pointing mechanisms (APMs) usually have to maintain a communication link between the spacecraft and a ground station. Therefore often a very quick and highly accurate pointing is required. For telescopes the pointing requirements typically are even higher but the pointing velocities usually are smaller. Sensor mirrors tend to have the highest requirements on slewing rates and tracking precision. Due to these high requirements on pointing mechanisms, the used components like bearings, motors, or gears also have to fulfill high quality standards. And furthermore, in contrast to deployment mechanisms, pointing mechanisms must operate during the whole life of the spacecraft.

The antenna pointing mechanism for ESAs ENVISAT Polar Platform drives a Ka-band antenna as part of a data relay satellite system. It provides the link between the spacecraft and ground. The mechanism is a two motorgear azimuth and elevation gimbal system and drives a 1 meter antenna. The mechanism comprises the wave guides and rotary joint as well as 52 cables in azimuth [22]. Two other APMs operated successfully in 1995 onboard the OFFEQ experimental satellite. The gimbal pitch over yaw arrangement provided the link to the ground station [5]. Also for the ETS-VI K-band single access (KSA) antenna a pointing mechanism was required. A two axis gimbal mechanism flew onboard the Engineering Test Satellite VI (ETS-VI) [1]. For X-band data downlink from a low Earth orbit (LEO) satellite, Airbus built the Extremely Compact Two-Axis X-Band Antenna Assembly. It was used to point a gimbaled horn antenna [23]. Surrey Satellite Technology Ltd (SSTL) designed a mechanism to point X-band horn antennas on small LEO satellites. The goal was the development of a steered X-band antenna for communication with ground station. This provided ten times more data transmission compared to a conventional static antenna. The mechanism had to maintain the data link whilst the satellite performs positioning manoeuvers. A mechanically-steered antenna was preferred over an electrically solution because it is more affordable and less restrictive on pointing range. Therefore a two axis azimuth-elevation assembly was designed. The two axis were balanced in a way that no hold down mechanism was required. Although the balancing is difficult and expensive in terms of complexity and weight, it is worth the effort. Because compared to a hold down release mechanism the effort is rather low. A total of 11 of these mechanisms were actually built [7]. For ESA’s mission to Mercury Ka-band and X-band communication was required.

Therefore an elevation over azimuth dual pointing mechanisms was developed. The high temperatures on Mercury were the main challenges during the design process [4]. For an optical communication laser terminal RUAG designed a two-axis azimuth-elevation coarse pointing system. The assembly provides high bandwidth data transfer between telecommunication satellites operating in different orbit [24]. Another coarse pointing mechanisms was developed to maintain an optical link between a LEO satellite and geostationary (GEO) satellite or two GEO satellites [25].

1.3.1.2 Mechanism Requirements

The primary design drivers for mechanisms are the requirements coming from the mission objectives. The space mechanism requirements can be divided into performance and system requirements [12]. Performance requirements describe how a mechanism must operate. For example how fast a pointing mechanism has to move or how many cycles a mechanism has to perform during the mission. System requirements consider the mechanism as part of the spacecraft system. Therefore the mechanism's weight or envelope is important. Also the environmental conditions the mechanism has to survive. An overview of the different requirements can be seen in Table 1-1 and Table 1-2.

Performance requirements
Operating life
Pointing accuracy
Slew (or scan) rate
Operating speed
Deployment time
Restow capability

Table 1-1: Mechanism performance requirements

System requirements
Weight
Stiffness
Envelope
Clearance
Alignment
Interfaces
Environments

Table 1-2: Mechanism system requirements

These requirements on mechanisms also influence the requirements on its components. Accuracy, pointing velocity, or weight of a mechanism are all dependent on the performance of the components. And since gear wheels are essential components in the drive train of a mechanism, they have a huge influence on the quality of a space mechanism.

The operating life of a gear wheel typically has to be the same as the operating life of the mechanism. Because the number of deployments, the number of cycles, or the hours of operations of a mechanism also has to be fulfilled by the gear wheel. The range of operating cycles is rather large. A gear wheel built in a deployment mechanism often is turned only once in order to move a solar array for example to the desired position after launch. In contrast, gear wheels used in rotating mechanisms like attitude control systems have cycle numbers of more than a million. Whereas pointing mechanisms with its gear wheels usually stay below one million revolutions. Another requirement on mechanisms which is strongly influenced by gear wheels is the pointing accuracy. The pointing accuracy describes how precise an instrument must be oriented or moved. In GEO-GEO scenarios for example a high pointing accuracy is required because the two satellites might have a distance to each other of 60 000 km. In LEO-GEO and LEO-LEO application, the mutual line of sight contact is limited to 20 minutes. So a fast beam acquisition is required. Therefore high pointing accuracy and pointing speed is needed [24]. Many factors play a role in the accuracy of mechanisms: misalignments, dynamic loads, thermal distortions, backlash, and many more [12]. Often backlash is the largest source in the pointing error budget [26]. Gear wheels are responsible for the backlash and the goal is to keep the backlash low and constant during mission duration. A low backlash in a gearing system is often required for a smooth running and can be considered in the calculations. But an increase in backlash during the life of a mission has to be avoided because with that uncertainties and inaccuracies are brought into the system. An increase of backlash can, for example, be caused by wear and a decrease of the gear tooth diameter. The accuracy requirement on the gear wheels strongly depends on the type of the mechanism. A high precision Laser pointing mechanism, for example, might require an accuracy in the range of arc-seconds. Whereas the deployment of a boom is less critical in terms of positioning.

Also the required operational speed of a mechanism depends on the performance of gear wheels. For high velocity mechanisms like those integrated in gyroscopes or reaction wheels the heating of the gear wheels is an issue. Pointing and deployment mechanisms typically have lower speeds which is less critical for the used gear wheels. Since the cost of a satellite launch rises with the spacecraft mass, low-mass components are desirable. Consequently the system requirement for low weight of the mechanism affects every single component which is integrated in the mechanism. But not only the component itself, also supporting structures like reservoirs for gear wheel lubrication or motor radiators have to be considered. Also the requirement to survive the harsh environment of space has to be

fulfilled by every component. But depending on the mission and application the environment requirements can be quite different. The temperature and radiation limits, for example, strongly depend on the mission and the position of the component inside the spacecraft. Also vibration and shock depends on the chosen launch vehicle. Whereas vacuum affects all components in the same way, as long as they are not used in a pressurized capsule.

Table 1-3 gives an overview of different requirements on space mechanisms. DM stands for deployment mechanism, RM for rotating mechanism, and PM for pointing mechanism.

Author	Year	Type	Cycles	Accuracy [°]	Velocity [°/s]	T min [°C]	T max [°C]	Torque [Nm]
[27]	2001	DM	1	1	4	-40	65	5.4
[28]	2001	DM	1	1	n/a	-75	105	0.15
[14]	2003	DM	1	n/a	0.38	n/a	n/a	22
[16]	2014	DM	1	n/a	n/a	-30	40	n/a
[15]	2014	DM	1	n/a	0.04	n/a	n/a	0.89
[29]	2011	DM	1	n/a	n/a	n/a	n/a	1.5
[30]	2003	RM	600000	1	0.7	n/a	n/a	10
[17]	2011	RM	70000000	0.02	192	0	50	4.5
[18]	2014	RM	40000	n/a	36	-272	77	0.015
[19]	2014	RM	90000000	n/a	212	n/a	n/a	n/a
[20]	2014	RM	100000	3	2	-30	60	n/a
[21]	2013	RM	9000000	n/a	34	-35	75	n/a
[31]	2011	RM	n/a	0.2	6	n/a	n/a	n/a
[22]	1996	PM	88000	0.01	4.2	-40	+100	0.27
[5]	1996	PM	n/a	1	10	-30	+60	n/a
[1]	1991	PM	n/a	n/a	0.3	n/a	n/a	0.45
[23]	2009	PM	20000	n/a	10	-50	+80	0.14
[26]	1994	PM	n/a	0.03	n/a	-50	+80	0.7
[25]	1996	PM	n/a	0.01	2	n/a	n/a	1.0
[32]	1996	PM	n/a	0.05	0.11	n/a	n/a	0.17
[24]	2010	PM	n/a	n/a	n/a	-30	+45	0.2
[4]	2013	PM	22000	0.015	n/a	n/a	n/a	n/a
[7]	2011	PM	280000	0.25	20	-40	60	2.3
[33]	1999	PM	n/a	0.005	5	n/a	n/a	0.3

Table 1-3: Mechanism requirements overview

As already mentioned, mechanisms can be divided into high cycle and low cycle mechanisms. High cycle mechanisms are for example pointing, rotating, or tracking mechanisms. Whereas deployment mechanisms would be among the low cycles mechanisms.

1.3.1.3 Components

The performance of a space mechanism highly depends on the quality of its components. Most of the components are well known from Earth applications but prior to be used in satellites they have to be qualified for the harsh space environment. Furthermore the components have to proof reliable performance throughout the mission of up to 15 years. Typical components used in space mechanisms are motors, bearings, gear wheels, position feedback devices, HF feedthroughs, signal and power transfers, and also the structure. An overview of these components and examples of applications are given in the following. The gear wheels are covered in more detail in chapter 1.3.2.

Motors

All pointing mechanisms require motors or actuators to provide the required motion. Therefore two types of motors are used most often: Stepper motors and DC servo motors. Stepper motors have the advantage that no positioning sensor is required. The actual position can be determined by simply counting the steps of the motor as long as no steps are lost due to too high loads. Furthermore very low velocities can be accomplished with a stepper motor and its volume and mass is rather low. Stepper motors also provide holding torques by design. Servo motors need brakes. Finally the drive electronics often in simpler for stepper motors compared to servo motors [1]. But nevertheless both types are popular in spaceflight and are described in the following with some examples from recent missions.

In [22] a stepper motor is used for the Ka-band Antenna Pointing Mechanism for the ENVISAT satellite. A motorgear precision of 0.010° is required for that mission. The motor is built by SAGEM (France) and provides a holding torque of 0.27 N·m. For redundancy reasons two motor windings are integrated in the system. With the motor a maximum pointing speed of 4.2°/s and maximum pointing acceleration of 1.0°/s² is provided. Furthermore, the motor assembly withstands temperatures from -40°C to +100°C.

A stepper motor is also used in [1] as a driving system for the K-band antenna pointing mechanism for ETS-VI. The motor is used with a 0.45 step angle and provides an output torque of 0.45 N·m. The required maximum speed for that mission is 10°/s and the maximum pointing acceleration 10°/s². Due to the large antenna mass of 10 kg and a large payload inertia of 13 kg·m² a relatively large holding torque of 10.3 N·m is required. This is

necessary to prevent rotation of the antenna during firing of thrusters. To achieve a high pointing accuracy one of the most important parameters is the step size of the motor. In the application for the ETS-VI APM a step size of 0.005° was chosen. To verify the mechanism, functional tests were conducted after vibration tests, after thermal-vacuum tests, and after life tests. The results show that the step size stays basically constant during all the tests. Also the holding torque did not change. Only the slew rate had some minor variations which were negligible.

A stepper motor in open loop configuration is integrated in the XAA by Astrium [23]. The motor is run in the micro-stepping mode to reduce jitter. The motor itself provides a running torque of 140 N·mm. It is connected to a Harmonic Drive to ensure a rotation velocity of 10°/s. The motor withstand temperatures from -50°C to +80°C for a lifetime of 4 years which means 20 000 operation cycles. Also the INTELSAT antenna pointing mechanism uses stepper motors [26]. 1.5° stepper motors are integrated in both axes. The stepper-HD (Harmonic Drive) configuration provides 0.009375°/step. The motor has to operate in a temperature range from -50°C to 80°C and has to withstand temperatures from -60°C to +85°C in a non-operational status.

A stepper motor is used for a pointing mechanism to steer a Laser beam experiment [25]. The reason to integrate a stepper motor was its micro stepping mode which is important for pointing accuracy. Because the pointing accuracy requirement for that mission is 0.01° and the pointing stability over 60 seconds per axis is even 0.007°. The angular velocity of 2°/s and the angular acceleration of 0.02°/s² are low compared to other missions. Stepper motors are integrated in the antenna pointing mechanisms for Ka- and L-band reflectors designed by [32]. To provide linear motion the stepper motor is used together with a screw gear. The motor is a dual-wound, four-phase hybrid stepping motor with step angle of 1.8° and a minimum dynamic torque value of 170 N·mm. With the motor-gear assembly, one single motor step provides a displacement of 0.01 mm at the reflector. The motor system reaches pointing angular resolutions of 0.0006° in azimuth and 0.001° in elevation which results in a pointing accuracy of 0.05°. The maximum slew rate of the reflector is 0.11°/s.
For the antenna pointing mechanism for the mercury mission BepiColombo [4] a high temperature permanent magnet stepper motor is used which is coupled to a gear wheel to point the output shaft. A planetary gear is integrated in the stepper motor and creates some backlash. The backlash is required to avoid abnormal wear in the gears. Due to high lifetime and thermal requirements some design changes had to be applied: Gluing of the sleeve of the motor was substituted by a hot mounting sleeve because the glue created bumps and bubbles. But also problems with the lubrication MoS_2 occurred. The main challenges for that mission were the high temperatures and the long lifetime. The lifetime requirement asks for 18.8 million motor revolutions. Furthermore a backlash of only 18'' to 24'' was allowed in the motor-gearhead because the maximum pointing error is required to be as low as 55''.

A brushless DC motor was used for the antenna pointing mechanism for the OFFEQ satellite. But during life test at -20°C a large increase in input voltage was observed without any change in input current. The reason was a cut in the motor windings. Consequently all motors had to be modified [5]. [24] used a brushless DC motor for a pointing mechanism for optical communication. The motor has dual windings for redundancy. To minimize mass a frameless design was chosen. In the Global Microwave Imager (GMI) Spin Mechanism Assembly a 3-phase DC motor is integrated to spin an instrument at 32 rpm [17].

Bearings

In general, all bearings are designed to transfer loads in radial and axial direction. The most common bearings used in space mechanisms are ball bearings. They provide high running precision, a good load capacity, are easy to lubricate, and have low friction. Depending on the application, also roller bearings, cylindrical-roller bearings, or tapered-roller bearings are sometimes integrated in mechanisms [6]. Bearings used in spaceflight have to fulfill some specific requirements compared to nonspace use. During launch they have to survive the high vibrational loads of the rocket and must not lose their accuracy. Once in space the lack of gravity may affect oil flow systems that are important for functionality. Also vacuum and extreme temperatures are critical parameters for bearings applied in space environment [11]. In the following some examples are shown where bearings have been applied successfully in space mechanisms.
In an antenna pointing mechanism for the OFFEQ satellite, 440C stainless steel, precision angular-contact ball bearings with double rows of balls were integrated. They are back-to-back preloaded and only the grooves were dry lubricated with sputtered MoS_2. The ball separators were made out of the synthetic based material Duroid [5]. For a Laser beam experiment a high accuracy pointing mechanism was developed and therefore the ball bearings had to be extremely precise. Due to the high accuracy requirements the spacers between the bearings were designed to be adjustable in the range of µm to control the rigid preload within 10%. So the preload adjustment was made by the bearing manufacturer. Due to thermal constraints the spacer, the housing, and the shaft have to be made out of the same material. To avoid torque noise (very important for good pointing performance) the bearing track has to be grinded with special care and has to be prevented from dust contamination [25]. High performance bearings were also required for the pointing mechanism of an optical communication system designed by [24]. The desired performance was enhanced by integrating a Bearing Active Preload System (BAPS). BAPS offer high and stiff preload during launch. In orbit the BAPS can be actively transitioned to a low and soft bearing preload state. This is important for smooth, low-jitter movements during beam tracking. Furthermore it allows large thermal gradients across the bearings which is an advantage for GEO application. With BAPS minimum resistance torque can be achieved when the mechanisms is in orbit as well as high preload to withstand the challenging launch loads. Furthermore angular contact ball bearings in back-to-back configuration were used.

The balls were made of ceramic and the spacers were made of steel. Kaydon thin section angular contact bearings are integrated in the mechanisms for the Beagle2 Mars lander. The thin-section bearings have a high load capacity despite their small dimensions [3]. Many different bearing concepts can be found in literature. From back-to-back matched duplex bearings [7] or preloaded inclined ball bearings [23] to single row deep-groove ball bearings [1].

Position Feedback Devices

For many mechanisms the determination of its actual position is required. Sometimes only a reference position is needed from where the mechanism starts operation. In other cases it has to be determined if the mechanisms has successfully moved an instrument to a certain position. But most of the time a position knowledge is required throughout the operation. Especially pointing mechanisms need to know pointing direction and pointing velocity continuously. Many solutions are available which have to be chosen depending on the application.

Rotary encoders determine the position and velocity of a rotating shaft and convert the angular motion into a digital code. In spaceflight, optical encoders are quite popular because they provide accuracies in the range of arc-minutes to less than 1 arc-second [6]. Optical encoders consist of a light source (often a LED), a rotating code disk with a certain pattern printed on it, a slit plate, and a detector. The detector translates the incoming, encoded light beam into electrical current. Encoders are for example applied to determine the motion of a motor or the position of a shaft. In [22] a 16-bit absolute encoder is located on the output shaft of a Ka-band antenna pointing mechanism to monitor its motion. Absolute encoders have the advantage of maintaining the position information even when power is turned off. A 24-bit high-resolution optical encoder is used in a pointing mechanism for optical communication. That encoder allows a very smooth control which improves jitter performance [24].

Furthermore, resolvers are used to measure rotation. They are excited with a high-frequency AC signal and producing two sinusoidal output signals 90° out of phase with each other. With that an accuracy from several arc-minutes to 10 arc-seconds can be achieved [6]. In the antenna pointing mechanism built by [5] a resolver is integrated for servo control feedback. For position feedback of a motor applied in the spin mechanism assembly for the Global Micromave Imager a resolver is used as well. It provides an accuracy of 30 arc-seconds [17].

Many other solutions are available for position determination. For example potentiometers are used as position indicators in [1] and [26]. They measure electric potential to convert mechanical motion into an electric signal in order to determine the position. Also inductosyn

transducers are used as position sensors. These types of sensors use the inductive principle to determine the position [4]. Furthermore light barriers and position switches are applied as position feedback devices. Hard end stops limit for example the elevation range of an antenna pointing mechanism in [23]. High precision end switches power the motor off before reaching the mechanical stop. For azimuth and elevation reference mechanic precision switches are used. Their accuracy is in the µm range.

HF Feed through

When space mechanisms are used to deploy, steer, or point antennas, the radio frequency signal has to be led through the mechanism. And since the mechanism with the antenna often is turning during the transmission of data the feed through is quite a challenge during the design process. A popular solution is the integration of a rotary joint (RJ). It has the big advantage of unlimited rotation. For example the antenna pointing mechanism for the BepiColombo mission to planet Mercury comprises a two axis rotary joint [4]. Titanium was selected as material for the RJ for thermal compatibility with the mechanism and the rest of the radio frequency chain. Due to the poor electrical conduction of titanium, gold plating was required. Since large temperatures are an issue during the mission, the external parts of the RJ were sandblasted to increase the emissivity of the titanium. Emissivity of up to 0.45 was tested. MoS_2 bearing are used for internal motion of the RJ. The RJs were successfully tested at temperatures up to 290°C. For an antenna pointing mechanism designed by [7] non-contact rotary joints were selected in preference of contact rotary joints. Contact rotary joints might produce mechanical wear which pollute sensible components like bearings. Since suppliers for space-rated RJs were hard to find, a COTS rotary joint was selected and modified regarding materials, lubrication, cleanliness, and bearing size for vibration strength. Later the product was tested and qualified for space application. Coax cables were used to complete the RF feed. Also in [5] and [23] rotary joints are used for RF feed through. To connect the RJs with the antenna or another RJ, coaxial cables are used.

Cable wraps or coaxial cables are also a possible solution for RF signal feed through. But recent missions and studies showed some problems with that solution. During the design of an X-band pointing mechanism [23] the first idea was to use coaxial cables in elevation. But the coaxial harness required large torques to bend the cables. And in addition to that they were not compatible to life requirement. So the design for the harness was changed. The new configuration showed improved performance but became larger and bulky. And the RF losses increased. So it was decided to use a rotary joint. Another problem with coaxial cables was that the harness torque was not reproducible over temperature and it depended strongly on number of performed cycles. So the calculation of a reliable torque budget was not possible. Now coaxial cables are only used to connect the elevation RJ with the azimuth RJ. In [7] the use of coaxial cables was evaluated to connect the X-band transmitter output with the antenna’s septum-polarizer subassembly. But it has been

decided against this solution because the dynamic slewing of the antenna imposes stressing and bending on the cable, especially at temperature extremes where cables become stiff when getting cold. To solve the bending problem, the cable had to be designed longer which results in higher RF losses. Because of these disadvantages of coaxial cables it was decided to use rotating connectors which provide more reliable solution over life. As rotating connectors non-contact rotary joints were selected.

Signal and Power Transfer

To transfer signals and power from the mechanism to the spacecraft typically either slip rings or cable wraps are chosen. A slip ring vs. cable wrap evaluation was done by [23] for the design of an X-band pointing mechanism and the study showed that the cable wrap is quite heavy and bulky so it was decided to go on with slip ring. With cable wrap a rotation angle of 540° would have been possible, with slip ring unlimited rotation. So a slip ring with 15 power and signal tracks was integrated. In Surrey Satellite Technology Ltd's antenna pointing mechanism [7], to transfer motor and telemetry channels from the control electronics to the upper axis also two solutions were identified: a slip-ring and a flexible harness. It turned out that a slip ring was too complex to be developed in-house and procuring the units from specialist-suppliers is expensive and takes a lot of time. Flexible harness is cheaper but concerns in life time require careful design and qualification. But it was decided to use the harness solution. These two examples show which trade-offs have to be considered to choose the proper solution for a certain mission. In another example [5] unexpected increase of contact resistance in the slip ring signal tracks was discovered during functional tests. After run-in the values were normal. It was believed that the reason for the increase of resistance were MoS_s particles from the gears which contaminated the slip ring. Furthermore galvanic deposit occurred in air and increased the contact resistance as well. Also high temperatures, for example during BepiColombo's mission to Mercury [4] prevents the use of a slip ring.

In a pointing mechanism for a Laser beam experiment [25] over 60 twisted pairs of wires, two coax cables, and one bonding strap were concentrated in one cable wrap. This was possible because the cable wrap only had to provide an angular coverage of 200°. But due to the soft nature of the cable wrap friction is generated when rotating under 1-g conditions. So special low-friction coating was applied to lower friction. Also the presence of insulation material around the wires increases friction. During the development of the cable wrap, cable stiffness has to be taken into account in order to calculate the torque required to bend the wrap. To transmit power and signals over one rotation axis to the next cable wrap is used in a pointing mechanism for optical communication [24]. The cable wrap is divided into three ribbons. This has the advantage to separate the power lines from the sensitive encoder signals. The cable wrap is made of flex prints which formed bumps and buckles and their roll-down had impacts on the torque noise of the global system, which would

reduce the smoothness and thus the accuracy of the mechanism. In another pointing mechanism [7] a flexible harness is used to transfer the motor and telemetry signals. The limiting factor with this technology was the deflection through tight bend radii. A coiled flexible-PCB (Polychlorierte Biphenyle) wrap arrangement was formed to minimize the bending of the harness.

Beside slip rings and cable wraps only a few other solutions for signal and power transfer were found in literature. [22] uses a cable drum for the Ka-band antenna pointing mechanisms for the Envisat mission. The goal with that choice was to minimize the resistant torque, control the cable motion during launch, and control temperature of the cables. In [4] an own developed twist capsule was used to route the 96 lines of electric connectors. With that a 360° rotation was provided. Unlimited rotation was not required. The cables were attached on both sides of a flexible support foil. When moving counter-clockwise the foil and attached wires are wrapped in the rotor. When moving clockwise the foil unwrap from the rotor. During life test high friction and debris generation was observed. After a redesign of the support structure the life tests were successful.

Structure Material

The structure of a mechanism has to provide enough strength and stiffness as well as fatigue life. Therefore the choice of the material plays an important role. Often aluminum frames are used as housing [32]. The main structure of the Ka-band mechanisms for the Envisat mission is made out of Ti6Al4V and the secondary structures are made of aluminum alloy 7075 [22]. Also for the mechanisms of the Beagle2 instrument arm all structural items were manufactured from titanium in order to closely match the thermal expansion of the bearings, whilst minimizing the mass. Titanium alloy was also investigated by [5] because its coefficient of thermal expansion (CTE) is close to the CTE of the 440C stainless steel bearing material. Furthermore titanium provides a good stiffness to weight ratio. But at the end the mass got to large and titanium was not chosen. Aluminum alloy (7075-T7351) was chosen instead due to lower mass and its good stiffness to weight ratio. But a problem was the big difference in CTE compared to 440C stainless steel. This results in either an increase of preload and friction or an off-loading of the bearings. But after detailed examination of these effects it was shown that pointing accuracy and stiffness will not be affected. For the pointing mechanism for a Laser beam experiment [25] beryllium was used for the main structural parts because very low weight was required. The advantages of beryllium are its large Young’s modulus and high stiffness. But beryllium is toxic when inhaled in small particles and difficult in handling and workmanship [3].

1.3.1.4 Testing

Testing is essential for space mechanisms in order to verify the functionality under space conditions. But testing also has the purpose to validate computer models which simulate the behavior of the mechanism. Basically three levels of testing can be distinguished: tribometer, component, and mechanism level. Tribometer level tests are carried out to determine material properties or the behavior of a certain lubricant. For example friction coefficients and wear rates of a bulk material can be measured with a pin-on-disk test. In order to qualify components for space application, which is essential for the application in any mechanism, specified component levels tests have to be conducted. These tests should be carried out as close to the real application as possible. Gear wheels have to be tested concerning backlash and life, for example. Especially when new materials are used for components a systematical test series is required. But the functionality of all components not necessarily means the functionality of the assembled mechanism. That is why mechanism level tests are absolutely mandatory. With these, pointing accuracies, backlash, torque margins, or rotation velocities are verified under space conditions [8].

The test environment describes the external conditions where the tests are carried out. In-air testing means the tests are carried out in a 1 bar, controlled laboratory environment at “ambient temperatures”. These are typically 20°C ± 2°C. Often, this is simply just called “lab environment” or “ambient environment”. Furthermore humidity has to be controlled during the test because, for example, similar friction and wear tests in different laboratories have shown different results. The thermal-vacuum test environment has to represent the conditions in space. The pressure inboard of a spacecraft in geostationary orbit is approximately 10^{-6} to 10^{-8} mbar. These pressure levels can be achieved in modern vacuum chambers. The temperature range where most components operate is between -40°C and +65°C, leading to a qualification temperature of -55°C to +80°C [12]. These numbers are confirmed by examples found in literature about thermal-vacuum tests of space mechanisms. Tests are conducted at temperatures from -40°C to +60°C at 10^{-6} mbar [5], [1].

A typical space mechanism runs through four stages of testing: development, qualification, acceptance, and refurbishment tests. Development tests are conducted in order to identify and solve design problems in an early stage of the project. The purpose of the qualification test is to verify that the design of the mechanism fulfills all requirements. It is the key test during the development phase of the mechanism and is conducted in operational environment with adequate margin of safety. The acceptance test demonstrates the quality of a specific mechanism. All requirements must be verified. The idea of refurbishment tests is to test flight mechanisms that have been stored for a long time or have been repaired [12].

The test program of a mechanism consists of many different tests like functional tests, performance tests, or system tests. The most important tests are vibration tests, thermal-vacuum tests, and life tests. The vibration test is divided into sinusoidal and random vibration. Sinusoidal tests typically run from 5 Hz to 2000 Hz and have the goal to identify the Eigen frequency of the mechanism. Random vibration tests simulate the launch loads and are mandatory during the qualification process of a space mechanism. The thermal-vacuum test is one of the most important tests because it demonstrates the functionality of a mechanism under representative conditions of vacuum and temperature. Also the thermal gradients must be simulated during the test because, since the spacecraft is orbiting the Earth, the thermal conditions are changing continuously. Life tests under thermal vacuum conditions are important to monitor the performance of the mechanism throughout mission life. But since the total mission life cannot be simulated entirely, often accelerated life tests are conducted. In [22] for example an accelerated life test was conducted to check performance of liquid lubrication on bearings and gears. Therefore the test was run with 10 times maximum speed and 100 times maximum acceleration. Also the three year mission duration of a K-band pointing mechanism was carried out in a five months TV test.

1.3.2 Gear wheel basics

All the equations introduced in this chapter are taken from [34].

1.3.2.1 Introduction

Gear wheels are elements of many industrial machines and are applied in nearly all engineering fields. Their main goal is the transmission of power and motion. The most popular gear trains are spur gears, bevel gears, spiral gears, and worm gears. Spur gears are used most often because of their large carrying capacity, low mass related to transmitted power, and efficiency. The axis of the spur gears in a system are parallel to each other. Whereas the shafts of bevel gears intersect and the axis of worm and spiral gearing do neither intersect nor are they parallel. The different types of gear trains can be seen in Figure 1-1. From left to right spur gear, bevel gear, helical gear, and worm gear.

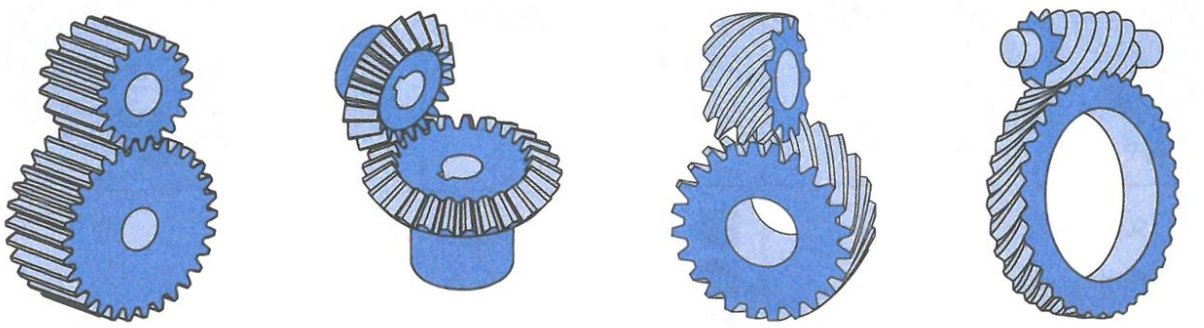

Figure 1-1: Different types of gear trains [34]

Beside the gearing type, the profile of the wheel is an important characteristics. The most relevant are cycloid toothing, cycle-shaped toothing, and involute toothing. These days, the latter is used most often because involute toothing has fundamental advantages like easy manufacturing, insensitive against changes in axis distance, or low-vibration operation. Consequently straight toothed spur gears with involute toothing are the most popular gear wheels and are typically just called “spur gears”. In Table 1-4 the most important parameters of spur gears are described.

Name ***German translation***	**Symbol**	**Unit**	**Description**
Module *Normalmodul*	m_n	mm	Scaling factor for tooth
Number of teeth *Zähnezahl*	z	-	Number of teeth of one gear wheel
Tooth thickness *Zahnbreite*	b	mm	Thickness of the tooth
Axis distance *Achsabstand*	a	mm	Distance of the axis of the two gear wheels
Reference center distance *Nullachsabstand*	a_d	mm	Theoretical value for calculation
Gear ratio *Übersetzungsverhältnis*	i	-	Ratio of the two gear wheels
Circular pitch *Teilung*	p_t	mm	Distance of the two adjacent teeth on the reference diameter
Base circle pitch *Grundkreisteilung*	p_b	mm	Distance of the two adjacent teeth on the base circle diameter

Normal base pitch *Eingriffsteilung*	p_e	mm	Normal distance between two flanks
Normal pressure angle *Normaleingriffswinkel*	α	°	Angle between a line tangent to a tooth surface and the line normal to the pitch surface
Operating pressure angle *Betriebseingriffswinkel*	α_w	°	Angle at pitch diameter
Transverse normal base angle *Stirneingriffswinkel*	α_t	°	For straight spur gears $\alpha_t = \alpha$
Helix angle *Schrägungswinkel*	β	°	For straight spur gears $\beta = 0$
Reference diameter *Teilkreisdurchmesser*	d	mm	Diameter where the pressure angle of the involute is equal to 20°
Base circle diameter *Grundkreisdurchmesser*	d_b	mm	Diameter where the involute starts
Pitch diameter Wälzkreisdurchmesser	d_w	mm	Diameter where no sliding occurs between the wheels
Root diameter *Fußkreisdurchmesser*	d_f	mm	Diameter of the tooth root
Tip circle diameter Kopfkreisdurchmesser	d_a	mm	Maximum diameter of the wheel
Tooth depth *Zahnhöhe*	h	mm	Hight of a tooth
Bottom clearance *Kopfspiel*	c	mm	Minimal distance of the root of one tooth to the tip of the other tooth
Normal backlash *Normalflankenspiel*	j_n	mm	Minimal distance of the flanks
Circumferential backlash *Drehflankenspiel*	j_t	mm	Actual backlash
Sliding speed *Gleitgeschwindigkeit*	v_g	m/s	Sliding speed at the contact of the teeth
Addendum modification coefficient *Profilverschiebungsfaktor*	x	-	Addendum modification normalized with module

Length of path of contact *Eingriffsstrecke*	g_α	mm	Length of path where the teeth are on contact
Trans-verse contact ratio *Profilüberdeckung*	ε_α	-	Average of teeth pairs being in contact
Trans-verse contact ratio pinion Teilprofilüberdeckung Ritzel	$\varepsilon_{\alpha 1}$	-	
Trans-verse contact ratio wheel Teilprofilüberdeckung Rad	$\varepsilon_{\alpha 2}$	-	

Table 1-4: Spur gear parameters [34]

1.3.2.2 Gear pairing parameters

According to DIN 867 (standardized gearing) [35] the profile angle of a standard gear is 20° and is called pressure angle α. This is the angle between the tangent at the involute and the line through the center of the gear wheel. The diameter of a circle through the contact point of the tangent with the involute is called reference diameter. The reference diameter can also be calculated by multiplying number of teeth *z* and module *m*.

$$d = z \cdot m \qquad (1)$$

The module describes the scaling factor of a tooth with the unit [mm]. It is one of the main factors for gearing calculations. In Anglo-Saxon countries instead of the module, often the diametral pitch P_d is used, which is the reciprocal value of the module.

$$P_d = \frac{z}{d} \qquad (2)$$

When multiplying the module *m* with π the circular pitch p_t is calculated which is the distance of two adjacent teeth on the reference diameter.

$$p_t = m \cdot \pi \qquad (3)$$

In order to realize a working gearing system the modules of the two gears have to have the same module. For manufacturing reasons the modules have been standardized in certain steps. According to DIN 780 [36] the nowadays used modules are shown in Table 1-5.

1	1.25	1.5	2	2.5	3	4	5	6	8	10	12	16	20

Table 1-5: Gear wheel modules [36]

For the creation of the involute the base circle diameter d_b is the essential parameter.

$$d_b = d \cdot cos\alpha \quad (4)$$

The distance of the two adjacent teeth on the base circle diameter is called base circle pitch p_b.

$$p_b = p_t \cdot cos\alpha \quad (5)$$

The normal distance between two flanks is called normal base pitch p_e and is equal to p_b.

$$p_e = p_t \cdot cos\alpha \quad (6)$$

According to DIN 867 [35] tip circle diameter d_a, root diameter d_f, and tooth height h can be calculated as followed:

$$h = 2.25 \cdot m \quad (7)$$

$$d_a = z \cdot m + 2 \cdot m \quad (8)$$

$$d_f = z \cdot m - 2 \cdot m \quad (9)$$

Figure 1-2 gives an overview of the relevant gearing parameters. a) describes the parameters at one certain gear wheels and b) at a gearing system.

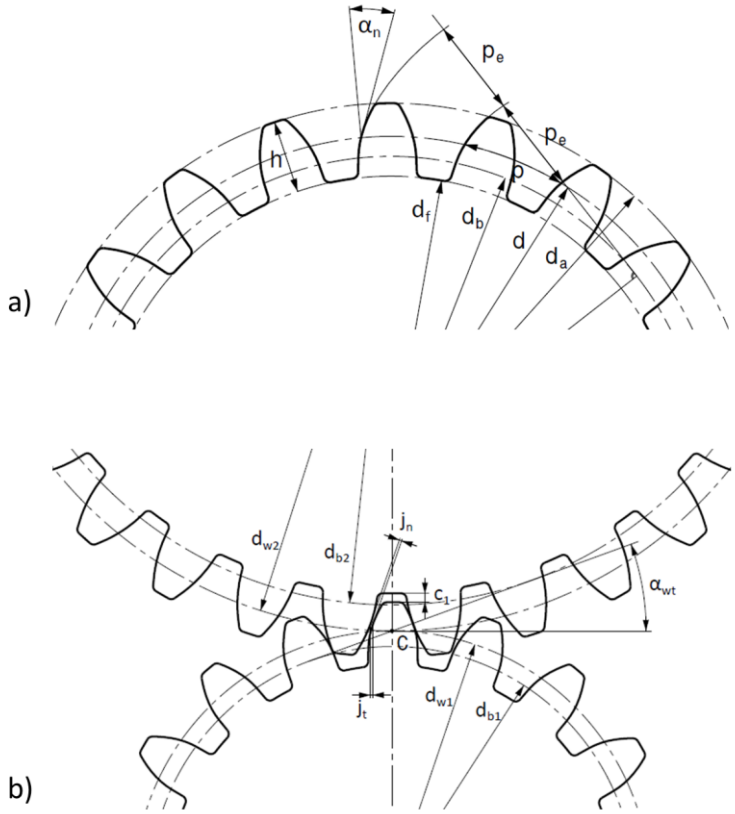

Figure 1-2: Gearing parameters [34]

Based on the mentioned parameters the geometry of gearing systems can be calculated. A gearing system includes a smaller gear wheel which is called “pinion” and the larger gear wheel which often is just called “wheel”. In the following calculations the pinion parameters are marked with index “1” and the wheel parameters with index “2”.

From the sum of the reference diameters d_1 of the pinion and d_2 of the wheel, the reference center distance a_d can be calculated.

$$a_d = \frac{d_1 + d_2}{2} \qquad (10)$$

The operating pressure angle α_w can be calculated with the normal pressure angle α, the reference center distance a_d, and the real axis distance a.

$$cos\alpha_w = \frac{a_d}{a} \cdot cos\alpha \qquad (11)$$

Further important gearing parameters are gearing ratio i, revolutions n, and pitch diameter d_w.

$$|i| = \left|\frac{d_{w2}}{d_{w1}}\right| \tag{12}$$

$$i = \frac{n_1}{n_2} = -\frac{d_{w2}}{d_{w1}} = -\frac{z_2}{z_1} \tag{13}$$

The real axis distance a can be calculated with the pitch diameters d_{w1} and d_{w2} of pinion and wheel.

$$a = \frac{d_{w1} + d_{w2}}{2} \tag{14}$$

With equation (15) and (16) the pitch diameters d_{w1} and d_{w2} can be calculated.

$$d_{w1} = \frac{2 \cdot a}{1 - i} \tag{15}$$

$$d_{w2} = \frac{2 \cdot a}{1 - \frac{1}{i}} \tag{16}$$

In the case of $\alpha_w = \alpha$, it follows $d_w = d$. For external gear pairing $i < 0$.

The length of path of contact is the distance where the teeth are in contact with each other and can be calculated as followed:

$$g_\alpha = \sqrt{\left(\frac{d_{a1}}{2}\right)^2 - \left(\frac{d_{b1}}{2}\right)^2} + \frac{z_2}{|z_2|} \cdot \sqrt{\left(\frac{d_{a2}}{2}\right)^2 - \left(\frac{d_{b2}}{2}\right)^2} - a \cdot sin\alpha_w \tag{17}$$

From g_α the trans-verse contact ratio ε_α can be calculated.

$$\varepsilon_\alpha = \frac{g_\alpha}{p_e} \tag{18}$$

1.3.2.3 Calculation of load carrying capacity

An overview of the relevant parameters for the calculation of the carrying capacity are summarized in Table 1-6.

Name ***German translation***	**Symbol**	**Unit**	**Description**
Torque *Drehmoment*	M_T	N·m	Torque acting on the gear wheel
Revolutions per minute *Drehzahl*	n	1/min	Number of revolutions of the gear wheel per minute
Angular velocity *Winkelgeschwindigkeit*	ω	°/s	Angular velocity of the gear wheel
Power *Leistung*	P	W	Power in the gearing system
Tangential force *Tangentialkraft*	F_t	N	Acting force at reference diameter d
Axial force *Axialkraft*	F_a	N	Force acting axial on the tooth
Radial force *Radialkraft*	F_r	N	Force acting radial on the tooth
Tooth root stress *Zahnfußbeanspruchung*	σ_F	N/mm²	Real acting stress at tooth root
Tooth root load capacity *Zahnfußgrenzfestigkeit*	σ_{FG}	N/mm²	The maximum allowable load at the root of the tooth
Application factor *Anwendungsfaktor*	K_A	-	Form factor
Dynamic factor *Dynamikfaktor*	K_V	-	Form factor
Transverse factor *Stirnfaktor*	$K_{F\alpha}$	-	Form factor
Face load coefficient *Breitenfaktor*	$K_{F\beta}$	-	Form factor
Form factor *Formfaktor*	Y_{Fa}	-	Form factor

Stress correction factor *Spannungskorrekturfaktor*	Y_{Sa}	-	Form factor
Coverage factor *Überdeckungsfaktor*	Y_{ε}	-	Form factor
Mass wear *Massenverschleiß*	M_W	g	Mass loss due to wear
Tooth area before operation *Ungelaufene Zahnfläche*	$A_{tooth,new}$	mm²	Tooth area of the novel gear wheel
Tooth area after operation *Gelaufene Zahnfläche*	$A_{tooth,op}$	mm²	Tooth area of the operated gear wheel
Material density *Dichte des Materials*	ρ	g/cm³	Density of the material
Mass wear rate *Massenverschleißrate*	M_{WN}	10^{-6}·g	Mass wear per revolutions
Cycle number *Lastwechselzahl*	N	-	Number of load cycles
Profile length *Profillänge*	l_{Fl}	mm	Profile length of the active flank
Tooth loss factor *Zahnverlustfaktor*	H_V	-	-
Safety factor *Sicherheit*	S_{Fmin}	-	-
Fatigue stress under fluctuating stress *Zeitschwellfestigkeit*	σ_{FlimN}	N/mm²	-
Deformation of tooth Zahnverformung	λ	mm	-
Young's modulus *Elastizitätsmodul*	E	N/mm²	-

Table 1-6: Parameters for gearing carrying capacity calculation [34]

From the torque M_T, the revolutions per minute n, and the diameter of the gear wheel, all the relevant operational parameters of the gearing system can be calculated.

The tangential forces F_t at the pinion (index 1) and the wheel (index 2) can be calculated from the torque M_T.

$$F_t = F_{t1,2} = \frac{M_{T1,2}}{\frac{d_{1,2}}{2}} \quad (19)$$

Turning velocity v [m/s]

$$v = \frac{d \cdot \pi \cdot n}{60 \cdot 10^3} \quad (20)$$

From the tangential force, the axial forces F_a and radial forces F_r at the tooth can be calculated.

$$F_a = F_t \cdot tan\beta \quad \text{for } \beta = 0 \quad F_a = F_t \quad (21)$$

$$F_r = F_t \cdot tan\alpha \quad (22)$$

Tooth root carrying capacity

The calculation of the tooth root carrying capacity considers bending stress at the tooth root resulting from a tangential force on the tooth flank. According to guideline VDI DIN 2736 [37], one can calculate the load carrying capacity of thermoplastic spur gears as followed:

The calculation of the actual acting bending stress at the root of the tooth of a spur gear requires the acting force, the tooth parameters tooth thickness and module, as well as different form factors.

$$\sigma_F = K_A \cdot K_V \cdot K_{F\alpha} \cdot K_{F\beta} \cdot \frac{F_t}{b \cdot m} \cdot Y_{Fa} \cdot Y_{Sa} \cdot Y_\varepsilon \quad (23)$$

According to DIN 867 [35]: for z = 30 and x = 0, the form factor Y_{Fa}= 2.60 and Y_{Sa}= 1.70
for z = 24 and x = 0, the form factor Y_{Fa}= 2.75 and Y_{Sa}= 1.65

The form factor Y_ε can be calculated with the trans-verse contact ratio ε_α.

$$Y_\varepsilon = 0.25 + \frac{0.75}{\varepsilon_\alpha} \quad (24)$$

Regarding DIN 3990 [38], when considering a rather slow and smooth running of the gearing system, the form factor K_A = 1 and K_V = 1.

According to [39], if $\frac{b}{m} \leq 12$, $K_{F\alpha} = K_{F\beta} = 1$.

In order to ensure the gear wheels survives the load, the acting bending stress σ_F at the wheel has to be smaller than the tooth root load capacity σ_{FG} of the wheel. For continuous operation the safety factor S_{Fmin} usually has the value 2.

$$\sigma_F \leq \frac{\sigma_{FG}}{S_{Fmin}} \quad (25)$$

$$\sigma_{FG} \approx 2 \cdot \sigma_{FlimN} \quad (26)$$

Values for the load capacity (fatigue stress under fluctuating stress σ_{FlimN}) are only available for some selected polymers. Table 1-7 shows σ_{FlimN} for POM [37].

Tooth root temperature [°C]	**σ_{FlimN} [N/mm²] at different cycle numbers N**			
	10^5	**10^6**	**10^7**	**10^8**
20	65	50	41	35
40	62	47	38	32
60	57	42	33	27
80	50	35	26	20
100	41	26	17	11

Table 1-7: Fatigue stress numbers for POM [37]

Wear

For the determination of wear with the tactile measuring method, the contour of a tooth is measured. Out of the contour, the area of a tooth can be calculated. With the difference of the tooth area before ($A_{tooth,new}$) and after ($A_{tooth,op}$) operation of the gear wheel, the mass wear M_W can be calculated.

$$M_W = \left(A_{tooth,new} - A_{tooth,op}\right) \cdot z \cdot b \cdot \frac{\rho}{10^3} \qquad (27)$$

In order to evaluate the wear behavior it is necessary to calculate the mass wear M_W based on the number of cycles N. This is called mass wear rate M_{WN}.

$$M_{WN} = \frac{M_W}{N} \cdot 10^6 \qquad (28)$$

To calculate the wear coefficient k_W, first the linear wear rate W_{mN} has to be determined.

$$W_{mN} = \frac{10^3 \cdot M_{WN}}{z \cdot b \cdot l_{Fl} \cdot \rho} \qquad (29)$$

$$k_W = \frac{W_{mN} \cdot b \cdot z \cdot l_{Fl}}{T \cdot 2 \cdot \pi \cdot H_V} \qquad (30)$$

With integrating equation (29) into equation (30), the wear coefficient can directly be calculated from the tooth area difference.

$$k_W = \frac{10^6 \cdot \left(A_{tooth,new} - A_{tooth,op}\right) \cdot z \cdot b}{N \cdot T \cdot 2 \cdot \pi \cdot H_V} \qquad (31)$$

For the mentioned calculations, the profile length l_{Fl} and the tooth loss factor H_V have to be known.

$$l_{Fl} = \frac{1}{d_b} \cdot \left[\left(\frac{d_a}{2}\right)^2 - \left(\frac{d_f}{2}\right)^2\right] \qquad (32)$$

In a first approximation, l_{Fl}can be calculated as $l_{Fl} = 2.0 \cdot m$

$$H_V = \frac{\pi \cdot \left(\frac{z_2}{z_1} + 1\right)}{z_1 \cdot \frac{z_2}{z_1} \cdot cos\beta} \cdot (1 - \varepsilon_\alpha + \varepsilon_{\alpha 1}^2 + \varepsilon_{\alpha 2}^2) \quad (33)$$

Equation (33) is valid for $1 \leq \varepsilon_\alpha \leq 2$.

$$\varepsilon_{\alpha 1} = \frac{1}{p_e} \cdot \left(\sqrt{\left(\frac{d_{a1}}{2}\right)^2 - \left(\frac{d_{b1}}{2}\right)^2} - \sqrt{\left(\frac{d_{w1}}{2}\right)^2 - \left(\frac{d_{b1}}{2}\right)^2} \right) \quad (34)$$

$$\varepsilon_{\alpha 2} = \frac{z_2}{p_e \cdot |z_2|} \cdot \left(\sqrt{\left(\frac{d_{a2}}{2}\right)^2 - \left(\frac{d_{b2}}{2}\right)^2} - \sqrt{\left(\frac{d_{w2}}{2}\right)^2 - \left(\frac{d_{b2}}{2}\right)^2} \right) \quad (35)$$

1.3.3 Gear wheels in spaceflight application

Gear wheels are fundamental components in most spaceflight pointing mechanisms. Gear wheels are typically used for speed reduction and increase of torque in mechanical power transmission systems. Beside the traditional spur gears, various novel gear concepts have been introduced over the last decades with new materials and new manufacturing techniques, including helical gears, internal gears, plain and spiral bevel gears, hypoid gears, worm gears, Harmonic Drives, and planetary gears. Due to their simplicity, robustness, and high efficiency, spur gears are the most popular gears used in spaceflight mechanisms. Planetary gears and Harmonic Drives are applied in mechanisms because of their compactness and high reduction ratios.

1.3.3.1 Spur Gears

The geometry of gear pairings can be clearly characterized by the shape of the gear body, the tooth traces, and the profile shape. The most common and simplest solution is the spur gear with involute profiles. Compared to other gear pairings, based on performance and efficiency, spur gears have high load capacities, low masses, are easy to manufacture and to install, and thus are used in many industrial applications [34]. With these advantages, spur gears are also the most popular gears for the application in spaceflight mechanisms. Spur gears achieve efficiencies of 98 to 99% [6]. The teeth of spur gears are parallel to the

shaft and are placed on the outside of a cylinder. The smaller driving gear wheel is called a pinion. The ratio of the number of teeth is equal to the gear ratio of the gear pair [12]. To minimize the backlash of spur gear mechanisms, the distance between the axes of the two interacting gear wheels is reduced during assembly. If done in a fixed manner, thermal expansion cannot be compensated anymore which might result in an increase of backlash (cold, too far apart) or an increase of friction (hot, too tight engagement).

The main challenge using spur gears is the inherent backlash. The goal of gear systems is to transmit power from one gear to the other. Therefore the teeth flanks of the two gears have to be in contact. When the rotational direction is changed, the tooth of the moving gear is initially without contact until it touches the next tooth of the driven gear. This moving without contact is called backlash and is most often measured in degrees [40]. Due to manufacturing inaccuracies and the necessity for a smooth running of the gear wheel, backlash typically cannot be avoided completely. To provide sufficient lubrication, a gap between the teeth is even required to ensure enough lubricant can flow between the flanks. However, the accuracy of pointing mechanisms decreases due to the backlash between gears [12], making low backlash one of the main design parameters for gear boxes [41]. Removing backlash has not only the advantage of greater position accuracy, but it also provides greater repeatability, higher effective stiffness, and simpler linear analysis [11].

An examples where spur gears were used in recent spaceflight missions is the Mars Science Laboratory (MSL) Mast Cameras. The Mast Cameras Zoom Lens, although finally not flown on MSL, used spur gears for the Focus Drive System and the Filter Wheel Drive System [42]. To focus the mirror at the Kepler mission, a pinion-spur gear solution was chosen were the pinion is driven by a stepper motor and both gears are made out of stainless steel [43]. Spur gears were also used in the antenna pointing mechanism that provided the data link between OFFEQ experimental satellite and ground control [5]. This design used a stainless steel pinion and an aluminum gear wheel, lubricated with sputtered MoS_2. Also for the mission to planet Mercury, the BepiColombo spacecraft uses spur gears in its solar array drive mechanism. A two stage spur gearbox was applied to provide the necessary transmission between the motor and the solar array output shaft. Due to the expected high temperatures of more than 100°C wet lubrication was not possible. Consequently MoS_2 was used as dry lubricant [31].

1.3.3.2 Spring-loaded split gears

Spring-loaded split gears are available from stock and are widely used to eliminate backlash in gear trains [12]. In space application they are used in high accuracy pointing applications [23]. The principle idea of spring-loaded split gears is to split a gear in two narrow width gears which are resiliently biased together. This is achieved by a preloaded coil spring. This

has the advantage that the flanks of each of the two split gears remain in contact with the driven gear and consequently no backlash appears when the rotation direction of the gear is changed. The disadvantages of the spring-loaded split gears are the large number of required parts and a limited load capacity. As soon as the inertia generated by turning the mass is larger than the load capacity of the spring, the anti-backlash principle does not work anymore [44].

The mechanism for the Extremely Compact Two-Axis X-Band Antenna Assembly (XAA) designed by Airbus [23] uses the split gear principle Figure 1-3. The horn antenna for X-band data downlink on LEO satellites require high precision and consequently a split and spring-loaded spur gear is used in azimuth for zero backlash. Furthermore the gear is lubricated with Maplup PF 101-a. Also for BepiColombo, the ESA mission to Mars, split gears are integrated in the Planetary Orbiter. The Ka- and X-band antennas require high accuracy pointing mechanisms which use an anti-backlash pinion to minimize backlash [4]. A problem with an anti-backlash pinion spur gear occurred during vibration test of the antenna pointing mechanism designed by Surrey Satellite Technology Ltd (SSTL). The pinion uses a single small-sized grub-screw to lock it to the motor gear-box output shaft. And during the test the pinion gear came loose from the shaft. The grub-screw was unable to provide enough force. Even a second grub-screw was not enough to attach the pinion reliable to the shaft. Only with an increase of the screw from M3 to M4 and an increase of the locking torque sufficient locking torque was provided to mount the gear onto the shaft. The gear is used in a pointing mechanism for an X-band horn antenna. The mechanism has to maintain the data link whilst the satellite performs positioning manoeuvers [7].

Figure 1-3: Spring-loaded split gear [23]

1.3.3.3 Harmonic Drive

Harmonic Drives (HD) were invented in 1957 so they are quite a new development in gearing. Since then they have become very popular in spaceflight because they have no backlash [1] and an optimal reduction/mass ratio [22]. Harmonic Drives consist of three

elements: the Wave Generator, the Flexspline, and the Circular Spline (Figure 1-4). The principle of the gear is described by the Harmonic Drive AG as followed[1]: The Flexspline is slightly smaller in diameter than the Circular Spline resulting in it having two fewer teeth on its outer circumference. It is held in an elliptical shape by the Wave Generator and its teeth engage with the teeth of the Circular Spline across the major axis of the ellipse. As soon as the Wave Generator starts to rotate clockwise, the zone of the tooth engagement travels with the major elliptical axis. When the Wave Generator has turned through 180 degrees clockwise, the Flexspline has regressed by one tooth relative to the Circular Spline. Each turn of the Wave Generator moves the Flexspline two teeth anti-clockwise relative to the Circular Spline.

Figure 1-4: Harmonic Drive[1]

As mentioned before Harmonic Drive gears are widely used in space applications. One is used, for example, in the antenna pointing mechanism for ESA's ENVISAT Polar Platform. The mechanism drives a Ka-band antenna which provides the link to the ground. The pointing mechanism is a two motorgear azimuth and elevation gimbal system and drives a 1 meter antenna. The Harmonic Drive gear HDUS-20-BLR with ratio 100 made of stainless steel is installed in the mechanism. Another example where HD gears are used is the antenna pointing mechanism for the ETS-VI K-Band Single Access Antenna. In the two axis gimbal mechanism the Harmonic Drive CS-32-SP was integrated with a reduction rate of 1/157. A drawback of the application of HDs was the production of wear debris. The above mentioned XAA mechanism designed by Airbus [23] uses a Harmonic Drive size 11 which is mounted on the output shaft of the stepper motor. The HD is wet lubricated with Maplup PF 101-a and it shows better jitter performance than planetary gear boxes. Also for the INTELSAT antenna pointing mechanism the HD is mounted on the output shaft of the stepper motor [26]. The gear provides a 160:1 ratio. But although the Harmonic drive design offers essentially zero backlash, a disadvantage arises in positional hysteresis. The flex spline of the harmonic drive acts as a spring and tends to wind up when driven into a stop. This wind up causes a step versus position error.

[1] http://harmonicdrive.de/en/technology/harmonic-driver-strain-wave-gears/

1.3.3.4 Others

Beside spur gears, spring loaded gears, and Harmonic Drive gears, many other gear solutions are used in space mechanisms. Airbus integrated in their XAA mechanism a bevel gear which is wet lubricated with Maplup PF 101-a. For minimum backlash it is adjusted by shimming the elevation actuator axially [23]. In an antenna pointing mechanism for a reflector a screw gear is connected to the stepper motor shaft to provide linear motion [32]. A worm-wheel transmission is used in the elevation assembly of the above mentioned SSTL antenna pointing mechanism. The reasons for that solution were good gear-ratio and the prevention of back-driving. With the large gear ratio a fine pointing resolution is provided without requiring additional planetary gear-heads. The worm gear is made out of stainless steel and its counterpart, the wheel, is made out of Delrin. With that solution the gear assembly can be operated without lubrication [7].

1.3.3.5 Lubrication

Metallic gear wheels have to be lubricated to reduce friction and wear as the turning gears result in movement between the metallic flanks of the gears. An appropriate lubricant can reduce these limiting effects, increase transmission efficiency, and prolong the lifetime of the components. Without lubricating the contact areas of the gears, the increased friction would result in a higher power consumption, not desirable especially in spaceflight applications with limited power. A failure in lubricating the gear wheels not only causes an increase in power consumption, but also a loss of accuracy in pointing mechanisms due to abrasion and increasing backlash [12]. Since lubrication and most of the moving parts in a mechanism cannot be designed redundant, a failure in lubrication often is a single point of failure in space mechanisms and has to be taken serious during the design process.

But lubrication is everything but easy in space applications: The lubricant has to be compatible with the high vacuum and extreme temperatures, a refilling or renewal of the lubricant is not possible, and the performance of the lubricant must not decrease during the mission. Two groups of lubricants are used nowadays in spaceflight applications: liquid and dry-film lubricants. Liquid lubricants provide a smoother operation and are less sensitive to process variations. But at low temperatures the viscosity of liquid lubricants increases, so the temperature should typically be kept above -30 °C. At high temperatures, the evaporation of the lubricant may also cause problems, limiting some lubricants to temperatures between -30°C and +40°C [6]. A disadvantage with liquid lubrication is, that there has to be a small gap between the flanks of the wheel to allow the lubricant to flow between them. But this small gap between the flanks already constitutes backlash and a loss of accuracy. Another problem is that liquid lubricants mitigate from the contact zones and the high vapor pressure of common oils leads to evaporative loss in vacuum. This

makes seals or oil reservoirs necessary in the gear box design which increases the mass and complexity of a mechanism. Furthermore the escape of lubricants creates a risk of contamination for solar cells or optical components [12]. Despite these limitations, liquid lubricants are frequently used in space missions despite their drawbacks. Maplup PF 101-a is used for Harmonic Drives and gears in Airbus' X-band antenna pointing mechanism [23]. Fluid lubrication was also used for a pointing mechanism for Laser beam experiments [25]. But anti-creep barriers had to be implemented to prevent oil depletion and pollution towards the optical elements. Other examples for liquid lubrications include Fomblin Z25 which is used in a pointing mechanism for optical communication [24], and Braycote 601EF which is used to lubricate a motor gearbox [7].

Two general types of dry-film lubricants are used: molybdenum-disulfide (MoS_2) and Teflon. These dry lubricants provide a low coefficient of friction and are less sensitive to temperature. However, at a relative humidity higher than 50%, MoS_2 accelerates corrosion [6]. Also a high number of operational cycles are a challenge for dry lubricants. In the antenna pointing mechanism for the BepiColombo mission, MoS_2 is used as a lubricant for the APM gears [4]. The authors remarked that gears with low or zero backlash would not be suitable to be used with solid lubrication, and the designers had to reduce the maximum allowable torque, as the lubrication failed in life tests at higher loads. At low temperatures, the wear rates increased for MoS_2 lubrication, thus, a heating of the component was required. Furthermore a depletion of dry lubrication from the gears was observed but this did not reduce the functionality. For the ENVISAT mission, MoS_2 was intended to be used as lubrication in the Ka-band antenna pointing mechanism [22]. However, during long-life tests, the lubricant failed already after 7 000 cycles (88 000 were required). Therefore, the ESA-qualified Fomblin Z25 oil lubrication was used for bearings and gears of the ENVISAT Ka-band APM. MoS_2 was successfully used to lubricate aluminum gears [5] and bearings [1] in other applications.

1.3.4 Synthetics Gear Wheels

1.3.4.1 Polymers

Compared to other materials the history of polymers is pretty short. In the 19th century synthetic materials were extracted from natural products for the first time. They were seen as cheap alternatives to metallic materials. Since the middle of the 20th century the variety of polymers has been increased enormously. Also the quality improved and soon high-performance polymers were invented which exceeded the properties of other materials. Due to their low mass, good machinability, and low wear they are standard in today's life.

Polymeric material can be divided into thermoplastics, elastomers, and thermosets. Thermoplastics are built up of linear or cross-linked macromolecules which can be in an amorphous or semi-crystalline state. Thermoplastics are made by adding together subunits to form long chains. The macromolecules are connected with van der Waals forces or hydrogen bond. With thermal energy these bonds can be broken up and the polymer can be transformed into a molten state. Elastomers, more commonly known as rubbers, can already be deformed at low temperatures and with low forces. But usually this deformation is reversible. Thermosets are made by mixing two components which react and harden. Thermosets are losing stiffness as soon as they are heated, but do not melt as they are heavily cross-linked. Thermosets therefore cannot be hot worked. For high-performance applications, thermoplastics are used most often.

An overview of different polymers is shown in Table 1-8 [45]. To make comparison between the materials easier, for each polymer type only the properties of the natural material is given. With different fabrication methods or added fillers these properties can be changed. The shown materials typically are divided into three categories: standard polymers, technical polymers, and high-performance polymers. The standard polymers (e.g. PE, PVC, PS) are used for mass applications like packaging, insulators, or covers. They do not provide great mechanical properties but have other advantages like chemical stability, good insulation properties, or good cost-performance ratio. Technical polymers (e.g. PA, PC, POM) are characterized by good mechanical, electrical, and thermal properties. They can be used at temperatures up to 150°C, have high strength, and good machinability. Their field of application is pretty wide and goes from slide bearings or wheels to seals and insulators. Also the high-performance polymers (e.g. PEEK, PTFE, PI) have good mechanical, electrical, and thermal properties. Compared to technical polymers which can be used up to temperatures of 150°C, the high-performance polymers withstand temperatures of more than 150°C even in long-term application. For that reason they are sometimes called high-temperature polymers. Also low temperatures down to -200°C is survived by some of these materials. Furthermore they provide extremely good wear behavior and resistance against radioactive radiation.

Polymer name	Humidity absorption [%]	Ultra-violate stability	Geometry stability	Young's modulus [MPa]	Melting temperature [°C]	Operating temperature [°C]	Friction	Wear
Acrylonitrile butadiene styrene (ABS)	0.30	Moderate	Satisfying	2400		-40 to +80	Moderate	Moderate
Polyamide 6 (PA 6)	3	Satisfying	Moderate	3200	220	-40 to +85	Satisfying	Satisfying
Polycarbonate (PC)	0.20	Satisfying	Satisfying	2300		-40 to +115	Moderate	Moderate
Polyethylene (PE)		Bad	Bad	900			Satisfying	Moderate
Polyetheretherketone (PEEK)	0.20	Satisfying	Good	4000	343	-60 to +250	Good	Good
Polyetherimide (PEI)	0.50	Satisfying	Good	3100		-50 to +170	Moderate	Moderate
Polyethersulfone (PES)	0.70	Satisfying	Good	2700		-50 to +180	Moderate	Moderate
Polyethylene terephthalate (PET)	0.25	Good	Good	3000	255	-20 to +115	Satisfying	Satisfying
Polyimide (PI)	1.30			3200		-200 to +300		
Polyoxymethylene (POM)	0.20	Moderate	Satisfying	2800	165	-50 to +100	Satisfying	Good
Polypropylene (PP)		Bad	Moderate	1400		0 to +100	Satisfying	Moderate
Polyphenylene sulfide (PPS)	0.02	Satisfying	Good	4150	285	-20 to +220	Satisfying	Satisfying
Polysulfon (PSU)	0.20	Satisfying	Good	2600		-50 to +160	Moderate	Moderate
Polyvinylchloride (PVC)	1	Good		2700			Moderate	Bad
Polyvinylidene fluoride (PVDF)	0.04	Very good	Moderate	2100	178	-30 to +140	Moderate	Moderate

Table 1-8: Polymer overview [45]

1.3.4.2 Synthetic gear wheels in general

Polymer-based materials have unique properties like low density, elasticity, or high strength per unit mass. They have high corrosion resistance in various environments and they are easy to machine. Furthermore, synthetics are usable over a wide temperature range, but some have a high coefficient of thermal expansion. Many different synthetic materials are available nowadays. Not all are suitable for the application in gear wheels. In general, thermoplastics like Polyamides (PA) or PEEK are appropriate materials for gears, as well as Polyimides (PI). They have properties which are highly desirable for gear wheel application [46]:

- Maintenance free
- High wear resistance when used in a dry-running application
- Low noise
- Vibration damping
- Corrosion resistance
- Low mass moment of inertia through low weight
- Cost-effective manufacturing

Table 1-9 gives a more detailed overview of materials which are recommended for gear wheels [47].

Material	Production mark
Polyamide	Various
Polyamide 66	Various
Polyamide 12	Vestamind (among others)
Polyoxymethylen (POM)	Delrin, Duracon (among others)
Polyimide	Kapton, Vespel, Kinel
Polyether ether ketone (PEEK)	Victrex

Table 1-9: Gear wheel material recommendations

Also [48] studied the application of synthetic materials for gear wheels. They point out the advantages of thermoplastics as gear wheel material: dry-running application, damping, corrosion resistance, low weight and low inertial mass, and good machinability. As possible materials polyamide 6, 66, and polyoxymethylene (POM) are suggested. Polyamide 6 (PA 6) is an all-round material for gear wheels in engineering. It is wear resistant but due to its tendency to absorb moisture it is less suitable for high precision wheels. Polyamide 66 (PA 66) has higher strength and stiffness compared to PA 6. It has better wear performance and

less moisture absorption. Polyoxymethylene (POM) has even higher strength and stiffness than PA 66. It has good wear behavior, almost no water absorption, and high mechanical strength. Also the load carrying capacity is better compared to polyamide. Consequently POM is applied as material for small-sized gear wheels in clocks, as well as in highly stressed applications. Additives like glass fiber increase strength and Young's modulus of PA and POM. With adding graphite or molybdenum disulfide strength and stiffness can be increased however toughness decreases.

Polymer gears are already used in various industrial applications. For example in automotive application, Metaldyne is building balance shafts and replaced the metallic gears with VICTREX® PEEK polymer gears. Using the polymer gear solution, the moment of inertia is reduced by 70% compared with metallic gears and consequently, the power consumption is reduced by 3% to 9%. VICTREX® PEEK polymers provide the material properties required for that particular application, withstanding temperatures up to 155°C at high fatigue strength, and good chemical resistance. Italian based company Saroblast integrated polymer gears in their harvesting tools. After metal parts had failed, Saroblast chose to use PEEK gears due to their superior wear and temperature properties. Furthermore the synthetic components helped to reduce mass, lowering power consumption and noise emissions.

Also another article [49] describes the application of PEEK gear wheels in the automotive industry. The present development in car industry towards weight reduction, increasing efficiency, and miniaturization leads to higher loads and higher operating temperatures. For this reason PEEK is getting more and more popular as material for these applications because it survives temperatures of more than 100°C. For example for electric seat adjustment synthetic gear wheels are used pretty often because of its low noise level. But after preliminary crash-tests, it was discovered that only PEEK gear wheels survive the high loads during a crash and allow an adjustment of the seat afterwards.

But beside the mentioned advantages, possible defects can result in the loss of the functioning capacity of the polymer gear. These are [47]:

- Broken tooth at the base
- Cracks on the working side of the tooth surface
- Tooth breaking in the gearing pole zone
- Bending of the tooth due to the material plastic flow
- Appearance of pitting on the lateral surface of teeth
- Wear

For PEEK gear wheels especially wear is together with root and flank failures the main failure parameters in dry-running applications.

1.3.4.3 Synthetic materials in space application

Synthetic materials are already used in spaceflight applications due to their advantageous properties. The low density of polymers reduces mass and the moment of inertia which often results in power savings. Furthermore, synthetics have almost no problems with corrosion which is an advantage during ground testing and launch preparation. Even in dry-running applications, polymers provide high wear resistance without lubrication. This results in easier handling and additional mass savings, as lubricant casings are not required. Polymers consist mainly of carbon-based molecules and have a high molecular weight, resulting in advantageous properties such as strength, resilience, high melting points, ability to be molded, or electric resistance [50].

Polymers have a wide range of application in spaceflight. They are used, for example, in circuit boards, temperature regulating blankets, lubricants, coatings, electric insulation, and high stiffness components. Polymers can be easily modified by the addition of other materials and consequently they can be adjusted for a certain application which makes them flexible usable in spaceflight. For example with the addition of MoS_2 the wear properties can be improved. This modification is used in gear and bearing design. But to be used successfully in space applications all polymers have to fulfill certain requirements (Table 1-10, [50]):

Capability to function in hard vacuum
Very low outgassing to prevent contamination of surrounding components
Resistance to extremely harsh ultraviolet light
Resistance to on-orbit charged particle radiation
Resistance to erosion from atomic oxygen
Endurance over wide temperature extremes
Ability to survive the life of the mission

Table 1-10: Requirements on polymers for space application

If the polymer material is used inside the spacecraft, requirements like resistance to UV light or erosion from atomic oxygen can be neglected.
Synthetic materials are for example used in thermal blankets. Thermal blankets are used to regulate the temperature of satellites. The blankets consist of a polymer film and many layers of these films build up the Multi-Layer-Insulation (MLI). The films usually are based on Mylar® (polyethylene terephthalate) or on Kapton® (polyimide) from DuPont Company. The layers are separated by fine scrim cloths made from Nylon® polymers. Polymers are also the standard material for wire insulation. Teflon therefore is used quite often due to its

chemical inertness. But is suffers from poor radiation stability. For high radiation application like RTGs or Jupiter orbiters, polymers of vinylidene fluoride (PVDF) has been developed for cable insulation [50].

Due to the positive performance of polymers regarding mass, wear, and corrosion, the material is also often used in space mechanisms. For the antenna pointing mechanism of the OFFEQ experimental satellite, Duroid is used as ball bearings toroid rings [5]. A mechanism designed for deployment and fine pointing of L-Ka antennas [32] uses parts made of Vespel as coupling between a lead screw body and its supporting case. The reason to choose Vespel was its low friction coefficient. In the same mechanism Teflon was used for the internal insert of the lead screw which is kinematic coupled with the steel gear screw. But due to wear, this coupling generated Teflon particles which could pollute sensitive components of the mechanism. Furthermore Duroid (PTFE, MoS2, glass fiber composites) is used for bearing cages.

Also the Rosetta mission, whose goal is to land on the nucleus of a comet, uses synthetic material. To minimize friction, the plain bearings, which are integrated in the Lander Anchoring System, are made out of Vespel. The polymer has to withstand temperatures between -160°C and -190°C for ten years. Vespel SP1 is also integrated in the lock and release mechanism for a Russian Phobos sample return mission [51]. An important device for the mission is the hammer-driven penetrator which is developed by the Space Research Center of the Polish Academy of Sciences (PAS). To lock and stow the penetrator, a lock and release mechanism was developed. The operating conditions are -100°C for ten years. As mating part materials for slide bearings titanium alloy with titanium nitride layer and polyimide-based Vespel SP1 were chosen. Vespel is used for bushings, sliders, and guides. This solution has been used in many other mechanisms built by PAS and is the result of experience and testing. During the testing, the coefficient of friction for the Vespel–Titanium combination was determined. The tests were conducted in an environment with 10^{-4} mbar, the load was 50 N, the sliding speed was 0.1 m/s, and the contact area was 10 mm². At room temperature as well as at -80°C the coefficient of friction was around 0.22. The tests showed that Vespel SP1 and titanium alloy are suitable mating materials for low temperature application. BepiColombo, the ESA mission to Mercury, integrated bushings and holders made out of Vespel in its High Temperature Antenna Pointing Mechanisms for Ka-band and X-band communication [4].
One part of the deployment mechanism of the Cubesat Xatcobeo [52] is built from a polymer. In a first design polyamide 6 was chosen as material and Selective Laser Sintering (SLS) as the manufacturing method. But during the development process it was decided to use polyamide 12 with fiberglass reinforcement. The reasons for that decision were that PA 12 is 10% lighter than PA 6, it absorbs less water, and the manufacturing of PA 12 using SLS is more precise. But according to [8] polyamides are unsuitable for use in vacuum.

Delrin, which is the tradename for Polyoxymethylene (POM), is frequently applied in spaceflight. In an antenna pointing mechanism, for example, a Delrin spur gear is used in combination with a worm gear. The Delrin gear was chosen to operate the system without lubrication. The counterpart of the Delrin gear is a stainless-steel worm gear [7]. In a low cost release mechanism built by [53] sleeves, guides, and strips are made out of Delrin. Also the Oscillation Mitigation System for the CEV Crew Pallet System used Delrin as material for pad stops, tube bushings, and dampers.

PEEK has been used as material in several recent spaceflight missions: For the ESA Rosetta comet mission, the MIDAS experiment built to collect dust particles, employed a PEEK plate, in which a conical pin is inserted [54]. [55] designed a high performance parallel antenna pointing mechanism for future optical, very high resolution, satellite missions. A radome, made out of PEEK material, protects the source of the antenna. In a work presented by [56] novel deployable booms were developed to deploy a gossamer sail. For the boom deployment system PEEK spindle bushings are used to facilitate the deployment at extreme temperatures. For linear guides, rails made out of PEEK provide low friction. PEEK was also chosen as material for a nut in the sample container separation mechanism used in the CHOMIK sampling device for the Phobos-Grunt mission [57]. The nut was required to lock the container against rotation.

The tribological behavior of PEEK composites in vacuum environment were studied with friction tests [58]. The friction tests were carried out with PEEK filled with solid lubricants against 304 stainless steel, in vacuum and at a temperature range from -40°C to +160°C. In general, the performance of PEEK can be improved with the addition of fillers and fibers like carbon fibers, PTFE, and graphite. In the above mentioned work, PEEK composites were filled with 10 vol.% carbon fibers, 10 vol.% PTFE, and 10 vol.% MoS2. The results of the test show, at 1 MPa contact pressure, a significantly decrease of friction and wear rate of the PEEK composite in vacuum when compared to ambient air. The PEEK composite also shows a temperature dependency. The friction coefficient increases continuously from -40°C to +160°C. The lower friction at low temperature can be explained with the behavior of MoS_2. At low temperature the polymer is harder and the deformation of the polymer decreases. A higher hardness produces higher contact pressure. The performance of MoS_2 improves at higher contact pressure and this results in a lower friction coefficient at lower temperatures (here -40°C).

In [10] the influence of solid lubricant fillers on the tribological behaviour of PEEK composites was studied. Possible fillers for PEEK are carbon fibers, PTFE, and graphite, or MoS_2. Some percent of PTFE improves the tribological properties although it has the tendency to cold flow. Graphite does not provide lubrication in vacuum because a certain amount of water is necessary for graphite lubrication. MoS_2 is widely used as solid lubricant in vacuum environments.

The tests performed by [10] are particular applicable to this study, because the boundary conditions are quite similar. Friction and wear are the measured parameters, vacuum is the test environment in both cases, and the temperature range is comparable. -80°C to +20 °C in [10] compared to our range of -40°C to +80°C. Also, the involved materials are the same: PEEK against steel. However, [10] used a PEEK pin as test device and not a gear wheel, and the PEEK was not in a natural state, but filled with graphite and MoS_2. Quite similar in both studies is the contact pressure (1 to 7 MPa vs. 3 MPa) as well as the sliding mode (continuous). At +20°C, the results show a wear rate of about $1 \cdot 10^{-6}$ mm³/(N·m) at 1 MPa contact pressure, and $1 \cdot 10^{-7}$ mm³/(N·m) to $3 \cdot 10^{-7}$ mm³/(N·m) at 7 MPa. In that case it does not have to be distinguished between natural PEEK and modified PEEK because above room temperature, the influence of solid lubricant is not significant. But, with decreasing temperature, the different PEEK compositions show a different behavior. Especially at low temperatures, PEEK with MoS_2 added showed better friction and wear performance when compared to PEEK added with graphite. The reason for that is a thin polymer transfer film on the counterface, with a higher concentration of MoS_2 at the surface of the composite.

The biggest challenge for polymers in space is the vacuum environment. The lack of atmospheric pressure results in outgassing of the polymers and subsequent mass loss, changing the polymer's properties and potentially contaminating sensible surfaces such as mirrors or optical surfaces. Consequently, only synthetic materials with low outgassing rates and excellent vacuum properties can be considered for spaceflight applications. A study by [59] compared PEEK and Vespel SP 1 as vacuum seals for fusion application. Vespel SP1 was used as insulation material for seals at pressures between 10^{-8} and 10^{-9} mbar and at temperatures up to 400°C. Due to the higher cost of Vespel, PEEK was considered as an alternative for ultra-high vacuum applications. Both materials also have good mechanical characteristics at high temperatures. A mass loss can be observed for both PEEK and Vespel when heated up to 150 °C and left at that temperature for one hour: PEEK loses 0.17% of its mass, Vespel SP1 0.99%. Additional tests showed that VESPEL SP1 has an outgassing rate two times higher compared to PEEK. The main advantage of PEEK is the lower cost (15 times less than Vespel).

Since low outgassing is one of the main requirements for polymers in space, Table 1-11 shows outgassing properties of synthetic materials [12].

Material tradename	**Polymer family**	**TML [%]**	**CVCM [%]**
Crossflon	PTFE	0.04	0.01
Fluon	PTFE	0.00	0.00
Hostaflon	PTFE	0.05	0.01

Lubriflon	PTFE	0.04	0.00
Armallon	PTFE / glass fiber	0.48	0.02
Duroid	PTFE / glass fiber	0.22 – 0.25	0.00 – 0.02
Delrin	POM	0.35	0.01
Kematal	POM	0.37	0.01
Hostalen	UHMWPE	0.42	0.03
Maranyl	PA	0.93 – 1.56	0.01 – 0.02
Nylartron	PA	0.53 – 2.19	0.00 – 0.02
Rislan	PA	0.91 – 8.70	0.00 – 0.05
Zytal	PA	2.26 – 2.68	0.01 – 0.02
Turlon	PAI (Polyamidimid)	2.51	0.01
Vespel SP 1	PI	0.95 – 1.58	0.00 – 0.01
Vespel SP 3	PI	1.13 – 1.16	0.00
Victrex	PEEK	0.20 – 0.31	0.00
ESA Requirement		< 1	< 0.01

Table 1-11: Synthetic materials outgassing properties [12]

The accepted limits for outgassing are defined by ESA's ECSS-Q-70-02A standard. They require a total mass loss (TML) of less than 1% and a collected volatile condensed material (CVCM) of less than 0.01% (for a component mass larger than 10 grams). In particular, PTFE, POM, and PEEK fulfill these requirements. PI and UHMWPE are close at the limit whereas PA in general does not fulfill the outgassing requirements.

Another work [60] studied the vacuum compatability of 3D-printed materials. 3D printed materials have the advantage of very easy fabrication of complex geometries. But since 3D printing is an additive process it is possible that there are small holes in the material where gas could be trapped and released later to the vacuum. So it is very interesting how these materials perform in a vacuum environment. To test the outgassing properties of different materials a waveguide was printed by Shapeways using an EOS printer with using the selective laser sintering (SLS) method. The outgassing test was conducted with a pressure of $1.2 \cdot 10^{-8}$ mbar. The results showed that Polyamide had an outgassing rate of about 3×10^{-8} to $4 \cdot 10^{-7}$ mbar·L/(cm²), which is comparable to Teflon and Viton materials. Consequently the conclusion of the test was that polyamide could be used sparingly in vacuum similar to Teflon and Viton.

1.3.5 Synthetic gear wheels in space / vacuum environment

The „Space Tribology Handbook“ [8] evaluates different synthetic materials regarding their application in space and as tribo-components. Table 1-12 gives an overview of commonly used polymers in space.

Polymer	**Tradenames**
PTFE	Teflon, Fluon, Hostaflon
PTFE / glass fiber	Duroid, Rulon, Armallon
Polyamides	Maranyl, Rislan, Zytal (*)
Polyimide	Vespel SP1, Kinel
Polyimide / MoS2	Vespel SP3
PEEK	Victrex
POM	Delrin, Kematal
HD polyethylene	Rigidex
UHMWPE	Hostalen, GUR

* all unsuitable for use in vacuum

Table 1-12: Commonly used polymers in space

The tribological behavior of PTFE is unaffected by vacuum consequently it also has good tribological performance in space. But in unfilled condition it shows poor mechanical properties. That is why PTFE is often used in combination with a filler. Polyamides have bad vacuum properties and should not be used in space. POM is widely applied for low precision gears in spacecraft mechanisms. HD polyethylene / UHMPWE are ultra-high molecular weight polyethylenes and are also often used for low precision gears in spacecraft mechanisms.

For the application as tribological components in spaceflight four polymers are recommended by [8]:

- Polyoxymethylene / Polyacetal (POM)
- Polytetrafluoroethylene (PTFE)
- Polyimide (PI)
- Polyether ether ketone (PEEK)

These materials provide low outgassing, high strength, and corrosion resistance. Consequently they are also interesting candidates for the application as gear wheel

material. Most common polymers employed as spacecraft gears are Vespel SP3, Duroid 5813, and polyacetal because of their proven flight application. But regarding vacuum performance PEEK (TML=0.20 to 0.31) has better outgassing properties than Vespel SP1 or SP3 (TML=0.95 to 1.58).

In a gearing system a synthetic–metallic gear combination is recommended because polymers in contact with metallic counter faces have good lubricity due to the effective transfer film formation in dry sliding. Surface engineering is not applicable for polymers and polymer composites. Glass fiber is not suitable as a solid filler as it is harder than many metals and may increase the abrasive wear. Graphitic fibers have poor tribological properties in vacuum.

Information about the behavior of gear wheels in the space environment can rarely be found in literature. In tests conducted by ESA [8] it is specified that adhesive wear, which is the most fundamental wear mechanism in dry sliding contact, is promoted by vacuum. Furthermore wear rate tests with synthetic gear wheels show large differences of specific wear rate of the polymers when tested in air compared to tests in vacuum. In some cases the wear rate increased in others it decreased. Some polymers also showed a dependency on temperature (+60°C compared to -30°C). A POM (Delrin) spur gear is integrated in an antenna pointing mechanism designed by [7]. The dry-running property of Delrin was the reason for its application. But altogether publications about synthetic gear wheels in space environment are pretty rare in literature.

1.4 Gap Analysis

As a result from the state of the art research, several knowledge gaps are identified as described below which then lead to the objectives for this work as outlined in chapter 1.5.

No experimental data could be found in the literature regarding the performance of synthetic gear wheels in the harsh spaceflight environment. This lack of information may be a reason why the application of synthetic gear wheels often is avoided and the traditional metallic wheels are used instead. However, for Earth applications, gear wheels are often made out of polymers, which have many advantages like low mass and low moment of inertia, low noise, corrosion resistance, or vibration damping. Furthermore, polymers have a high wear resistance even when used in a dry-running applications where no lubricant is applied. Some of these advantages would be very desirable in space application: mass saving is always desired in spaceflight applications, since more mass means higher launch costs. With a lower moment of inertia, power can be saved and be used elsewhere. The ability of some polymers to be run without lubrication, to prevent corrosion, and to decrease micro-vibration is also of interest to spaceflight applications.

Criteria for excluding polymers from space applications include low strength, outgassing, or a high coefficient of thermal expansion. But with the development of novel high-performance polymers in the last decades, these concerns can now be addressed. High quality synthetic components are already used in the automotive, medical, and aerospace industries. Spacecraft applications could also benefit from these high performance polymers because some examples combine the advantages of synthetics like dry-running ability or vibration reduction with the requirements for space missions, such as vacuum compatibility. In some applications, polymers are already used in spaceflight. Examples include wire insulation, bearing rings, sliders or guides (chapter 1.3.4).

Recent spacecraft are facing more and more demanding performance requirements for higher accuracy mechanisms: pointing mechanisms, for example, must achieve accuracies better than 0.1°, have to avoid micro-vibration, and be able to maintain their performance characteristics over many years without servicing while operating under extreme environmental conditions. Components which significantly influence the performance of a mechanism are the gear wheels (chapter 1.3.2), which are traditionally made out of stainless steel because of its high strength and well known behavior under spaceflight conditions. But steel also has its drawbacks like the need for lubrication, the potential for introducing micro-vibrations, backlash, or corrosion. With synthetic gear wheels, some of these concerns could be avoided. Synthetics can be used without lubrication, reducing inaccuracies through tighter tolerances in the system, simplifies integration, and makes heavy seals or oil reservoirs (chapter 1.3.4) unnecessary. With that the mechanism system gets simpler, more accurate, and more robust. The corrosion resistance of synthetic wheels

would simplify ground testing and storage of components. A decrease of micro-vibrations is especially interesting for missions which require very smooth running of the mechanism to avoid perturbations.

Consequently, synthetic gear wheels might be an interesting alternative in order to advance performance capabilities of space mechanisms. But in order to be integrated in a space mechanism, synthetic gear wheels have to proof their performance in relevant space-similar environment. As mentioned at the beginning of this chapter, published experimental data are pretty rare about that topic. One can therefore conclude that it is important to systematically study the performance of synthetic gear wheels in simulated spaceflight environments. This leads to questions like: Which polymers can generally be considered for gear wheel application in space? What influence does vacuum and extreme temperatures have on wear and strength? How does backlash of a gearing system change in orbit? Are temperature limits of the polymer reached during operation? Or does the space environment have no influence at all? And how can the in-orbit performance of a synthetic gear wheel be tested on Earth?

1.5 Thesis Objective

The questions stated at the end of the last chapter can be summarized to one overarching research question:

Research questions:

How does the spaceflight environment influence the performance of PEEK and POM gear wheels as selected representatives of high performance synthetic materials, and do the wheels made of PEEK and POM fulfill the requirements for space mechanisms?

These research questions lead to the objective of the thesis:

Thesis objective:

The goal of this doctoral thesis is to evaluate the behavior of PEEK and POM gear wheels in a simulated spaceflight environment and their applicability in space mechanisms.

The general thesis objective can be divided into several sub-objectives:

(1) Study of space mechanism requirements as applicable for gear wheels.
In order to decide whether synthetic gear wheels are suitable for the application in space mechanisms, the requirements on gear wheels coming from different mechanisms have to be evaluated. Depending on the type of mechanism, these requirements may be different and a gear wheel which might be suitable for a deployment mechanism may fail when used in a pointing mechanism.

(2) Preselecting promising polymers for space and gear wheel application.
Possible polymers have to fulfill the requirements which come from the space environment as well as the requirements coming from the application as gear wheels. Concerning the space environment, the synthetic material has to be compatible with vacuum, extreme temperatures, and space radiation. The demands for the gear wheel application are sufficient strength, low friction, and low wear rate. So one goal of the thesis is to find synthetic materials which combine these characteristics. The characterization tests will then be performed with the promising candidates.

(3) Wear characterization of PEEK and POM gear wheels in a simulated space environment.

Development of a test method to study the wear of the gear wheels under relevant spaceflight environments: Most gear wheel test rigs that already exist are not meant to be used in vacuum conditions and at very low and high temperatures. Therefore, a new test method and test setup has to be developed to conduct the wear tests in simulated spaceflight environments.

Determine the wear of the gear wheels in spaceflight environment: With the novel built test rig, the tests have to be conducted in order to determine the wear coefficient of the different materials.

(4) Strength characterization of PEEK and POM gear wheels in a simulated space environment.

Development of a test method to study the influence of the spaceflight environment on the strength of the gear wheels: In order to make a statement about the influence of the spaceflight environment on the strength of gear wheels, a test method has to be developed.

Determine the strength of the gear wheels as a function of simulated spaceflight environments: With the developed test method, the tests have to be conducted in order to determine the strength of the different materials.

(5) Characterization of the environmental impact on the geometry of PEEK and POM gear wheels.

Development of a test method to study the influence of the spaceflight environment on the geometry of the gear wheels: In order to make a statement about the influence of the spaceflight environment on the geometry of gear wheels, a test method has to be developed.

Determine the geometry change of the gear wheels as a function of the simulated spaceflight environment: With the developed test method, the tests have to be conducted in order to determine environmental impacts on the geometry of the gear wheels.

(6) Temperature characterization of PEEK and POM gear wheels in a simulated space environment.

Development of a test method to study the influence of the spaceflight environment on the temperature of the gear wheels during operation: A new test method and test setup has to be developed to conduct the temperature tests in a simulated spaceflight environment.

Determine the temperature of the gear wheels during operation as a function of the simulated spaceflight environment: With the developed test method, the tests have to be conducted in order to determine the temperature of the gear wheels during operation.

(7) Evaluation of the applicability of PEEK and POM gear wheels in space mechanisms.

After all the tests and after evaluating the results, the performance of the gear wheels has to be brought in context with the requirements for the mechanism, and the appropriate applications for which synthetic gear wheels can be used have to be identified.

2 Test preparations

2.1 Test Overview

The goal of this thesis is to evaluate synthetic gear wheels in space simulated environment. In order to evaluate a gear wheel, the load-carrying capacity has to be considered, which, for synthetic gear wheels, is characterized by the following parameters [37]:

- Tooth root carrying capacity
- Tooth flank carrying capacity / Pitting
- Wear
- Partial melting

Beside the load-carrying capacity, typically different performance parameters are chosen to describe the behavior of gear wheels [61]:

- Gear tooth quality
- Temperature and humidity caused geometry change
- Critical temperature
- Deformation of teeth
- Power loss
- Dynamic pressure

Tooth root carrying capacity
The tooth root carrying capacity considers the bending stress at the tooth root as a result from the tangential force at the tooth flank [34]. For synthetic gear wheels failure due to insufficient tooth root carrying capacity is one of the most important failure modes [61]. Also [48] describes tooth root damage as one of the main failure modes of polymer gear wheels. Consequently testing the tooth root carrying capacity as a function of the test environment is one of the main tests conducted in the context of this work.

Tooth flank carrying capacity / Pitting
The flank of a synthetic tooth can be damaged by either wear or pitting [62]. The wear behavior is described later. Pitting mainly occurs in wet-lubricated gearing systems [61], not applicable in spaceflight applications, and therefore not considered in this study.

Wear

According to DIN 50320, wear is defined as a continuous loss of material from the surface of a solid body. Wear is generated by contact and relative motion of a solid, liquid, or gaseous counterpart and can be categorized as adhesion, abrasion, and fatigue. For steel gear wheels, assuming a correct lubrication, wear has only in exceptional cases been considered as a lifetime limiting factor [34]. For polymeric materials however, wear is a significant factor in the calculation of load-carrying capacity [63]. Negative consequences of wear include a decrease in tooth thickness resulting in an increase in circumferential backlash. Various approaches for calculating the wear of synthetic gear wheels can be found in literature, however according to [61] the results obtained through different methods are inconsistent with each other. Consequently the wear coefficient has to be determined experimentally for each new material combination and application. And thus, measuring the wear of the polymer gear wheels is another major test run in this thesis.

Partial melting

Although partial melting happens especially in dry-running operation it is not considered here because the operating speed is too low. Partial melting only occurs at circumference velocities of more than 5 m/s [64], and is therefore not relevant here due to the much lower velocities (0.1 m/s) in our pointing mechanism study.

Gear tooth quality

The gear tooth quality depends on the manufacturer and the machine that is used. Typically the quality of metallic wheels cannot be achieved by synthetic gear wheels. The gear tooth quality is tested during this work in order to increase reliability and reproducibility of the results.

Temperature and humidity caused geometry changes (Backlash)

Compared to metallic components, polymers have significantly larger coefficients of thermal expansion and a quite relevant absorption of humidity. These two effects cause a change in geometry of the wheels which occurs especially in space environment (vacuum and large temperature change). A change in geometry directly leads to a change in backlash of the gear train. And since a changing backlash is crucial in space mechanisms the temperature and humidity caused geometry changes is also tested in this thesis.

Critical temperature

The properties (in particular) of synthetic materials is dependent on the temperature and also the maximum operational temperature of synthetic materials is limited. Consequently, the temperature is a key parameter in the design of gear wheels made out of polymers. Therefore not only the ambient temperature has to be considered but also the temperature which results from the operation of the component. Because friction and damping may result in an increase of the temperature. Often it is not necessary to calculate the temperature of

the wheel in all detail but knowing the core temperature and the surface temperature of the wheels is highly recommended. The core temperature influences the fail by rupture and deformation. The surface temperature has an impact on surface failures (e.g. wear) [63]. Consequently measuring the temperature in the tooth of a gear wheel is recommended and the tests are conducted in this work. Especially because the vacuum and extreme temperature environment might influence the wheel temperature as well.

Deformation of teeth

Due to the lower Young's modulus of synthetic materials, the deformation of teeth has to be taken into account. In the context of this work a calculation will consider the influence of the deformation. Thus, no separate test will be conducted.

Power losses

Power losses or efficiency is another parameter for the characterization of gear wheels. It is mainly important in high-velocity and high-performance applications. In this thesis power losses are not considered for various reasons: space mechanisms typically are machines with lower velocities and lower loads with a high margin. Consequently little variations in power or efficiency do not make such a big impact. Furthermore power losses are the results of wear and temperature increase [61]. And since wear and temperature is extensively tested in separate tests, conclusions about the power losses can be drawn from these measurements. Finally, the test setup to measure power losses is quite complex, especially when the test rig has to be designed for a test series under thermal vacuum conditions. Thus, it was decided not to test power losses separately.

Dynamic performance

Due to the damping properties of synthetic materials, dynamic performance is not considered in VDI 2736 (characterization of synthetic gear wheels) [37] and consequently it is not considered in this work.

An overview of all performance parameters and whether they are tested, calculated, or not considered at all is given in Table 2-1.

Performance Parameter	Test	Calc.	Not cons.
Tooth root carrying capacity	X		
Tooth flank carrying capacity / Pitting			X
Wear	X		
Partial melting			X
Gear tooth quality	X		
Temperature and humidity caused geometry changes	X		
Critical temperature	X		
Deformation of teeth		X	
Power losses			X
Dynamic performance			X

Table 2-1: Performance parameter test overview

2.2 Test devices

2.2.1 30 mm Pinion

For all but one tests, the test device is a pinion with standard spur gearing. For the other test, the tooth root carrying capacity test, another wheel has to be used which is described in section 2.2.2. There have been various reasons to choose that type of gearing. First, the chosen geometry of the gear wheel corresponds to a pinion which is used for an antenna pointing mechanism being developed at the Institute for Astronautics [65]. Thus, it is possible to apply the test device in a later design of the mechanism if testing is successful. Furthermore, this thesis shall provide a basis for further investigations and therefore it was decided to start here with standard gearing with standard geometry. In a next step other types of gear wheels could be tested. And finally, compared with metallic gear wheels, the increase of carrying capacity reached with helical gearing is rather small [48]. A face width of 6 mm was chosen for the pinion. Because the face width should be six to eight times the module [48].

All pinions required for the tests were milled at the same company to ensure equal manufacturing processes and reproducibility of the tests. A summary of the pinion's main manufacturing parameters can be seen in Table 2-2.

Pinion Manufacturing Data			
Manufacturer	GEWO Feinmechanik GmbH		
Manufacturing type	Milling with profile cutter		
Gear type	Straight toothing		
Module	m	mm	1
Number of teeth	z	-	30
Normal pressure angle	α	°	20
Tooth thickness	b	mm	6
Addendum modification coefficient	x	-	0
Helix angle	β	°	0

Table 2-2: Pinion manufacturing data

Pinion parameter	**Symbol**	**Unit**	**Value**
Reference diameter	d	mm	30
Tip circle diameter	d_a	mm	32
Root diameter	d_f	mm	28
Base circle diameter	d_b	mm	28.19
Tooth depth	h	mm	2.25
Circular pitch	p	mm	π
Base circle pitch	p_b	mm	2.95
Normal base pitch	p_e	mm	2.95
Transverse normal base angle	α_t	°	20

Table 2-3: Pinion gearing parameters

With the equations from chapter 1.3.2, the other relevant gearing parameters for the pinion can be calculated and are summarized in Table 2-3.

Due to possible geometry changes of the pinion as a result of thermal expansion, it is recommended to use a form-locking connection to fix the pinion on the shaft [48]. In our case a special bore hole geometry was designed for mounting the pinion gear on the shaft (Figure 2-1), to assure a fixation without backlash and to avoid drilling or screwing into the polymer.

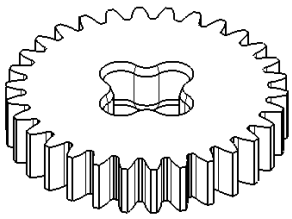

Figure 2-1: Pinion wheel with backlash free mounting interface according to own design

2.2.2 120mm Pulsator Test Wheel

For testing the synthetic gear wheels regarding tooth root load carrying capacity, the 30 mm pinion cannot be used. This has two reasons. First, in order to study the tooth root load carrying capacity of gear wheels, pulsator tests have to be conducted. Therefore a test rig ("Pulsator") at the Institute of Machine Elements is used and 30 mm pinions are too small to be tested. And second, there exists a standard gear wheel size with which the Institute of Machine Elements conducts all its tests. Therefore it is wise to use the standard gear wheel parameters for our tests as well, in order to make comparison of the test results easier. These parameters, from which the wheels are manufactured are summarized in

Table 2-4 and all the relevant calculated parameters are shown in Table 2-5.

Pulsator Test Wheel Manufacturing Data			
Manufacturer	Ilmberger GmbH		
Manufacturing type	Milling with profile cutter		
Gear type	Straight toothing		
Module	m	mm	5
Number of teeth	z	-	24
Normal pressure angle	α	°	20
Tooth thickness	b	mm	30
Addendum modification coefficient	x	-	0.48
Helix angle	β	°	0

Table 2-4: Pulsator test wheel manufacturing data

Gear wheel parameter	Symbol	Unit	Value
Reference diameter	d	mm	120
Tip circle diameter	d_a	mm	130
Root diameter	d_f	mm	110
Base circle diameter	d_b	mm	112.76
Tooth depth	h	mm	11.25
Circular pitch	p	mm	15.71
Base circle pitch	p_b	mm	14.76
Normal base pitch	p_e	mm	14.76
Transverse normal base angle	α_t	°	20

Table 2-5: Pulsator test wheel gearing parameters

2.3 Pinion material selection

Polymers used for pinions applied in space mechanisms have to fulfill the requirements coming from tribology and from space environment. From a tribological point of view, generally only technical and high-performance polymers are possible materials for gear wheels. Standard polymers like Polyethylene (PE) or Polyvinylchloride (PVC) do not provide well enough mechanical properties for high accuracy applications. Whereas technical polymers like Polyamide (PA) or Polyoxymethylene (POM) and high-performance polymers like Polyimide (PI) or Polyetheretherketone (PEEK) are characterized by excellent mechanical and thermal properties. In [47] PA, POM, PI, and PEEK are also recommended as materials for gear wheels. The reasons therefore are the low humidity absorption, large Young's modulus, low coefficient of thermal expansion, and good wear behavior of the mentioned materials.

Considering the requirements coming from the space environment, especially the outgassing properties of materials have to be taken into account. Large outgassing rates mean a change in property of the chosen materials or a possible contamination of sensitive components integrated in the spacecraft like optics or mirrors. The European Space Agency (ESA) characterizes the outgassing properties of materials with two factors: total mass loss (TML) and collected volatile condensed material (CVCM). Due to ESA standard ECSS-Q-70-02A a TML smaller than 1% and a CVCM smaller than 0.01% is required. POM and PEEK fulfill these requirements with TML in the range of 0.2 to 0.4% and a CVCM of less

than 0.01%. PI like Vespel is at the limit with TML varying between 0.95 and 1.58% (CVCM less than 0.01%). PA exceeds the TML requirement with values up to 8%.

Additional to PEEK, POM, and PI, [8] also recommends PTFE for the use in space. But in an unfilled state, PTFE does not provide well enough mechanical properties for the application as gear wheel. Generally with adding fillers to all the mentioned materials the properties could be improved. But it was decided to proceed with the materials which fulfill the tribological and environmental criteria already in their natural state.

Polyimides like Vespel are widely used materials in space [66] and also as gear wheels in Earth application, but they were excluded from our consideration because of two reasons: first, their outgassing rates are larger than those of PEEK and POM. And secondly, Vespel is very expensive and consequently an extensive test series would not have been possible with the budget available for this thesis. An own study was done by [59] to evaluate whether the expensive Vespel SP1 could be replaced by the cheaper PEEK as vacuum seals. The results show PEEK as an actual alternative.

Consequently, for this thesis, the polymers PEEK and POM were chosen as promising materials for pinions in space application. All the tests are conducted with these two materials. PEEK is used in its natural state without added fillers mainly because of its good vacuum, temperature, wear, and strength behavior. But furthermore PEEK is characterized by many other advantageous parameters [59]:

- good dimensional stability
- good handling in milling machines
- good dielectric strength
- retains tensile properties at temperatures of 250 °C
- very good creep resistance at higher temperatures
- excellent wear and abrasion resistance
- does not absorb water
- survives exposure to boiling water for 200 days

See Table 2-6 for detailed material properties of PEEK and POM.

Property	Unit	Value for PEEK	Value for POM
Density	g/cm³	1.32	1.41
Tensile strength	MPa	110	67
Young's modulus	MPa	4000	2800
Melting point	°C	343	165
Thermal conductivity	W/(m·K)	0.25	1.5
Coeff. of thermal expansion	$1/10^6$ K	50	110
min operation temperature	°C	-60	-50
max operation temperature	°C	+250	+100
Dimensional stability at heat	°C	152	110
TML	%	0.20 – 0.31	0.35 – 0.37
CVCM	%	0.00	0.01

Table 2-6: PEEK and POM material properties as used for the test pinion [45]

Also POM is used without any modifications. POM was chosen as less expensive alternative to PEEK with almost the same mechanical properties. The cost of POM is about $1/10^{th}$ the price of PEEK.

2.4 Test rigs

2.4.1 Wear Test Rig

The core setup of the wear testing is the back-to-back test rig, which rotates the pinion and generates the wear, which is measured using the gear tooth. The basic idea of the test rig is state of the art [67], [8] and several of these test stands are operated at our department. But nevertheless a new test rig had to be designed and built for our application because vacuum compatibility was required which is not fulfilled by the other rigs. The main requirements and characteristics of the test rig are summarized in Table 2-7.

Vacuum compatibility down to 10^{-5} mbar
Temperature compatibility from -55°C up to +80°C
Adjustable torque acting on the pinion
Constant torque acting on the pinion over half a million revolutions
Fit inside the LRT thermal vacuum chamber
Constant turning velocity of the pinion
Monitoring of torque acting on the pinion
Ability for long-term testing (emergency stops)
Testing of pinions with z = 30 and m = 1 mm

Table 2-7: Test rig requirements and characteristics

The basic principle of the test rig is a four-square arrangement with four gear wheels (Figure 2-2). The pinion under test (PUT) is one of the four gear wheels. An additional two wheels and one supporting pinion are required to close the circle. The 30 mm PUT has as counterpart one of the 120 mm wheels (see Table 2-8). This results in a gearing ratio of 1:4, and a nominal distance of axis of 75 mm. The test rig provides means to adjust the distance between the two axes from 70 mm to 85 mm. With that a small backlash can be set. Because regarding [48] a small backlash has to be provided between the gear wheels in order to allow thermal expansion. The required backlash can be calculated with equation (36).

$$S_E = 0.04 \cdot m + 2 \cdot l \cdot sin\alpha \cdot (\alpha_{th} \cdot \Delta\vartheta + \varepsilon_f) \qquad (36)$$

With l being the distance between the turning axis which is made out of polymer. In our case this value is 15 mm. α_{th} is the thermal expansion coefficient of the polymer, $\Delta\vartheta$ the temperature difference, and ε_f the humidity factor of the polymer. Since POM is the material with the larger thermal expansion coefficient compared to PEEK, the provided backlash is designed for POM. With α_{th} = $110 \cdot 10^{-6}$ 1/K, and ε_f = 0.0035 and a maximum thermal expansion of $\Delta\vartheta$ = 80 K, a backlash of 0.17 mm has to be provided. This value correlates very well with a statement in [8] where a backlash between 0.075 and 0.250 mm is recommended for center distances between 25 and 125 mm.

The counterpart of the pinion, the larger wheel, has a face width of 10mm to make sure the entire flank of the pinion is in contact with the flank of the wheel. The counter wheel is made out of steel because polymer-steel pairings provide the best life performance, good load carrying capacity, and advantageous heat transfer. Typically the pinion is made out of steel because it is exposed to higher loads [48]. In our case, it was decided to make the smaller pinion out of polymer to keep the thermal expansion of the gearing system as low as

possible. Furthermore the expected loads are rather small, consequently steel is not necessarily required for the pinion.

The gear preloading is applied by winding up the arrangement with a loading clutch. The loading clutch is a component which consists of two slightly elastic disks. Each disk is mounted on one of the wheel shafts and as soon as the two disks are screwed together the load path is closed. Before tightening the screws holding the two disks together, the disks are rotated against each other to generate the preload in the test rig arrangement. The load is measured with a measuring shaft which connects the shafts of the two pinions. The measuring shaft determines the preload by measuring the voltage of two strain gauges mounted on the surface of the shaft. The voltage can be converted to torque in newton meters on the shaft. Since the shaft with the stain gauges is turning during the testing the load can only be measured when the gear wheels are standing still. The torque is determined before, during, and after the test to detect any change or loss in torque during the tests. The testing is stopped once a day for a couple of minutes to verify the test load. The torque verification could only be conducted at ambient condition, as an interruption during the vacuum tests would require too much time. Pretests verified that the strain gauges work reliable under vacuum and thermal environments.

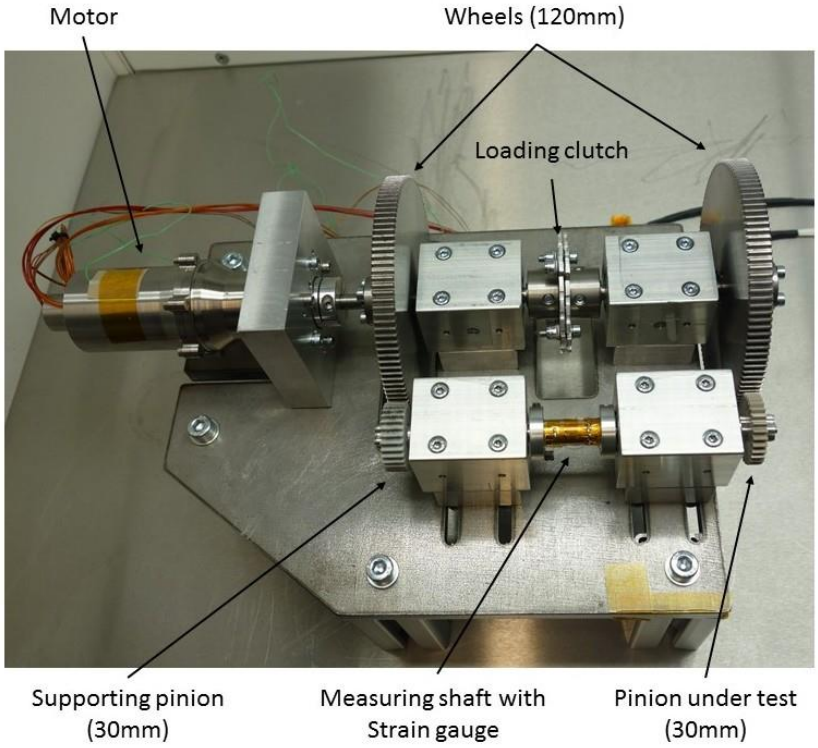

Figure 2-2: Test rig as designed for the wear tests

Counter Wheel Manufacturing Data			
Manufacturer	Maedler GmbH		
Manufacturing type	Stainless Steel 1.4305		
Gear type	Straight toothing		
Module	m	mm	1
Number of teeth	z	-	120
Normal pressure angle	α	°	20
Tooth thickness	b	mm	10
Addendum modification coefficient	x	-	0
Helix angle	β	°	0

Table 2-8: Counter wheel manufacturing data

The test rig (Figure 2-2) is driven by a Phytron stepper motor (Table 2-9). The stepper motor is connected to the shaft of one of the wheels with a bellows coupling. The stainless steel bellows coupling transmits the torque lossless while accommodating parallel and angular misalignment, as well as axial motion. The drive mechanism has a maximum velocity of 15 revolutions per minute (rpm) after the gear box. With a gear ratio of 1:4 for the pinion, this results into a turning velocity of 60 rpm for the pinion. The stepper motor is operated in a 64 microstep mode.

The stepper motor is equipped with a thermo-element to measure the winding temperature. Since exceeding the critical winding temperature of +180°C may destroy the motor it is monitored throughout the test. An automatic shut-down was implemented as soon as the winding temperature reaches a value larger than +150°C. Furthermore the temperature on the surface of the motor is monitored. The continuous monitoring of critical values and the automatic shut-down was implemented to allow unattended continuous long-term tests over several days. The test is also interrupted if the encoder on the end of the motor shaft no longer reports any rotation, which could be an indication of gear blockage by foreign objects or bearing failure.

The stepper motor is controlled by a Trinamic Motor Control Module, operated through a LabView™ program and a CompactRIO data acquisition and control unit by National Instruments. The program allows the control of motor velocity, motor power, maximum allowable motor winding temperature, and rotation direction. All data is also recorded.

Manufacturer	Phytron
Motor ID	VSS 42.200
Motor type	Stepper motor
Step number	200 per revolution
Working temperature	-40 °C to +80 °C
Max. winding temperature	+180 °C
Material	Stainless Steel 1.4305
Gear type	20:1 Planetary gear box
Bearing lubrication	Braycote 601
Gear lubrication	Maplub 101 A
Running torque	90 N·mm
Turning velocity after gear box	15 revs/min
Angular resolution on drive shaft	1.4 m°

Table 2-9: Properties of the Phytron stepper motor [68]

2.4.2 Pulsator

The Pulsator test rig (Figure 2-3) is run by the Institute of Machine Elements at the Technische Universität München and is provided us for the tooth root load carrying capacity tests. The Pulsator generally is used to determine static and dynamic strength values of components. The main focus of the test rig is the determination of the strength at the root of spur gears. Therefore the gear wheel is mounted with clamping jaws and a preload is chosen to fix the wheel. The test rig and the test device form an oscillation system which is activated by a pulsating load into a sinusoidal resonance oscillation. The test frequency is determined by the spring stiffness of the test device and the load. The best value for the test frequency, in our case, was found experimentally. The average load is set with the preload and is adjusted automatically throughout the test.

Figure 2-3: Pulsator test rig at FZG

2.4.3 3D Measurement Unit

For the contour measurement of the gear wheel teeth a CNC controlled gear measuring center P40 by Klingelnberg is used. It is operated by the Institute for Machine Elements at the Technical University Munich. It has a resolution of 1 µm and is designed for a module range from 0.5 to 15 mm. The CNC machine scans the contour of the tooth flank in steps of 0.01 mm to define the gear wheel surface. An example measurement is shown in Figure 2-4.

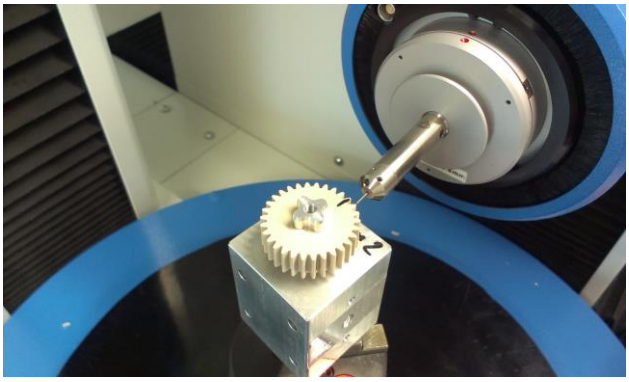

Figure 2-4: Tooth measurement setup at FZG

2.4.4 TV Chamber

For the tests in space-similar environment the LRT thermal-vacuum chamber is used. It is equipped with two pumps. A pressure of as low as 10^{-3} mbar can be achieved with the first roughing pump, and a pressure of lower than 10^{-5} mbar can be achieved with the turbo-vacuum pump. Three independent pressure sensors are mounted inside the chamber to monitor the vacuum pressure. The temperature inside the chamber can be regulated from -90°C to +110°C with a thermostat. Inside the chamber a total of 28 thermo-elements are available to measure temperatures. Eight of them are taken to observe the shroud temperature, but the other twenty thermo-elements can be used to monitor the temperature of the test setup. The thermal vacuum chamber is operated with a NI CompactRIO. The inner dimension of the chamber is 950 mm long, 450 mm wide, and 350 mm tall. A picture of the thermal-vacuum chamber can be seen in Figure 2-5.

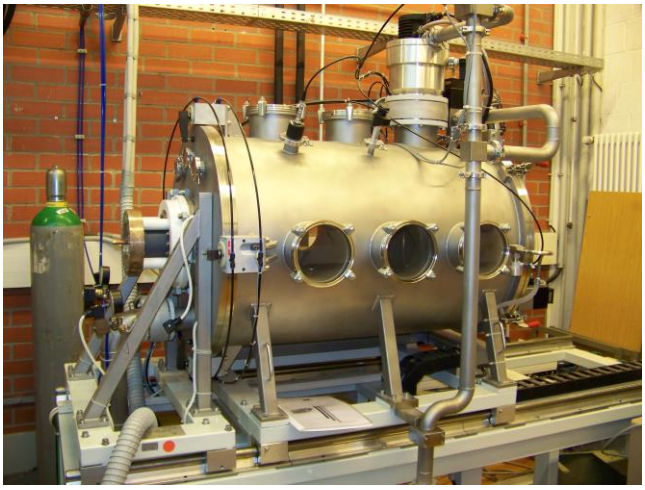

Figure 2-5: Thermal-vacuum chamber at LRT

2.4.5 Radiation Facility

The radiation tests of the Pulsator wheels were carried out at the Helmholtz Zentrum München at the Research Unit Medical Radiation Physics and Diagnostics. The irradiation chamber Gammacell220 (Figure 2-6 and Figure 2-7) is equipped with a Co^{60} source which is emitting gamma rays. It has a radiation rate of 9.3 Gy/min which is equal to 930 rad/min. For the required total dose of 100 krad, the wheel has to be exposed to the radiation for 108 minutes. Therefore the test device is placed inside a chamber which has a diameter of 20.6 cm which is just perfect for our 12 cm gear wheel. After closing the chamber it automatically drives downwards into the radiation area. The Co^{60} is installed circular around the chamber which results in an even irradiation of the wheel from all directions.

Figure 2-6: Gammacell220

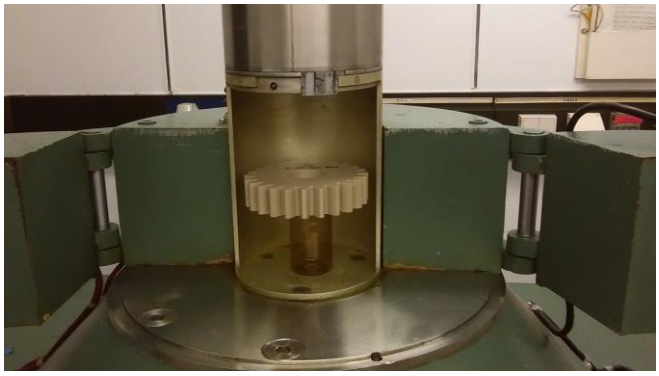

Figure 2-7: Gear wheel inside Gammacell220

2.4.6 Digital Camera

To test the environmental impact on the geometry of the pinions, a digital camera is placed outside the thermal-vacuum chamber and takes photos of the gear wheel inside the chamber. For these tests a Canon EOS 5D Mark camera with Canon Macro lens ef 100 is used. Its specifications are summarized in Table 2-10.

Canon EOS 5D Mark II
Canon Marco lens ef 100
21 megapixel CMOS sensor
ISO 100 – 6400 calibrated range
DIGIC 4 processor
High ISO noise reduction

Table 2-10: Digital camera properties

All photos are taken with the following adjustments:

Aperture	4.5
Time of exposure	15 sec
ISO	200
Distance from lens to gear wheel	10 cm

Table 2-11: Digital camera adjustments

The illumination conditions are kept constant during the test.

2.5 Test environment

The objective of this work is to describe the behavior of synthetic gear wheels in space application and to evaluate what influence the space conditions have on the performance of the wheels. Therefore the space environment has to be simulated as close as possible. The operational environment of the gear wheels is characterized by vacuum, extreme temperatures, zero gravity, and radiation. Zero gravity is not further considered as test environment because its impact on gear wheel performance is assumed insignificant compared to vacuum or temperature. Furthermore zero gravity testing is very expensive and complex and consequently the scientific gain does not justify the expenses.

The largest effect on the tribological behavior of gear wheels have the surrounding temperatures and pressure [8]. Consequently all gear wheel parameters have to be determined depending on thermal-vacuum (TV) environment. Therefore TV conditions have to be provided for all the tests. For qualifying space components, according to [8] these TV conditions have to be -55°C to 80°C and 10^{-5} mbar. These values can be provided with the thermal-vacuum chamber at the Institute of Astronautics which is described in detail in chapter 2.4.4.

Since polymers are much more sensitive to radiation than metals, radiation also has to be considered as test environment. But not for all tests. Wear is mainly unaffected by irradiation. But radiation can cause a loss in stiffness and consequently the strength evaluation has to consider space radiation. The tests can be conducted in air because effects of radiation are less severe in vacuum [8]. Also not every possible appearing kind of radiation has to be considered because space mechanisms with their gear wheels are typically integrated in the inside of spacecraft. And according to [69], atomic oxygen only degrades materials at the surface of the spacecraft. Also ultraviolet radiation is only a problem for components exposed to the sun. The same with charged particles.

Consequently gamma radiation is the only type of radiation which is tested in the context of this thesis because only gamma radiation has the potential to degrade components in the inside of a spacecraft. Therefore typical radiation dose rates in space are 10^5 rads/year in an unprotected location at the spacecraft. But since gear wheels usually are integrated inside a satellite the 10^5 rads are assumed for the whole mission duration. All gamma radiation tests can be conducted in air because gamma radiation in air produce more degradation of polymers than irradiation in vacuum [69].

Table 2-12 summarizes the environmental conditions in which the different tests are conducted:

Test	Temperature	Pressure	Radiation
Wear	-55°C to +80°C	10^{-5} mbar	---
Tooth root carrying capacity	-55°C to +80°C	10^{-5} mbar	10^5 rads
Environmental impact on geometry	-55°C to +80°C	10^{-5} mbar	---
Gear tooth temperature	-55°C to +80°C	10^{-5} mbar	---

Table 2-12: Environmental conditions for tests

In order to be able to make a statement about the influence of the space environment, all tests are also conducted in ambient conditions. This means +20°C and a pressure of 1 bar.

2.6 Functional Tests

In order to verify the functionality of the test setups, different functional tests were conducted in advance to the real tests. These tests only had the objective to show the reliability of the test rigs. The most relevant of these functional tests are described in the following.

2.6.1 Behavior of strain gauges at vacuum and temperature extremes

Strain gauges are used for the wear test rig. The test rig is designed to generate the wear of the polymer gear wheels in the different environments. Therefore a constant torque has to act on the wheels. And since this torque is an essential parameter in the calculation of wear its value has to be determined. The acting torque is measured indirectly with strain gauges which are placed at the surface of the shaft which connects the two pinions (Figure 2-8). The output of the strain gauges is measured in volts and can be converted to newton meters. Since the voltage can only be measured when the shaft is not turning, during the real test it cannot be determined whether the voltage stays constant during operation and at different environment. This has to be tested in a separate test. Therefore a preload

functional test is conducted which is described in the next section. Before doing that test, the vacuum / temperature dependency of the strain gauges have to be determined. Because otherwise it would not be possible to distinguish between a real loss in torque and voltage change of the strain gauge as a consequence of the environment. To measure the environment dependency of the strain gauge, the shaft with the mounted strain gauges is mounted at the test rig but not preloaded. The test rig is place inside the thermal vacuum chamber and the environmental conditions are set which are also planned for the real test. Throughout the test, the output voltage is measured. Table 2-13 shows the voltage values at different conditions.

Pressure [mbar]	Temperature [°C]	Output Voltage [V]
1000	20	4.63
10^{-5}	20	4.61
10^{-5}	-55	4.80
10^{-5}	20	4.65
10^{-5}	83	4.44
10^{-5}	20	4.61
1000	20	4.62

Table 2-13: Strain gauges functional test results

The results show that vacuum does not influence the output voltage of the strain gauges at all. At low and high temperature the tests show a small variation from the value at ambient temperature. But this can be explained with the functionality of strain gauges. Their integrated wires change length at different temperatures and consequently the output value changes although the actual torque stays constant.

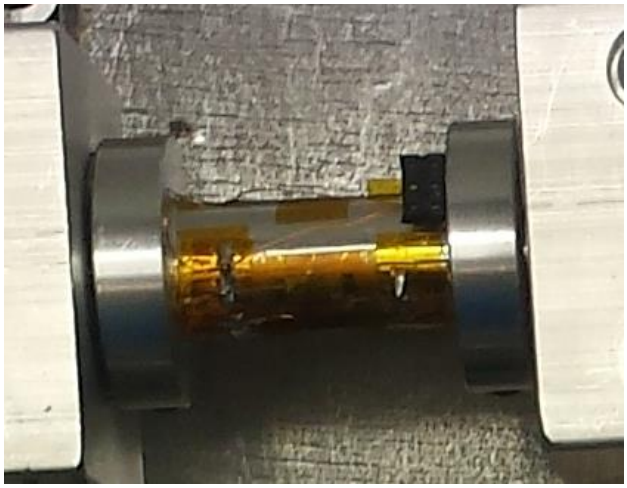

Figure 2-8: Shaft with strain gauges

2.6.2 Stability of preload throughout the test

As described in the previous chapter, an important parameter during the wear tests is the preload which is brought into the test rig. Because the preload generates the torque which is acting on the pinion. And the torque plays an essential role in the calculation of the wear. Therefore it has to be assured that the preload is staying constant throughout the test. This is accomplished in the design of the test rig by the installation of the loading clutch. But nevertheless pretests have to be conducted to prove the stability of the torque, because during the test it cannot be measured. With knowing the vacuum / temperature behavior of the strain gauges from the strain gauges functional test, this dependency can be taken into account when studying the preload. To measure the preload the test setup is mounted equal to the real tests but instead of turning the wheels (and the shaft) continuously, they are cycled. They are only turned by 90° and so the strain gauges do not have to be disconnected and the voltage can be measured throughout the operation at the different environmental conditions. The output voltages at the different pressures and temperatures are shown in Table 2-14.

Test time [h]	Pressure [mbar]	Temperature [°C]	Output Voltage [V]
0	1000	20	3.88
18	10^{-5}	20	3.87
24	10^{-5}	-55	4.08
38	10^{-5}	20	3.93
45	10^{-5}	83	3.63
48	10^{-5}	20	3.84
49	1000	20	3.87

Table 2-14: Preload stability test results

The results show that output voltage and with that the preload is not influenced by vacuum. At extreme temperatures a small variation from the starting value can be observed. An increasing voltage at low temperature and a decreasing voltage at high temperature. But since the same variation was also observed in the previous strain gauges test, it can be stated that it is not the preload which is changing, but the strain gauges voltage. And furthermore the initial value of 3.88 V almost returns at the end of the test it can be assumed that the torque at the shaft does not change during the test.

2.6.3 Miscellaneous functional tests

Beside the two described major functional test, other minor tests were conducted to improve testing. One of them had the goal to find the best aperture and exposure time of the digital camera for the gear wheel geometry test. Since the quality of the photo has quite an impact on the evaluation accuracy it was decided to take a series of photos with different aperture and exposure times to find the optimum. Finally an aperture of 4.5 and an exposure time of 15 seconds were chosen. With that combination the photo has enough brightness and depth of field for the analysis without having overexposure at any part of the wheel.

Also the distance between camera lens and pinion was varied as well as different lighting conditions were tested. The results showed, that the lightning does not have a big influence on the photo as long as a uniform illumination is provided and is not changed throughout the test. Furthermore, it was found out that the distance between lens and pinion should be as small as possible to increase resolution. Consequently the distance was given by the geometry of the thermal-vacuum chamber since the wheel was placed inside the chamber and the camera outside. This resulted in a distance of 10 cm.

Also the characteristics of the motor winding temperature was tested prior to the main tests. Overheating the motor would result in destroying the motor which would have meant a major

delay in the test series. Consequently, knowing the behavior of the winding temperature is essential. The maximum winding temperature for the used motor is 180°C. In a test series the temperature of the winding was monitored during various test scenarios. The test was conducted in vacuum environment, because the absence of air results in a stronger heating since radiation and conduction is the only way the motor can get rid of the heat. Three parameters were increased steadily during the test: motor power, motor velocity, and surrounding temperature. The parameters were slowly increased up to 20% over the expected values during the real test. At that point the winding temperature showed 150°C which is still 30°C less than the critical temperature. That gave us enough confidence for a save operation during all test phases. But nevertheless the motor winding temperature is monitored throughout all tests and as a backup function, an automatic motor shut down was implemented as soon as the motor winding increases above 150°C.

3 Wear

3.1 Test objective

Wear is one of the most critical parameters for gear wheels in general and for polymer gear wheels in particular. Due to the lower stability of synthetics compared to metallic materials, their wear rate is larger. Wear results in an increase of backlash and a weakening of the gear wheel. The increase in backlash in particular is a critical parameter for space mechanisms. Although wear cannot be avoided, at least it has to be understood for a reliable design. Since only a small number of published studies are available to the author about the behavior of synthetic gear wheels in the space environment, the goal of this test is to systematically evaluate the influence of the space environment on the wear of gear wheels made out of PEEK and POM. Therefore, the wear coefficients of PEEK and POM gear wheels in four different environments are determined: (1) in the lab environment with ambient pressure and a temperature of 20°C, (2) in vacuum with 20°C, (3) in vacuum with 80°C, and (4) in vacuum with -55°C.

3.2 Test method

In general, three methods are available for wear measurement: gravimetric wear measurement, tactile wear measurement, and loss of load torque of the test rig [61]. Since the tests in the context of this thesis are conducted in a vacuum environment, gravimetric measurement is not accurate enough since a loss of mass of the pinion might not only be caused by wear but also by volatiles. Also the loss of load torque is considered to be not sufficiently accurate.

Consequently it was decided to use the tactile method in order to measure the wear coefficient of the PEEK and POM pinions. The core of this method is to determine the loss of material of a gear wheel tooth after running through a test cycle (Figure 3-1). With the loss of material, as well as with knowing the torque acting on the pinion and the number of revolutions, the wear coefficient can be calculated. In order to determine the loss of material, before and after operation of the gear wheel, the cross-sectional area of a tooth must be measured. This is accomplished by scanning the contour of a tooth with a CNC-controlled gear measuring center by Klingelnberg at the Institute for Machine Elements at the Technische Universität München. In between the repeated contour measurements, the pinion is operated in a back-to-back gear test rig to generate wear. With that test rig, which is described in section 2.4.1, a constant torque is acting on the pinion. The number of revolutions is recorded throughout the test.

To conduct the wear test three test setups are required: the CNC controlled gear measuring center to measure the tooth cross-section area, the back-to-back gear test rig for operating the pinion, and the thermal vacuum chamber to simulate the space environment.

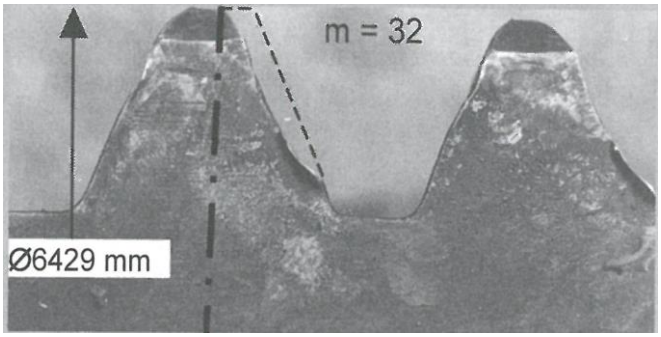

Figure 3-1: Tooth wear [34]

3.3 Test parameters and calculations

The gear wheels used in the wear test are the 30 mm diameter synthetic pinion and the 120 mm diameter steel counter wheel. Their parameters are summarized in section 2.2.1 and section 2.4.1. For the wear test these two gear wheels form a gear wheel pairing with certain specifications coming from the test requirements such as torque, revolutions per minute, and axis distance (Table 3-1).

Test parameter	Symbol	Unit	Value
Torque at pinion	M_T	N·m	0.3
Pinion revolutions per minute	n	1/min	60
Number of cycles	N	-	350000
Axis distance	a	mm	75.3

Table 3-1: Wear test specifications as derived from space mechanism requirements (Table 1-3)

With these specifications and the equations in chapter 1.3.2 the following parameters of the pinion as part of the pinion-wheel system can be calculated. These numbers are required in order to determine the wear after the tests and are reported in Table 3-2.

Pinion parameter	Symbol	Unit	Value
Operating pressure angle	α_w	°	20.61
Pitch diameter	d_w	mm	30.12
Sliding speed	v_g	m/s	0.09
Length of path of contact	g_α	mm	4.35
Transverse contact ratio	ε_α	-	1.47
Transverse contact ratio on pinion	$\varepsilon_{\alpha 1}$	-	0.77
Transverse contact ratio on wheel	$\varepsilon_{\alpha 2}$	-	0.71
Tangential force	F_t	N	20
Axial force	F_a	N	20
Radial force	F_r	N	7.28
Application factor	K_A	-	1
Dynamic factor	K_V	-	1
Transverse factor	$K_{F\alpha}$	-	1
Face load coefficient	$K_{F\beta}$	-	1
Form factor	Y_{Fa}	-	2.60
Stress correction factor	Y_{Sa}	-	1.70
Coverage factor	Y_ε	-	0.76
Profile length	l_{Fl}	mm	2.13
Tooth loss factor	H_V	-	0.08

Table 3-2: Pinion parameters for wear test as calculated with equations in chapter 1.3.2.

3.4 Testing

In order to identify the influence of temperature and pressure on the wear behavior of the PEEK and POM pinions, four different test series are conducted, one for each environmental condition (Table 3-3). The test parameters motor current and rotation rates are kept unchanged over the four test series (Table 3-4).

Environment	Temperature [°C]	Pressure [mbar]
Ambient	+20	~ 1000
Vacuum 20°C	+20	$1 \cdot 10^{-5}$
Vacuum 80°C	+80	$1 \cdot 10^{-5}$
Vacuum -55°C	-55	$1 \cdot 10^{-5}$

Table 3-3: Wear test environment

Maximum motor current	0.8 A
Rotational direction	Clockwise / “left”
Motor shaft output speed	15 rpm
Pinion speed	60 rpm

Table 3-4: Wear test motor parameters

All test are conducted with a torque of 0.3 N·m acting at the pinion. The cycle number of 350 000 was chose for three reasons. First, literature research showed that these high number of cycles can occur in spaceflight missions (see Table 1-3). Second, preliminary calculations and tests showed that after 300 000 cycles, a significant and measurable change in worn area can be obtained to yield reproducible results. And third, with four days total duration, the duration of the tests is kept within acceptable limits. The pinion rotation speed is 60 rpm, limited by the maximum speed of the geared stepper motor. Under those limitations, and with a desired cycle number of 350 000, one test series takes four days. A faster and vacuum-compatible motor was not available for this study. Due to the low rotation speed of the pinion, additional effects such as partial melting, do not have to be considered. Furthermore, spaceflight mechanisms often operate at low velocities around 10°/s (see Table 1-3) which corresponds to 1.7 rpm. Consequently, 60 rpm is a good compromise between realistic rotation speed and accelerated testing time. The motor current of 0.8 A is chosen as a compromise between sufficient torque to turn the wheels and as little power as possible to reduce the risk of overheating. In pretests at vacuum and +80°C ambient temperature, a maximum winding temperature of +150°C was observed which is within the allowable limit of +180°C.

Throughout the entire test series, the clockwise direction of rotation is not changed to produce as much wear as possible on one side of the tooth flank to get significant results in shorter test times. So “rotate left” is selected for motor rotation direction in the LabView test control program, which means clockwise rotation of the pinion as seen from the front.

The axis-center distance is 75.3 mm to intentionally provide a small amount of backlash between the pinion and the wheel (75 mm nominal distance = ½ · (120 mm + 30 mm diameter)). For proper functionality, backlash is required between gear wheels [34]. For a center distance from 25 to 125 mm, and a module of 1, a backlash of 75 to 250 µm (in the normal plane) is recommended [8]. The measured backlash in the test setup (100 µm) lies within that recommended range.

Each test series starts with mounting the new PEEK (POM) pinion on the shaft. Next, the flank contour of four teeth of the pinion is scanned and the teeth are marked to make sure always the same teeth are measured. Since the measurement unit is limited in the number of data points it can record, not more than four teeth can be measured at the same time. During tooth measurement, the pinion and the shaft remain assembled. This prevents introducing inaccuracies during remounting of the pinion. After mounting the pinion-shaft assembly in the test rig for the next test, the pinion is preloaded with 0.3 N·m through the loading clutch. The preload is determined with strain gauges. The test rig is placed inside the thermal-vacuum chamber, even for ambient pressure tests, to provide equal test conditions (Figure 3-2). Before the chamber is closed, the thermal elements are connected and the preload is measured to ensure it did not loosen during the integration process. Depending on the test conditions, the thermal-vacuum chamber can then be evacuated and the desired temperature is set. Once the desired pressure and temperature levels are reached, the motor is activated and the pinion begins rotating. During both the ambient pressure and room-temperature vacuum tests, each experiment day the test is stopped for five minutes to check the preload of the measuring shaft. For the hot and cold vacuum tests, the preload is only verified before and after the test. Parameter monitoring of motor winding temperature and encoder incrementing signals ensure save operating conditions. After 350 000 cycles (rotations), the motor is stopped and the thermal vacuum chamber is brought to ambient laboratory conditions. The preload of the arrangement is checked, and the contour of the pinion is scanned.
Finally, with the two tooth scans before and after operation, the volume loss can be calculated and the wear coefficient can be determined.

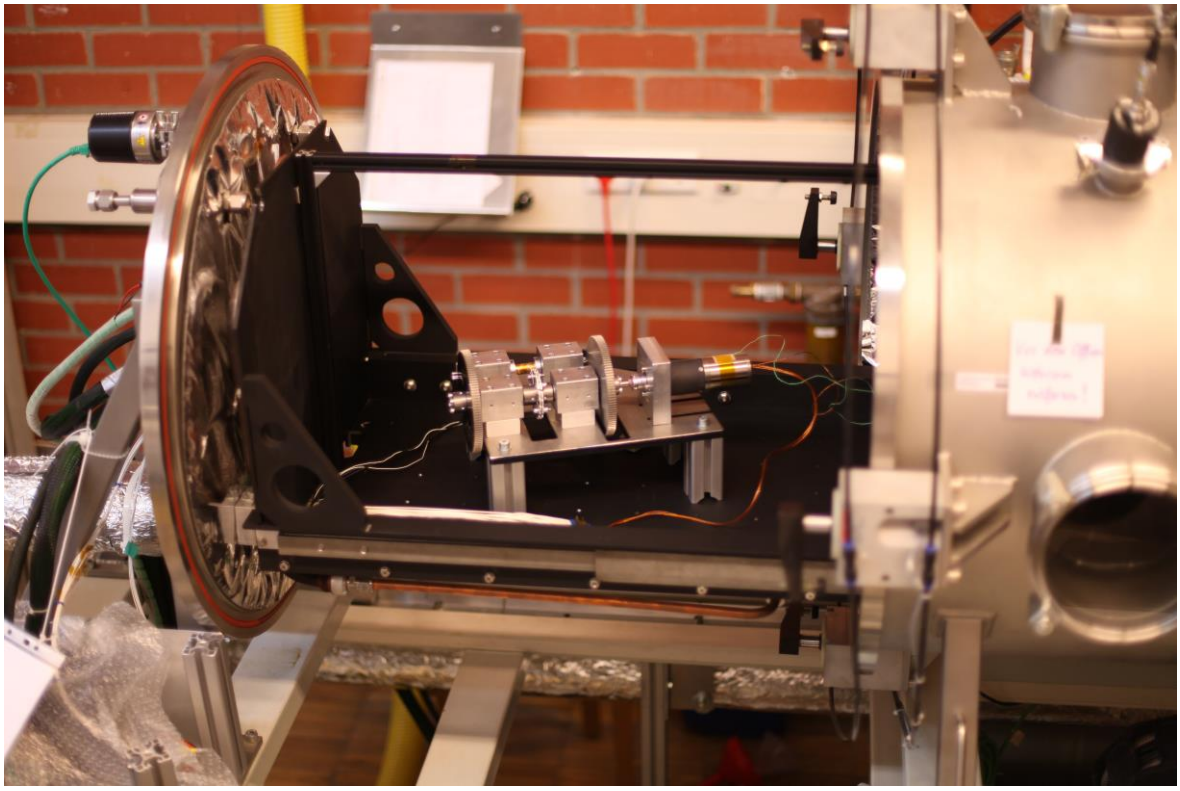

Figure 3-2: Wear test setup in thermal-vacuum chamber at LRT

3.5 Results

To evaluate the wear behavior of the PEEK and POM gear wheels, the decrease of the tooth area after 350 000 cycles is measured in the four different test environments and the wear coefficients are calculated. The numbers for the area decrease and wear coefficients of the PEEK gear wheels are shown in Table 3-5 and of the POM gear wheel in Table 3-6. Figure 3-3 provides an overview of all wear coefficients and their standard deviations.

Environment	**Area decrease PEEK [mm^2]**	**Wear coefficient PEEK [10^{-6} mm^3/Nm]**
Ambient	0.0011	3.8
Vacuum / +20°C	0.0005	1.8
Vacuum / +80°C	0.0130	44.4
Vacuum / -55°C	0.0042	14.4

Table 3-5: Area decrease of PEEK pinion due to wear

Environment	Area decrease POM [mm²]	Wear coefficient POM [10⁻⁶ mm³/Nm]
Ambient	0.0017	5.6
Vacuum / +20°C	0.0034	11.6
Vacuum / +80°C	0.0764	259.8
Vacuum / -55°C	0.0057	19.3

Table 3-6: Area decrease of POM pinion due to wear

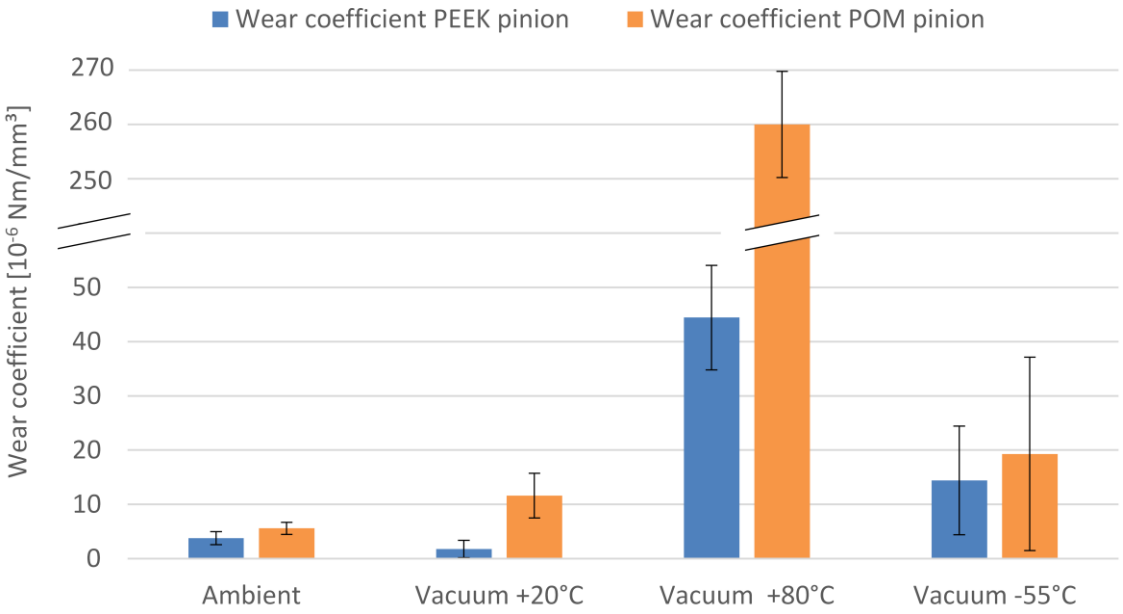

Figure 3-3: Wear coefficients for PEEK and POM

At all four environmental conditions, the results show for PEEK a lower wear coefficient than for POM. With k_W = 1.8·10^{-6} mm³/N·m the lowest wear rate is measured for PEEK at vacuum/20°C conditions. PEEK has its largest wear coefficient with 44.4 ·10^{-6} mm³/N·m at vacuum/80°C. At these conditions also POM shows its largest k_W with 259.8·10^{-6} mm³/N·m. But other than PEEK, POM has its lowest wear coefficient with 5.6·10^{-6} mm³/N·m at ambient environment. The author has to point out, that for vacuum/-55°C conditions, the standard deviation is quite large, and consequently these numbers shall only be considered as approximate values. At ambient environment both materials show a similar wear behavior.

3.6 Discussion of wear results and conclusion

The results show an environmental dependency of the wear rate of PEEK as well as of POM gear wheels. This can be extrapolated to similar effects under spaceflight conditions. The presented results are in the same order of magnitude as those wear coefficients available in literature for PEEK but under slightly different test conditions [70], [10]. A direct comparisons of the results with wear data for PEEK gear wheels are not possible since no such data were found in the reviewed literature. Only for POM gear wheels, wear coefficients are available to the author. In [37] a wear coefficient of $3.4 \cdot 10^{-6}$ mm³/N·m is presented for a POM-steel gearing system in ambient conditions. This correlates well with the wear coefficient of $5.6 \cdot 10^{-6}$ mm³/N·m found in the present tests, with the same test parameters.
In [8] tests are presented which show the wear behavior of different polymer gear wheels in a spaceflight environment. The polymer wheels show large differences in specific wear rate when tested in air compared to vacuum. In addition, a temperature dependency is shown. This corresponds to the results of this research. Additionally, a general increase of adhesive wear of gear wheels in vacuum is mentioned in that work. However, the present tests show an increase of wear in vacuum compared to air only for POM.
When comparing the two materials PEEK and POM under the different test conditions, PEEK shows lower wear coefficient than POM in all four environments. This fits the available descriptions of the mechanical properties and wear behavior of PEEK, resulting from the way it is produced. PEEK is produced with the polycondensation method which results in wear stability and also radiation resistance. Furthermore, the larger Young's-Modulus of PEEK compared to POM can lead to better wear performance.
Both PEEK and POM show the same wear tendency at ambient, vacuum/-55°C and vacuum/80°C, but not at vacuum/20°C. At vacuum/20°C, the wear coefficient of PEEK is decreasing compared to ambient condition, the wear coefficient of POM is increasing. This observation is difficult to explain. The results for PEEK correlate with findings reported in [71] and [58]. These studies also tested the wear of PEEK in vacuum conditions and observed a decrease in wear. The authors of [71] conclude that the decrease of water vapor in the material in vacuum environment leads to the decrease in wear. The behavior of POM in vacuum cannot be conclusively explained based on existing literature. One possible explanation might be the surface roughness of POM, as a dependency of wear in vacuum on surface roughness is reported in [69].

After evaluating the influence of vacuum on the wear behavior, the dependency on temperature shall be discussed in the following. PEEK as well as POM show the same tendency for the three tested temperatures (20°C, 80°C, and -55°C). In short, the wear coefficients of both materials are lowest at 20°C, largest at 80°C, and somewhere in between at -55°C. But again, it must be pointed out that the standard deviation of the vacuum/-55°C tests is large and consequently the results at this condition can only be seen

as approximate values. But nevertheless, the difference in wear between 20°C and 80°C is noticeable. Especially for POM where at 80°C the wear rate is a factor of 20 larger than at 20°C. That increase is not surprising, as an increase of wear for POM gear wheels at larger temperatures was also observed in [70]. The closer the temperature comes to the melting temperature of the material, the larger the wear rate. And since POM has a lower melting temperature than PEEK, it is more sensitive to wear at high temperatures. In this study, an additional factor has to be considered. As the authors of [72] assume, in normal atmospheric conditions, the heat generated by friction at the tooth flank of polymer gears would be entirely removed to the surrounding air. But in vacuum there is no air that would absorb the heat. Consequently, the surface is getting even hotter and the wear increases. Furthermore, [73] confirms an increase of wear for PEEK at larger temperatures. The theory behind the increase of wear at larger temperatures is the thermal decomposition of the polymer. Temperature influence causes large inflation pressure or triaxial tensions in the material which results in the creation of subsurface cracks during frictional sliding. This effect accelerates abrasion. This thermal decomposition theory could also explain the wear behavior at -55°C. Despite the large fluctuation of the test results, a tendency to larger wear rates compared to 20°C can be identified. This behavior is also evident in the tests reported in [10]. However, it must be mentioned that PEEK filled with MoS_2 and graphite was tested in that study, so the results cannot be directly transferred to this study.

In addition to the wear rate, the influence of wear on the accuracy of the mechanism must be evaluated. Accuracy is defined with the wear rate dependent backlash as the main parameter. The increase in gear backlash is derived from the wear depth per tooth encounter [8]. The loss in material of the gear tooth must be converted into a decrease of tooth thickness, and thus, an increase of distance between the teeth followed by an increase of backlash. Assuming the wear is constant over the line of contact of the tooth flank, the increase of backlash can be calculated and is displayed in Table 3-7 for a torque load of 1 N·m and 350 000 cycles.

Environment	Increase of backlash for PEEK pinion [°]	Increase of backlash for POM pinion [°]
Ambient	0.002	0.003
Vacuum / 20°C	0.001	0.005
Vacuum / 80°C	0.021	0.120
Vacuum / -55°C	0.007	0.009

Table 3-7: Increase of backlash as a function of environmentally induced wear

Referring back to Table 1-3, were mechanism requirements of recent missions are summarized, it can be seen that pointing mechanisms have the highest requirements on

accuracy which must be in the range of 0.01°, sometimes even better. Backlash is not the only factor influencing the accuracy of a pointing mechanism, but a critical one. Since other factors such as misalignments or thermal distortions are difficult to estimate, it is assumed that the accuracy requirement is the maximum allowable backlash [12]. The accuracy requirement of 0.01° is only met by PEEK and POM gear wheels at temperatures around 20°C. The exposure to vacuum does not influence the backlash of the wheels significantly. The operation at low temperatures seems also to be tolerable, the accuracy margin is getting smaller, though. When it comes to the hot vacuum environment, things change. PEEK pinions can still be applied for accuracies in the range of 0.02° but POM pinions are no option anymore for high accuracy mechanisms at an operational environment of 80°C, with a backlash change of 0.12°.

3.7 Summary

The objective of this section was to make a statement about the applicability of polymer gear wheels in spaceflight mechanisms. Therefore, pinions made out of PEEK and POM have been tested for wear in different environments. Since no test rigs were available for the test in space simulated environment, a new test rig was designed. The main challenge here was to develop a setup which produces reliable results under thermal-vacuum conditions. After an appropriate solution was found, initial functional tests were conducted to verify the test setup. The subsequent main tests were run in four different atmospheric environments. The results show that the wear rate is dependent on the environmental conditions. At ambient and vacuum environment the wear rate for both materials is lowest. A significant increase of wear was observed at temperatures of 80°C. The tests at low temperatures have the potential of some improvements since a large fluctuation of the results was observed. But despite these fluctuation, both materials seem to work satisfying at -55°C.

At temperatures around 20°C the increase of backlash caused by wear is within the limits of accuracy requirements of pointing mechanisms. For mechanisms with accuracy requirements which do not exceed 0.02°, PEEK is a suitable material for gear wheels over the whole temperature range from -50°C up to 80°C. With POM gear wheels, larger temperatures must be avoided since a significant increase in wear was observed at 80°C. No total failure of a gear wheel was observed throughout the tests, which shows the promise these polymer wheels hold for future space applications.

4 Tooth Root Load Carrying Capacity

4.1 Test objective

The tooth root load carrying capacity is a key parameter in the evaluation of gear wheels. It is used to calculate the maximum transmittable torque of a wheel. Polymer materials in general have lower strength than metals. This makes an evaluation of the tooth strength particularly important. In addition, the space environment can have an impact on the strength. With the application in a spacecraft, gear wheels are exposed to vacuum and extreme temperature changes as well as to radiation. Consequently, the main goal of this test is to find out whether the space environment (thermal-vacuum and radiation) has an influence on the strength of PEEK and POM gear wheels.

As described in the following, the tests are not conducted with the 30 mm pinion which is used for all the other tests and which is a potential candidate for a space mechanism. But nevertheless an estimation of the tooth root load carrying capacity of that pinion is required in the context of a gear wheels characterization and is described in an extra chapter at the end of section 4.

In the context of carrying capacity, also a possible deformation of the teeth has to be considered. The deformation of the teeth of the 30 mm pinion is calculated in chapter 4.9 which shows that the deformation is too small and can be neglected.

4.2 Test method

In the context of this thesis the fatigue strength of gear wheels is determined as a function of the environment to which the wheels were exposed before the test. The fatigue strength is a certain range in the Woehler Diagram where the trend is linear in a logarithmic plot. The objective of this test is to compare the strengths of different gear wheels with each other. For a more detailed analysis of the strength, also the other ranges of the Wohler Curve would have to be determined.

To test the fatigue strength, a pulsating load is applied to the wheel until the tooth of the wheel fails. The number of load cycles until failure is recorded and is the critical parameter for the test. In order to conduct the test, the Pulsator test rig is used which is operated by the Institute of Machine Elements (FZG) at the Technische Universität München.

The Pulsator is not built for the application in a thermal-vacuum chamber. Consequently the load carrying capacity test cannot be conducted while the gear wheel actually is in a

simulated space environment. Therefore, the gear wheel is exposed to a space-like environment first and the test with the Pulsator is conducted afterwards. Three different sets of gear wheels are prepared for each material (PEEK and POM). The first set is not exposed to any space condition. These “untreated” wheels represent the reference value for the other wheels. The second set is exposed to thermal-vacuum environment. A total of 50 temperature cycles from -55°C to +80°C are run in a vacuum environment of $1 \cdot 10^{-5}$ mbar for a duration of 17 days. The third set of wheels is exposed to 100 krad of gamma radiation (Table 4-1).

Gear wheel set	**Environmental exposure**
PEEK Ref	none
PEEK TV	50 thermal-vacuum cycles from -55°C to +80°C
PEEK Rad	100 krad gamma radiation
POM Ref	none
POM TV	50 thermal-vacuum cycles from -55°C to +80°C
POM Rad	100 krad gamma radiation

Table 4-1: Environmental exposure of gear wheels

The Pulsator test is the only test that is not conducted with the same pinion as the wear, geometry, and tooth temperature tests. The reason is the Pulsator test rig. Its design does not allow the test of wheels with small diameters as a 30 mm pinion. Thus, a wheel with a different geometry is required. The FZG, who operates the Pulsator, has a standard test geometry which has proven to be appropriate for the test over many years. Consequently it was decided to use that geometry for the tested gear wheels as well, facilitating the comparison with results from literature.

4.3 Test parameters and calculations

For the tooth root load carrying capacity test different settings have to be made at the Pulsator in order to provide reliable test execution. These settings are shown in Table 4-2 and Table 4-3. Because of the different stiffness of the two materials, the best test parameters have to be found experimentally for each material.

Test parameter PEEK wheel	Symbol	Unit	Value
Frequency	f	Hz	35
Preload	F_0	N	1
Load level 1	ΔF_1	N	10
Load level 2	ΔF_2	N	11

Table 4-2: Pulsator test parameter for PEEK gear wheel

Test parameter POM wheel	Symbol	Unit	Value
Frequency	f	Hz	20
Preload	F_0	N	0.6
Load level 1	ΔF_1	N	6
Load level 2	ΔF_2	N	7

Table 4-3: Pulsator test parameter for POM gear wheel

4.4 Testing

Three sets of gear wheels are tested for each material. One set serves as reference where the wheels have not been exposed to any space environment. The other one was exposed to thermal-vacuum cycles, and the third one was exposed to gamma radiation. For each set, four wheels were prepared for the test. Before the actual test can start, the different settings for the Pulsator must be selected. The test frequency is a compromise between testing time and heating of the gear wheel. During preliminary tests the temperature of the wheels is monitored during the test and a frequency is selected where temperature does not exceed 50°C. This temperature was suggested by the experts at the FZG because up to 50°C the temperature influence on the test results is negligible. The preload F_0 is required to hold the wheel in the Pulsator and is determined experimentally. The load levels are also determined with the help of preliminary tests. For the tests, a single wheel is mounted in the Pulsator and the load cycle starts. As soon as the tooth of the wheel breaks the Pulsator stops automatically and the number of cycles the wheel survived is recorded. After that the next wheel can be tested.

The space-similar environment to which the gear wheels were exposed to prior to the Pulsator test is described in chapter 2.5. The number of thermal-vacuum cycles was a critical parameter during the preparation of the test. It is obvious that the cycle number during the test cannot correspond to cycle numbers during a real mission (depending on

the orbit up to 6000 cycles can happen per year). To find a realistic number for the TV cycles a literature review was conducted. For the deployment mechanism of a pointing system a test program with 100 cycles was run [16]. 15 cycles in a TV chamber (5 at -20°C, 5 at +40°C, and 5 at room temperature) and 85 cycles at ambient conditions. For testing the Bi-Axial Solar Array Drive Mechanism [20] 12 cycles were conducted in a thermal vacuum chamber between -30°C and +80°C. And in [74] a total of 14 thermal vacuum cycles were conducted during qualification and life tests of a mechanism. Consequently the 50 thermal-vacuum cycles chosen for the present tests shall be sufficient for representative results.

4.5 Results

For the PEEK and POM gear wheels, two load levels are tested for each material. The appropriate load levels are determined with preliminary tests. For PEEK the load levels are 10 kN and 11 kN, for POM 6 kN and 7 kN. At each load level the gear wheel is tested until it fails and the number of survived load cycles is recorded. If the variance of the results is considered as too large more tests are conducted in order to increase the significance. The results of the six test series are shown in Figure 4-1 to Figure 4-6. For each test series all available measuring points are plotted in the graph and a line of best fit is added. For these kind of graphs it is the norm to use a logarithmic scale at the x-axis.

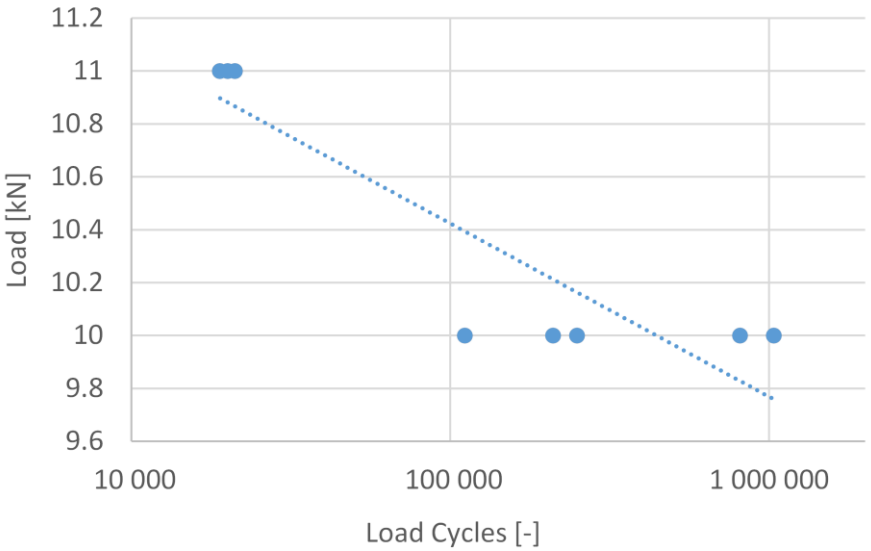

Figure 4-1: Load cycles until failure for PEEK reference wheels

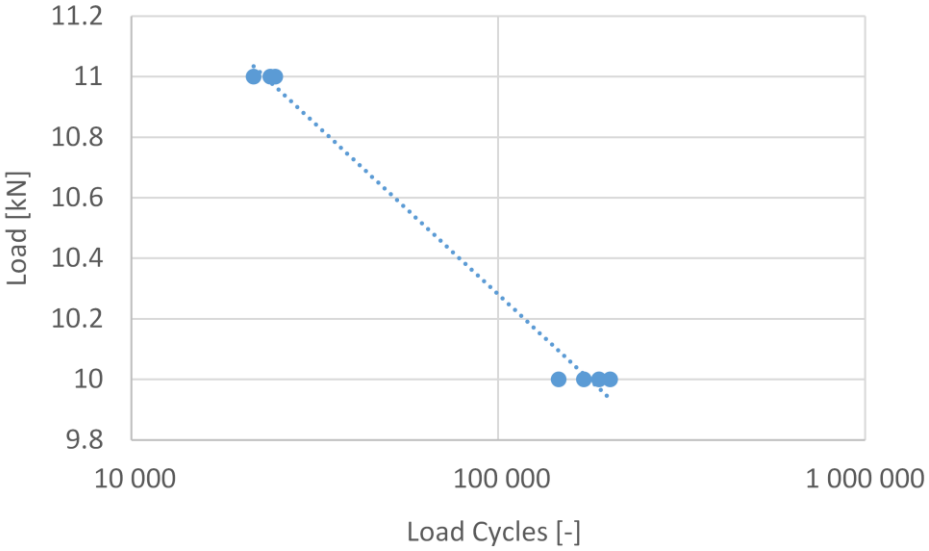

Figure 4-2: Load cycles until failure for PEEK wheels exposed to thermal-vacuum

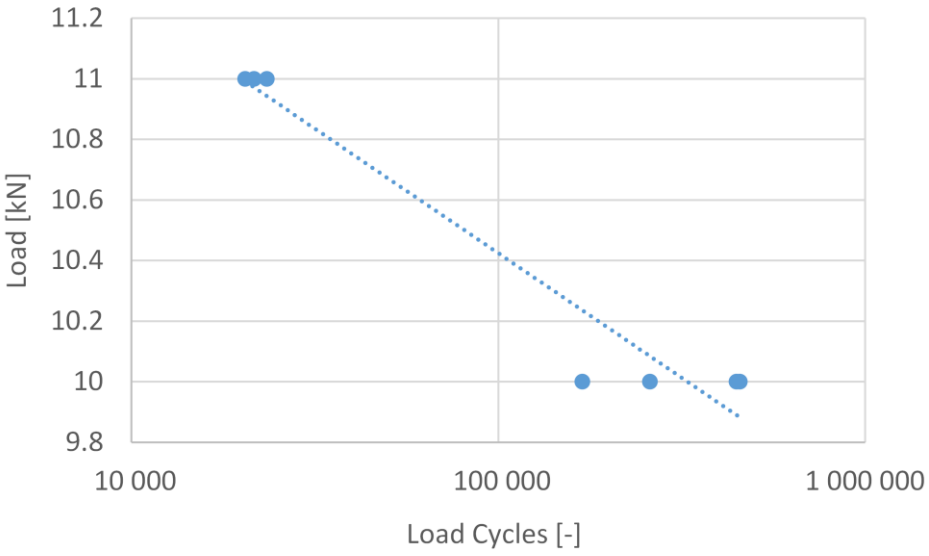

Figure 4-3: Load cycles until failure for PEEK wheels exposed to radiation

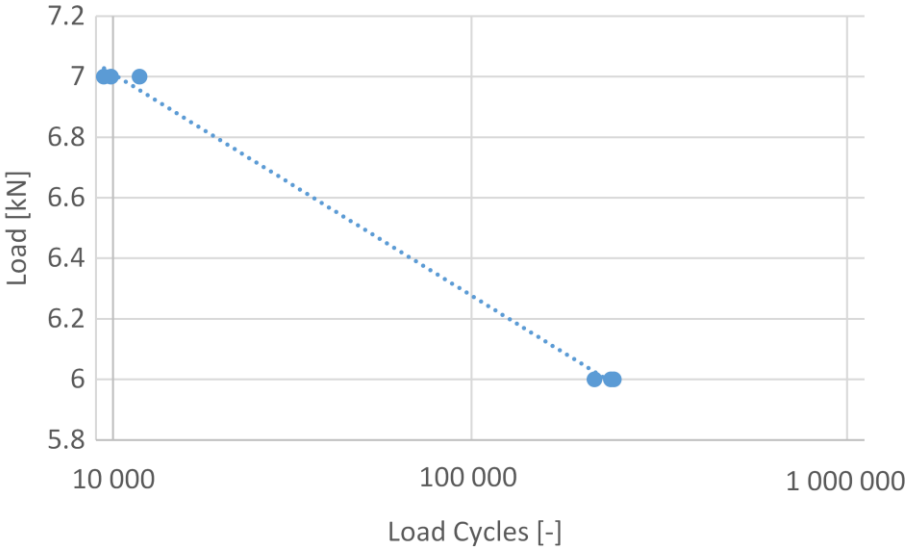

Figure 4-4: Load cycles until failure for POM reference wheels

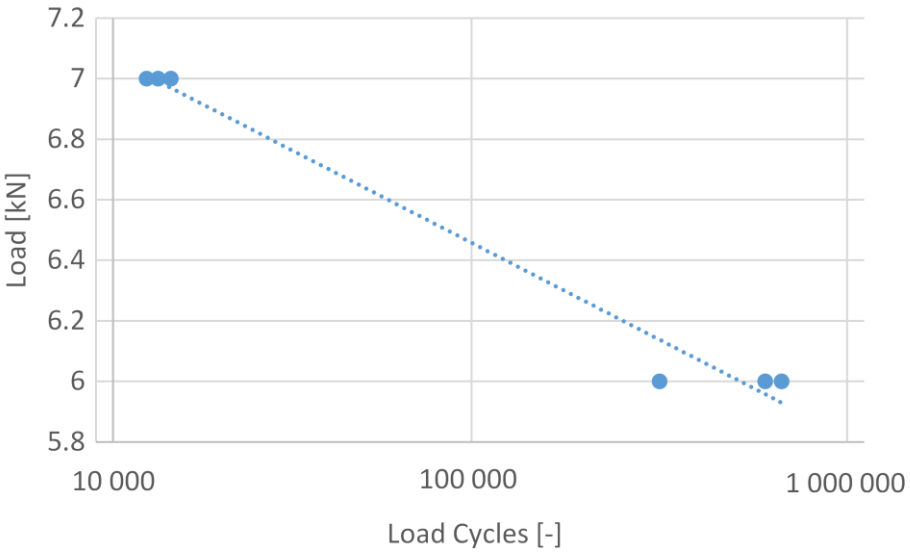

Figure 4-5: Load cycles until failure for POM wheels exposed to thermal-vacuum

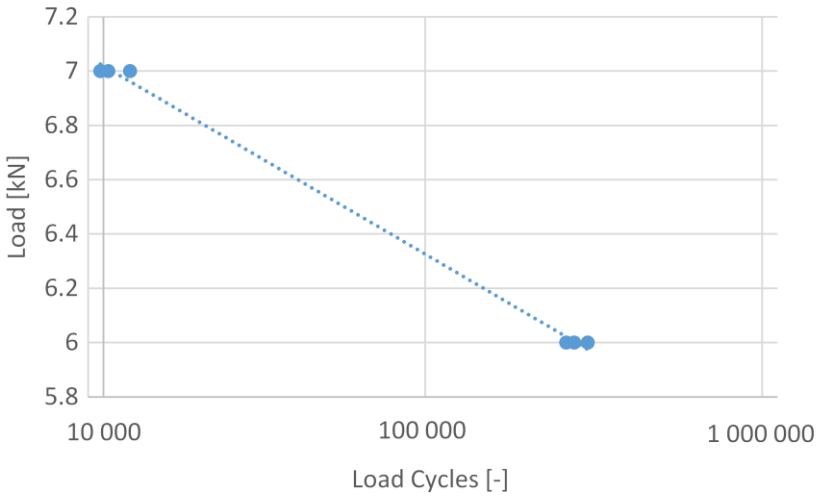

Figure 4-6: Load cycles until failure for POM wheels exposed to radiation

In general the results show low deviations of the measuring points at the larger load levels (11 kN for PEEK and 7 kN for POM) and larger deviations at the lower load levels (10 kN for PEEK and 6 kN for POM). For a better comparison of the results, the geometric mean value is calculated from the single measurement points for each test series. The geometric mean value describes a 50% probability of failure. In the context of these tests the geometric mean value describes the cycle number at which 50% of the gear wheels would fail. This value is appropriate to compare different tests with each other [75]. Furthermore, according to [75] and in order to get a feeling for the variance of the results, the logarithmic standard deviation *s* can be calculated. The geometric mean values for the tests and the standard deviation are summarized in Table 4-4 and the numbers are plotted in Figure 4-7.

Test series	**Geometric mean value of load cycles [-] for specific load level with standard deviation *s* in parentheses**	
	10 kN (Std. dev. s)	**11 kN (Std. dev. s)**
PEEK Ref	345 347 (0.41)	20 040 (0.02)
PEEK TV	175 731 (0.05)	23 349 (0.02)
PEEK Rad	307 525 (0.18)	21 757 (0.02)
	6 kN (Std. dev. s)	**7 kN (Std. dev. s)**
POM Ref	205 598 (0.02)	10 312 (0.04)
POM TV	453 835 (0.12)	13 202 (0.02)
POM Rad	252 251 (0.02)	10 657 (0.03)

Table 4-4: Geometric mean values of load cycles until failure

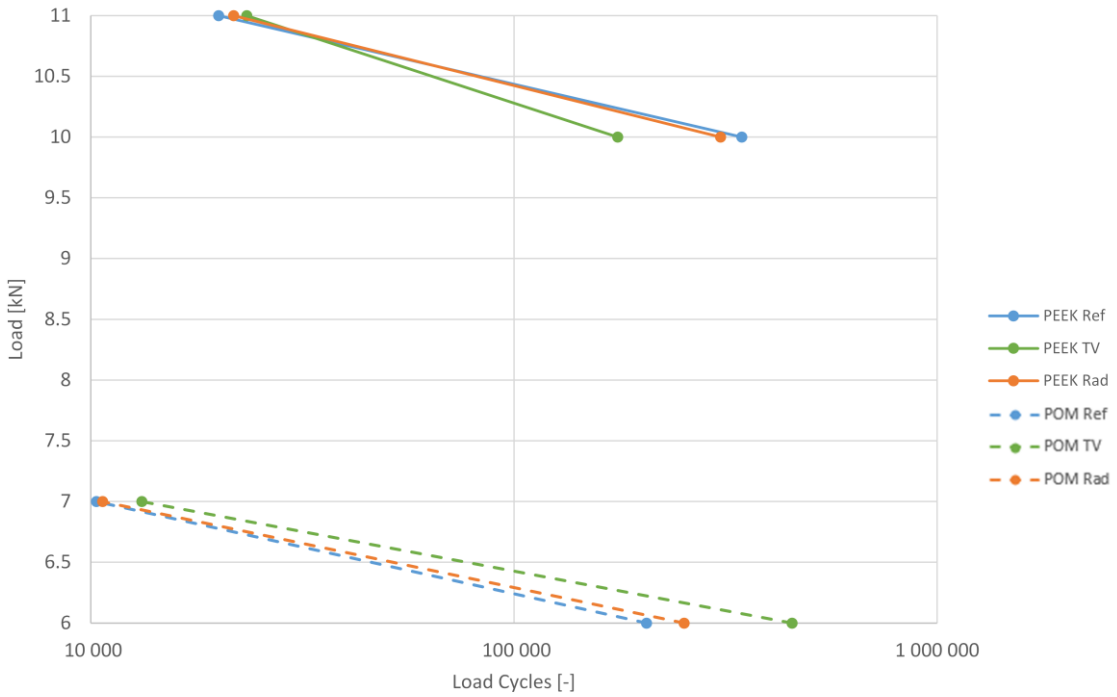

Figure 4-7: Geometric mean values for PEEK and POM wheels

The Pulsator test settings are adjusted in a way that all gear wheels break between 10 000 and 1 000 000 load cycles. For the PEEK wheels, therefore, a larger load level (10 kN to 11 kN) is required than for the POM wheels (6 kN to 7 kN). The PEEK wheels show a quite uniform behavior at 11 kN. Failure happens after between 18 000 and 25 000 cycles. At 10 kN the PEEK reference wheels and the radiation wheels survive longer than the TV wheels. However the larger variation of values for the reference wheels and radiation wheels must be noted. Also the POM wheels show a quite uniform behavior at the larger load level of 7 kN. At 6 kN the TV wheels show the best performance, albeit a large standard deviation.

4.6 Discussion

There are two conclusions of the tests which can be drawn immediately from the results. First, PEEK is stronger than POM, and second, the tooth root load carrying capacity is dependent on the thermal-vacuum environment the wheels were exposed to. The larger strength of PEEK compared to POM can be concluded from the larger load level which is necessary to break the gear wheel. Although this results is already state of the art and consequently not surprising, it brings confidence in the test method.

The dependence of the load carrying capacity on the environment is not so easy to explain. No information in literature was found where similar experiments have already been conducted. Consequently no data is available with which the results of the present experiments can be compared. At the larger load values, 11 kN for PEEK and 7 kN for POM, no significant difference in strength can be identified for the different environments. At the lower load levels, 10 kN for PEEK and 6 kN for POM, the differences, however, are noticeable. In particular interesting is that the performance of the two materials is very different. PEEK shows its best performance for the reference and radiation gear wheels, whereas POM performs best at thermal-vacuum conditions. Furthermore, it is noticeable that the results with larger cycle numbers also have larger standard deviations, especially the PEEK reference wheels show clearly larger variations than the others. According to the experts at the Institute for Machine Elements, this behavior is not unusual and is also a characteristic for a given material.

Explaining the environmental dependency of the materials is difficult. In general, the existing literature shows that gamma radiation increases the degradation of mechanical properties. Many polymers undergo main chain scission when irradiated in air which leads to degradation of the material [69]. This could neither be observed for the PEEK wheels nor for the POM wheels. For both materials, the cycle numbers for the irradiated wheels are in the range of the cycle numbers of the reference, “untreated”, wheels. For PEEK this is not surprising since, based on manufacturer information, PEEK is known for its resistant against gamma radiation [46]. POM on the other hand, is seen as more sensitive against gamma radiation. This was also evident during the radiation tests. After the tests, when the POM wheel was removed from the radiation chamber, a slight yellow color change was observed on the surface. However, this did not have any measurable influence on the load capacity of the material.

The thermal-vacuum influence resulted in an increase in strength for the POM wheels and a loss of load capacity for the PEEK wheels. This is a very surprising result. Especially since the trend for the two materials is different. According to [76] thermo-cycling may act in two different ways on PEEK. Due to post-polymerization the strength can increase but the thermal stress may also lead to mechanical stress which would decrease strength. In the present study, not only the temperature change but also the influence of vacuum leads to mechanical stress which may accelerated the loss of strength for the PEEK wheel. The reason for the improvement of the strength behavior of the POM wheels is unclear. POM is a more sensitive to temperature differences and vacuum than PEEK. Somehow the thermal-vacuum environment has a positive effect on the strength. Despite a detailed literature research, this effect cannot be explained, thus more specific experiments have to be conducted to be able to explain that interesting phenomena in more detail.

4.7 Summary

The goal of this test was to evaluate the influence of the space environment on the strength of PEEK and POM gear wheels. The Pulsator test rig used for the measurement is not built to be used in any space-similar conditions. Therefore, the gear wheels were exposed to simulated space environment first and then tested with the Pulsator. The two environments which were evaluated are thermal-vacuum and radiation. The exposure to thermal-vacuum conditions took place in a TV chamber where the wheels were cycled from -55° to +80°C for a total of about 17 days which corresponds to 50 cycles. The radiation exposure was provided by a gamma radiation chamber with a total radiation dose of 100 krad. Another set of gear wheels which was not exposed to any space conditions served as reference wheels.

The results show a significantly larger strength for the PEEK gear wheels compared to the POM wheels in all tested environments. For both materials, the gamma radiation had no impact on the load capacity of the wheels. The exposure to thermal-vacuum environment resulted in an improved strength behavior for the POM wheels and a loss of load capacity for the PEEK wheels.

4.8 Evaluation of the 30 mm pinion

The critical pinion to be evaluated regarding tooth root load carrying capacity is the POM pinion because of its lower strength confirmed with the previous tests. Therefore, the occurring bending stress at the root of the tooth must be calculated for a certain application. As in previous sections, an acting torque at the pinion of 0.3 N·m is assumed. The bending stress can be calculated with equation (37) which is described in detail in section 1.3.2. The required parameters are shown in Table 4-5.

$$\sigma_F = K_A \cdot K_V \cdot K_{F\alpha} \cdot K_{F\beta} \cdot \frac{F_t}{b \cdot m} \cdot Y_{Fa} \cdot Y_{Sa} \cdot Y_\varepsilon \qquad (37)$$

Symbol	Unit	Value
F_t	N	20
b	mm	6
m	mm	1
K_A	-	1
K_V	-	1
$K_{F\alpha}$	-	1
$K_{F\beta}$	-	1
Y_{Fa}	-	2.60
Y_{Sa}	-	1.70
Y_ε	-	0.76

Table 4-5: Pinion bending stress calculation parameters [34]

This results in a bending stress of:

$$\sigma_F = 11.2 \frac{N}{mm^2}$$

This value is valid for PEEK and POM pinions, since only the geometric parameters are relevant for the calculation.

The bending stress σ_F must be smaller than the load capacity σ_{FG} of the gear wheel including a safety factor of 2. And with $\sigma_{FG} \approx 2 \cdot \sigma_{FlimN}$ the equation can be simplified to [37]:

$$\sigma_F \leq \sigma_{FlimN} \qquad (38)$$

See chapter 1.3.2 for a detailed description of the equations.

Assuming a maximum cycle number of 1000000, the critical load capacity for the POM pinion occurs at a temperature of 100°C with

$$\sigma_{FlimN} = 26.2 \frac{N}{mm^2}$$

And with that, equation (38) is true and the load capacity criteria fulfilled.

The results from the Pulsator tests showed that the POM gear wheels exposed to radiation have about the same strength than the reference wheels and the TV wheels perform even better. Consequently no decrease in load capacity is expected for POM gear wheels in space environment. This means, for an acting torque of 0.3 N·m, POM wheels provide enough strength for the application in a space mechanism. Also the PEEK wheels can be considered as appropriate because they have even higher strength than the POM wheels.

4.9 Teeth deformation of 30 mm pinion

Due to the lower Young's modulus of synthetic materials compared to metallics, deformation of the synthetic gear wheel's teeth has to be taken into account. The deformation in circumferential direction λ can approximately be calculated with equation (39) [37].

$$\lambda = \frac{7.5 \cdot F_t}{b \cdot cos\beta} \cdot \left(\frac{1}{E_1} + \frac{1}{E_2}\right) \qquad (39)$$

With E_1 being the Young's modulus of the synthetic material. E_2 is the Young's modulus of stainless steel which is the material of the counter wheel. The following numbers are calculated with a tangential force F_t = 20 N and a Young's Modulus for stainless steel of 210 000 N/mm² [34].

Material	Young's Modulus [N/mm²]	Deformation λ [mm]
PEEK	4 000 (Table 2-6)	0.006
POM	2 800 (Table 2-6)	0.009

Table 4-6: Tooth deformation of PEEK and POM pinion

The acceptable maximum deformation λ_{max} for synthetic gear wheels is according to VDI DIN 2726 [77]:

$$\lambda_{max} \leq 0.07 \cdot m$$

With m=1 $\lambda_{max} \leq 0.07$ mm

Both materials, PEEK and POM, fulfill the deformation criteria by one order of a magnitude. Consequently no further tests are conducted to measure the gear wheel deformation.

5 Environmental Impact on Geometry

5.1 Test objective

One drawback of synthetic gear wheels compared to metallic materials is its larger coefficient of thermal expansion. Also the outgassing performance of synthetic materials in vacuum is not so good compared to metallic. The result of outgassing and especially of thermal expansion is the change in geometry of the gear wheels. But change in geometry has an immediate impact on the backlash of the gearing system. For example, with a decrease of the wheel diameter and the tooth thickness, the gap between two flanks would increase and this consequently results in a higher backlash which is not desired in most of the space mechanisms. On the other hand, as soon as the diameter of the wheels increases, for example because of heating, the desired gap between the flanks may vanish and this results in larger wear and less efficiency.
So the goal of this test is to monitor the geometry of a PEEK and POM gear wheel during different environmental conditions: vacuum at 20°C, vacuum at -50°C, and vacuum at +80°C. With that the change in geometry of the wheels in space conditions shall be determined and the impact on the backlash performance shall be evaluated.

5.2 Test method

To monitor the geometry of the gear wheel a digital camera is used which takes pictures of the wheel during the different environmental conditions. The idea of using digital imaging tools for measuring gear wheels has become popular in recent years since digital cameras are getting better and cheaper [78]. Doing that, it is important that the resolution of the camera is large enough to detect any geometry change of the wheel. The camera has a total resolution of 21 megapixel. The size of the taken photos and the camera resolution provides a geometry resolution of 0.01 mm.

Beside the digital camera, a mounting device for the gear wheel is required and, of course, the thermal-vacuum chamber is a part of the experiment in order to create the space environment. The test device is fixed on the mounting device and it is place inside the chamber. Through a window in the chamber the photos are taken from the outside which has the huge advantage that the camera has not to be vacuum and temperature compatible. Photos are taken every hour. The test starts with ambient pressure and ambient temperature, followed by vacuum at 20°C, vacuum and -55°C, and finally vacuum and +80°C. And then back to vacuum at 20°C and ambient environment (Figure 5-2). The total test cycle lasts about three full days. The taken photos are processed with Matlab in order to get the contour of the gear wheel. With another self-programmed Matlab script, out of the

contour the change in geometry of the gear wheel is calculated and with that the gaps between the flanks of the teeth in order to calculate the change in backlash.

5.3 Test parameters and calculations

To evaluate the geometry change of gear wheels as a function of the environment, the area of the pinion and the distance between adjacent teeth is measured. The pinion area is called A_{pin} and the distance between teeth is called space width e. It describes the distance between the teeth at the reference diameter d. But with an expanding gear wheel an expanding reference diameter comes along. And with that also the position of the space width measurement is changing. But in this work the change of space width at a fixed position relative to the axis shall be measured in order to determine the backlash change of the gearing system. In the context of this thesis it is called fixed space width e_{fix} and it describes the space width at 15 mm from the center of the pinion (Figure 5-1).

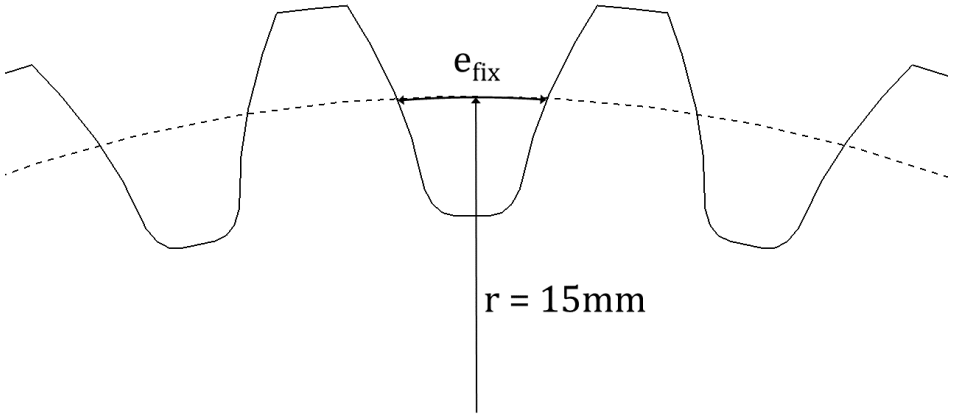

Figure 5-1: Space width

As described the data analysis is done with Matlab which delivers pinion area in mm² and space width in mm. The pinion area does not have to be preprocessed. The change in space width has to be converted to backlash change Δj. This is realized with the following equation:

$$\Delta j = 360° \cdot \frac{\Delta e_{fix}}{d \cdot \pi} \tag{40}$$

5.4 Testing

For the tests to identify the geometry change of the PEEK and POM gear wheel depending on the environmental condition, gear wheels with the same properties than those for the wear tests are used (Table 2-2): module 1, tooth number 30, and width 6 mm. The wheel is fixed on a 20 mm long shaft which is horizontal and points towards the camera. The shaft is used later to align the camera with the gear wheel. The shaft with the wheel is fixed on the mounting device which provides a rigid fixation and is insensitive against temperature changes. Directly behind the wheel a black surface is placed in order to create good contrast between the wheel and the surroundings. On the backside of the gear wheel (which cannot be seen by the camera) two thermo elements (Type K) are mounted in order to measure the actual temperature of the wheel. This is particular important since the knowledge of the exact temperature of the wheel is required for the evaluation of the geometry change. The thermo elements are connected with a NI cRio and are controlled with a LabView program.

The mounting device with the gear wheel is placed inside the thermal-vacuum chamber and the camera is positioned outside. With that solution a commercially available camera can be used which has not to be vacuum and temperature resistant. The pictures are taken through a window in the chamber. With pretests it was assured that taking photos through the window does not affect the results. As soon as the wheel is placed into the chamber, the chamber is closed. The camera is positioned in axial line to the shaft outside of the chamber. The correct alignment can be checked by watching at the shaft through the camera. As soon as only the front side of the shaft is visibly and not the long side, camera and shaft are in line. Once aligned, the test setup is not changed throughout the whole test which increases the accuracy of the measurement because the risk of changing alignment can be eliminated.

Photos are taken every hour and the first photo of the wheel is taken when the chamber is still pressurized and has room temperature (20°C). After that the chamber is evacuated down to a pressure of 10^{-5} mbar while holding the temperature constant to measure the influence of vacuum on the geometry of the wheel. This state is kept by about 12 hours. Than the temperature in the chamber is set to -55°C. The chamber takes about two hours to cool down but it takes about six hours until the gear wheel has the desired temperature. The two thermal elements on the back of the gear wheel provide its actual temperature. As soon as the wheel temperature stays constant at around -55°C for a couple of hours it is set to +80°C. It takes about three hours to warm up the chamber and eight hours to warm up the wheel. Again the hot temperature is kept for a couple of hours before the temperature is set back to room temperature. Back at 20°C another steady state condition is awaited and finally the chamber is pressurized to measure the geometry again at ambient environment and then the test is finished. Although photos are taken every hour, six measurements are particular interesting for comparing the geometry change: (1) ambient

pressure and ambient temperature, (2) vacuum and a temperature of 20°C, (3) vacuum and -55°C, and (4) vacuum and +80°C. But also the behavior of the wheels after the temperature cycle is measured. (5) Vacuum at 20°C (post test) and (6) ambient environment at 20°C (post test). See Figure 5-2 for an overview of the test cycle.

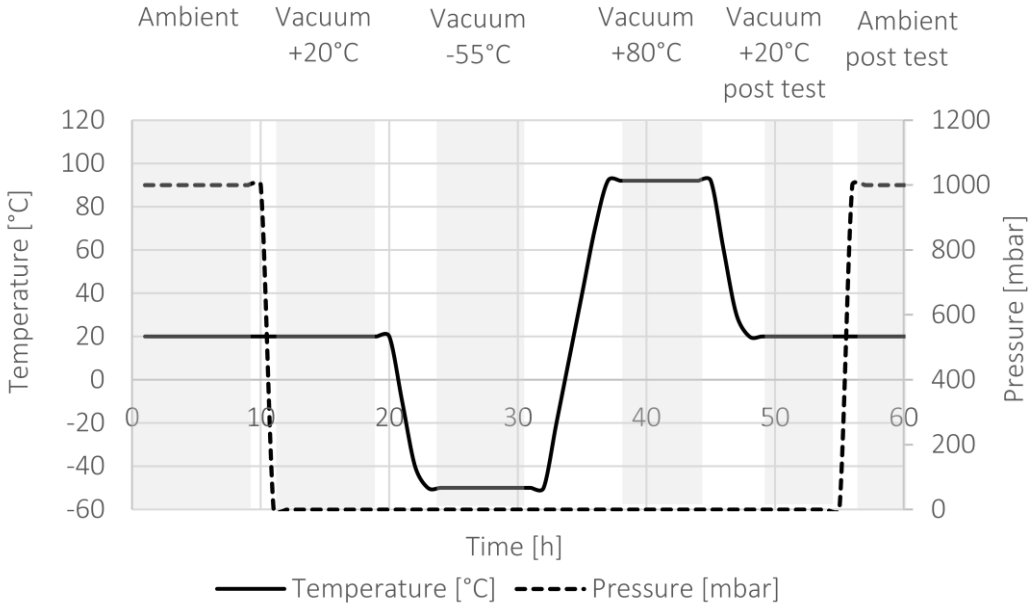

Figure 5-2: Test cycle overview

5.5 Results

The goal of this test is to describe the change in pinion area and space width as a function of the environment for gear wheels made out of PEEK and POM. The base environment to which all results are related to, is the so called ambient environment which means a pressure of 1 bar and a temperature of 20°C. The change relative to the ambient environment is particular interesting because it describes the change in geometry between integration in spacecraft on Earth and operating environment in space.

The absolute sizes of the PEEK and POM pinions are shown in Table 5-1 and its relative size change based on ambient environment is shown in Figure 5-3.

Environment	PEEK pinion size [mm²]	POM pinion size [mm²]
Ambient	696.42	699.26
Vacuum +20°C	695.32	698.28

Vacuum -50°C	689.71	688.32
Vacuum +90°C	701.62	711.80
Vacuum +20°C post test	695.36	698.01
Ambient post test	695.91	698.46

Table 5-1: Pinion size depending on environment

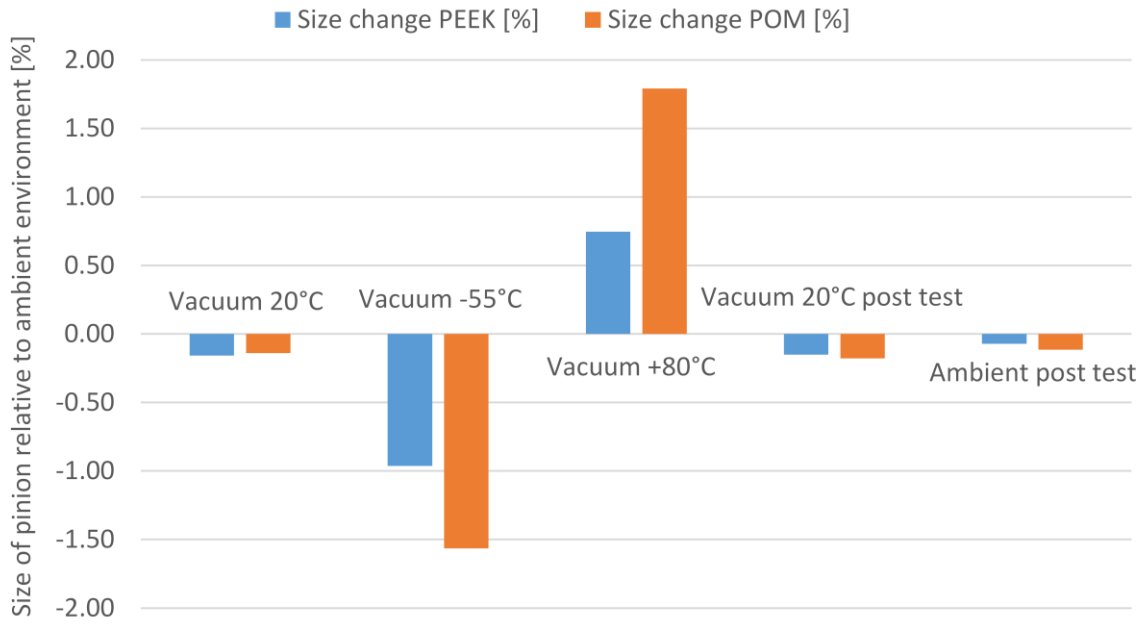

Figure 5-3: Pinion relative size change

Generally the two materials show a similar tendency in changing its geometry. PEEK as well as POM decrease their size in vacuum although temperature is not changed. PEEK is losing 0.16% of its original size, POM 0.14%. When cooling down the chamber until the wheels reach a temperature of -55°C, both pinions further decrease their sizes. PEEK by 0.96% and POM by 1.57%. When heating up the chamber to a gear wheel temperature of +80°C, the PEEK pinion increases by 0.75% and the POM pinion by 1.79% compared to their original size. When going back to +20°C (still in vacuum), the two pinions show a quite similar size compared to the first vacuum / +20°C measurement. The PEEK wheel is still 0.15% smaller the POM wheel 0.18%. When returning to pressurized environment at +20°C the two pinions still have a slightly changed size and do not return to their original size. The PEEK pinion is still 0.07% smaller, the POM pinion 0.11%. The error of the measurements is in the range of 0.001% and consequently not displayed in the plot.

As stated before, with the geometry variation, a change in backlash comes along. The numbers are shown in Table 5-2 and are plotted in Figure 5-4.

Environment	PEEK backlash change [°]	POM backlash change [°]
Vacuum +20°C	0.0019	0.0024
Vacuum -55°C	0.0122	0.0223
Vacuum +80°C	-0.0108	-0.0238
Vacuum +20°C post test	0.0017	0.0030
Ambient post test	-0.0005	0.0009

Table 5-2: Backlash change due to geometry variation

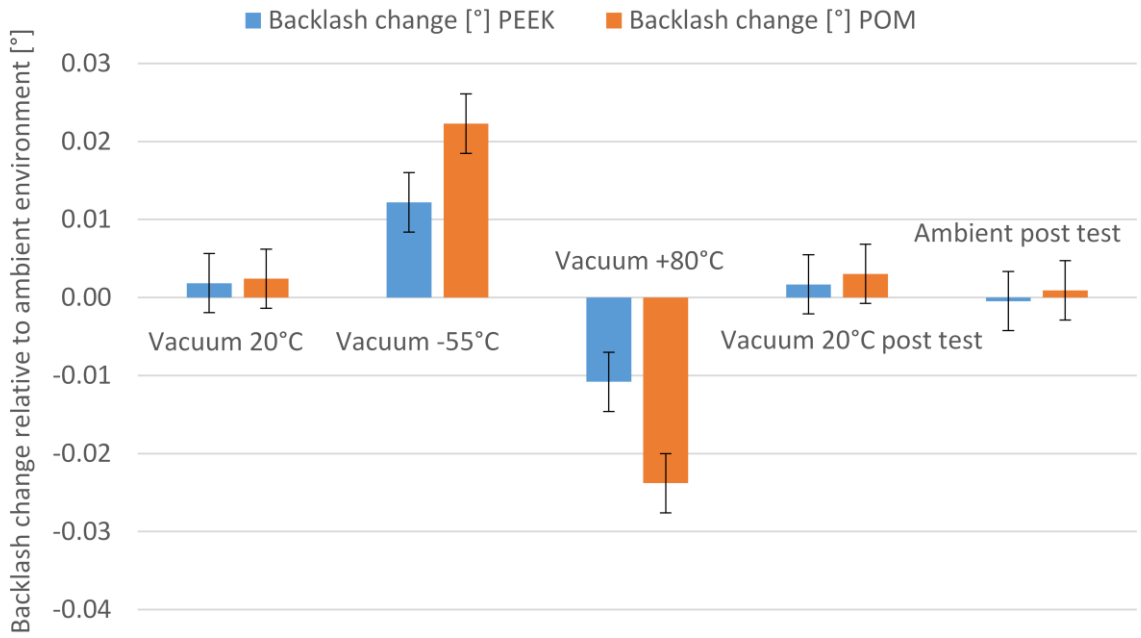

Figure 5-4: Backlash change relative to ambient environment

The backlash change, of course, is showing an opposite trend compared to the wheel size variation. A decrease of pinion size causes an increase in backlash. This can already be observed in vacuum conditions at +20°C. Due to the decrease in size, the backlash of a gearing system would increase by 0.0019° for PEEK gear wheels and by 0.0024° for POM wheels. In vacuum at -55°C the backlash increases further. The PEEK pinion would have a backlash of 0.0122° larger than in ambient environment, the POM pinion 0.0223°. When increasing the temperature to +80°C in vacuum, the backlash decreases. For the PEEK wheel by 0.0108°, for the POM wheel by 0.0238°. This means, in total there is a backlash

change between the -55°C and +80°C environment of 0.0302° for PEEK gear wheels and 0.0461° for POM gear wheels. Returning to +20°C in vacuum environment the backlash change also returns to numbers comparable to the numbers at the beginning. When pressurizing the chamber, the backlash change compared to the starting backlash almost vanishes. Only 0.0005° are left for the PEEK pinion and 0.0009° for the POM pinion. The standard deviation for this test is 0.0038° and is displayed in the plot with error bars.

5.6 Discussion

The test method, to take pictures of the gear wheels in order to measure the geometry, proved to be a good alternative to other methods. Especially to place the camera outside of the chamber and take the pictures through the window simplified the test a lot. The accuracy seems to be absolutely sufficient for the measurements conducted in this thesis. Another important factor for high test quality, is to provide steady state conditions (for pressure and temperature) at the gear wheels. Therefore a high degree of automatically test operations is required. With that the tests can be run over night and enough time to reach steady state conditions can be provided. Also mounting two thermo-elements at the pinion to measure the actual temperature proved to be important because a temperature difference between thermal-vacuum chamber shroud and gear wheel of up to 3°C was observed. Not only for higher accuracy but also for easier evaluation of the taken pictures it turned out that equal camera settings (aperture and time of exposure) is helpful. Another step towards high test accuracy was reached by not changing the camera–gear wheel alignment throughout the test. Even if there was a slight misalignment, the same error affects all the photos and since only relative statements are made, the error cancels out.

The change in size of the pinion has two reasons which have to be evaluated separate: vacuum and temperature. Due to exposing the gear wheels to a vacuum environment of $1 \cdot 10^{-5}$ mbar (and keeping the temperature constant) their size decrease by 0.16% (PEEK) and 0.14% (POM). Compared to the temperature influence, this change is rather small but nevertheless it cannot be neglected. The decrease of size can be generally explained by the outgassing of the synthetic materials. Although they provide good vacuum compatibility compared to other polymers, they still have volatiles which escape in vacuum environment. Temperature, of course, has a bigger influence on the size of the gear wheels. PEEK has a coefficient of thermal expansion (CTE) of $50 \cdot 10^{-6}$ 1/K, POM of $110 \cdot 10^{-6}$ 1/K. Therefore it is obvious that POM shows larger size variation than PEEK. The CTE ratio of 2.2 can also be observed when comparing the size change of PEEK and POM at +80°. At -55°C the difference is smaller. Only 1.6. This might be explained with a rather unknown behavior of the two synthetic materials at these low temperatures. Probably the CTEs of PEEK and POM are not constant over this large temperature range.

In terms of space mechanism accuracy, the backlash change in a gearing system is much more relevant than the size change of the wheels. When testing a mechanism on ground, the engineer has to know how backlash develops as soon as the spacecraft is in orbit and is exposed to vacuum and extreme temperatures. Similar to the other tests, the temperatures go from -55°C up to +80°C because this seems to be the most popular temperature range for space mechanisms. But since mechanisms often are mounted inside the spacecraft in a quite protected environment the temperature range might be even small but nevertheless, during this evaluation, the rather extreme temperatures are assumed. Similar to the wheel size test, the backlash change also has to origins: the vacuum and the temperature. But in this case the vacuum effect can be neglected because its influence on backlash is quite small (0.0019° and 0.0024°) and with a standard deviation of 0.0038 the significance of the numbers is limited. When looking at the backlash change due to different temperatures, the results show a favorable behavior for the PEEK pinion compared with the POM pinion. Because of the low coefficient of thermal expansion, also the temperature influence on the backlash is smaller for gear wheels made out of PEEK. But even for the PEEK wheels the backlash change is in the range of 0.01° at extreme temperatures compared to the 20°C baseline. For POM the change is around 0.022°. This results in a total backlash change between -55°C and +80°C of 0.023° for PEEK and 0.0461° for POM. Referring back to Table 1-3 where the accuracy requirements of different space mechanisms are summarized, it can be seen that especially pointing mechanisms often require accuracies better than 0.01° and this can neither be accomplished with PEEK pinions nor with POM pinions. At least in the large temperature range. Whereas for deployment or rotating mechanism the accuracy might be good enough. They often do not require accuracies better than 0.1° and this can be accomplished with both gear wheels. Independent of the type of mechanism there is one thing that has absolutely be taken into account during design. The decrease of tooth distance at high temperatures. This can become a problem as soon as not enough backlash is left in a gearing system. In that case the two gear wheels may get loaded when expanding due to the higher temperatures. This results in an increase of friction and a larger wear coefficient. Also the wheels may even get stuck because the motor power is no longer larger enough to provide enough torque to turn the wheels. In extreme scenarios teeth could even break.

5.7 Summary

This test had the objective to evaluate the geometry of a PEEK and a POM pinions as a function of the test environment. From the geometry, conclusions on the backlash of a gearing system can be drawn. It was assumed that backlash changes depending on the different test environments. And since backlash is one of the key parameters in the design of space mechanisms, an own test series was conducted to evaluate its behavior. A test setup was developed to monitor and measure the geometry of the wheels at the test

environments ambient conditions, vacuum at 20°C, vacuum at -55°, and vacuum at +80°C. From the measurement the change in gear wheel size and the change in backlash was calculated. The results for the size showed an expected behavior for both materials. A slightly decrease in size for vacuum conditions and a larger variation at the extreme temperatures. Thereby the polymers performed corresponding to their coefficients of thermal expansion. The backlash calculation showed an insignificant change in backlash at vacuum at 20°C compared to a pressurized environment at 20°C. The critical issue is the backlash behavior at low and high temperatures. A total change in backlash by 0.023° for PEEK and 0.0461° for POM was observed. For high accuracy pointing mechanisms, these numbers are too large. Whereas for deployment or rotating mechanisms, the wheels might still meet the requirements.

Overall one could state, that gear wheels made out of PEEK and POM, which are exposed to extreme temperatures from -55°C to +80°C, are not applicable in space mechanisms which require accuracies better than 0.03° (PEEK) to 0.05° (POM). But if these accuracies are not required, PEEK and POM might still be interesting material alternatives for space gear wheels.

6 Gear Tooth Temperature

6.1 Test objective

Polymers are more sensitive to higher temperatures than metallic. The determination of a synthetic pinion's temperature is absolutely necessary [48]. For example PEEK has a dimensional stability at heat of 152°C and POM of only 110°C. Consequently one has to make sure that the critical temperature of the polymer gear wheels is not exceeded during operation. Although the temperatures in mechanisms usually are lower than 152°C, respectively 110°C, due to friction between the teeth of the wheels, a locally increase of temperature may happen and the critical temperature may be exceeded. In space environment that risk is even higher, because with the absence of air, no conductive heat transfer from the pinions to the air is possible and consequently the polymer is heated more. An accurate calculation of the gear wheel's temperature is very difficult because the heat dissipation of rotating wheels can only be estimated roughly [48].
The objective of this test is to measure the heating of the gear wheel tooth during operation in order to find out whether the critical temperature is reached or not. The test is conducted at different turning velocities to be able to detect a possible velocity dependence of the temperatures. Furthermore the influence of vacuum on the temperature behavior of the pinions shall be detected because no information in literature was found that describes the temperature development in a gear wheel at vacuum environment.

6.2 Test method

The idea of the test is to measure the temperature at the tooth of the gear wheel during operation. For redundancy reasons two teeth are measured at each wheel. The tests are conducted as a function of turning velocity, environment, and gear wheel material. As material, like in all the other tests, PEEK and POM are used. To study the temperature dependency on vacuum as well as on temperature four different test environments are defined: (1) ambient at +20°C, (2) vacuum at +20°C, vacuum at +80°C, and vacuum at -55°C. In each environment three different velocities are run: 15, 30, and 60 revolutions per minute in order to test the influence of velocity on the temperature development.

6.3 Test parameters and calculation

Similar to the wear and geometry test, also for the measurement of gear tooth temperature a 30 mm pinion is used. Also the 120 mm diameters steel counter wheels is the same. The test parameters are summarized in Table 6-1.

Parameter name	Symbol	Unit	Value
Torque at pinion	M_T	Nm	0.3
Revolutions per minute	n_1, n_2, n_3	1/min	15, 30, 60
Axis distance	a	mm	75.3

Table 6-1: Gear tooth temperature test parameter

The temperatures at the wheels are measured at three different turning velocities n_1, n_2, n_3. These numbers can be calculated into turning velocity v_1, v_2, v_3, and angular velocity ω_1, ω_2, ω_3 (Table 6-2).

	Test 1	Test 2	Test 3
Revolutions per minute n [1/min]	15	30	60
Turning velocity v [m/s]	0.024	0.047	0.094
Angular velocity ω [°/s]	90	180	360

Table 6-2: Turning velocities during tooth temperature test

6.4 Testing

In order to measure the temperature of the gear wheels, a small hole is drilled into the wheel's tooth and a temperature sensor is place inside the hole (Figure 6-1). With that the core temperature can be measured during operation. The position of the hole was drilled as close to the flank as possible. Because due to friction at the flank, it is believed, the largest temperature increase would happen near the flank. The bore hole has a diameter of 0.5 mm. The tip of the temperature sensor has a diameter of 0.6 mm and is carefully inserted in the bore hole. With the slightly larger size of the sensor, it is made sure that the sensor is in uniform contact with the synthetic material and that there is no gap between sensor and the wall of the bore hole. Especially in vacuum condition a little gap would falsify the results.

Figure 6-1: Gear wheel teeth with drilled holes

The test setup is quite similar to the wear test since the same test rig is used. The tested 30 mm pinion and its steel 120 mm counter wheels are preloaded by 0.3 N·m which is roughly the maximum the test rig can handle before results are getting inaccurate. The value of the preloaded torque can be determined with strain gauges at the pinion shaft. With that the actual load acting at the pinion is known quite precisely. After preloading the wheels, the test rig is placed into the thermal-vacuum (TV) chamber. Also the tests in ambient environment are conducted inside the chamber in order to provide equal test conditions. As mentioned before, the temperature of two teeth at each pinion are monitored throughout the test. Also the motor temperature is measured in order to stop the test in case the motor is getting too hot. All the temperature sensors are type K sensors and are compatible with the TV chamber. Since the temperature sensors are mounted on the pinions, an infinite rotation of the wheels is no longer possible. The idea of integrating a slip ring, in order to provide unlimited rotation, would have been way too complex and was excluded pretty soon since another and much simpler solution was possible. Instead of turning the wheel infinite, it is only turned back and forward by 180°. With that cycle solution no unlimited rotation is required and also different turning velocities can be chosen. To operate and monitor the test basically the same LabView program is used as for the wear test. Only slightly modifications had to be made in order to allow the back and forward motion with a certain velocity. Beside the program to operate the test rig, another program is used to control the TV chamber. It is also based on LabView and controls the vacuum pumps as well as the thermostat. The program allows to choose steady-state conditions for the different thermo-elements. With that the maximum temperature change per time can be defined in order to know when a certain thermo-element reaches steady-state condition.

Before the measurement can start, the test rig is placed inside the TV chamber and all the required thermo-elements are connected. For the ambient environment test, obviously the

vacuum pumps are not turned on. Only the thermostat controls the temperature at 20°C. It is waited until steady-state condition is reached. Steady-state is defined for all tests as a temperature change of less than 0.1°C within 30 minutes. This value was chosen from experience from other tests and as a good compromise between test accuracy and test duration. For the 20°C ambient and also vacuum environment it takes about six hours until steady-state is reached. For 80°C and -55°C vacuum environment, steady-state condition was not reached before 24 hours. As soon as having steady-state the motor is started in order to cycle the pinion back and forward at a velocity which corresponds to 15 revolutions per minute. Not before the new steady-state temperature at the pinion is reached, the velocity is increased to 30 revs/min and then further to 60 revs/min. When finishing one test series with the three different velocities the motor is stopped and the next test environment is set. But again the next test series is not started before steady-state is reached. For the tests in vacuum conditions, the pressure inside the chamber is regulated to be $1 \cdot 10^{-5}$ mbar. Throughout the whole test the pinion temperatures are recorded for later evaluation at a sample rate of 1 Hz.

6.5 Results

The following plots show the temperature development of the PEEK and POM pinions at different turning velocities at different test environments. For easier comparison of the four plots, the scale in x-axis is kept the same. The first plot (Figure 6-2) shows the temperature at the teeth of the wheels at ambient environment, the second plot (Figure 6-3) at vacuum condition at 20°C, the third one (Figure 6-4) at vacuum environment at 80°C, and the fourth plot (Figure 6-5) at vacuum condition at -55°C. The standard deviation is the same for all measurement: 0.07°C.

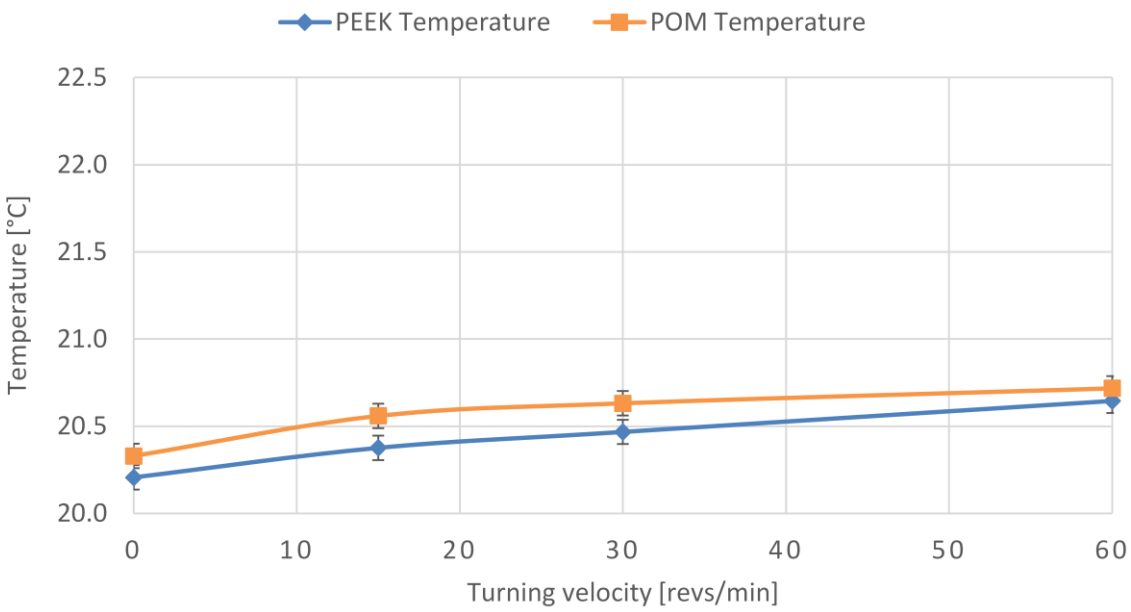

Figure 6-2: Tooth temperature at ambient environment

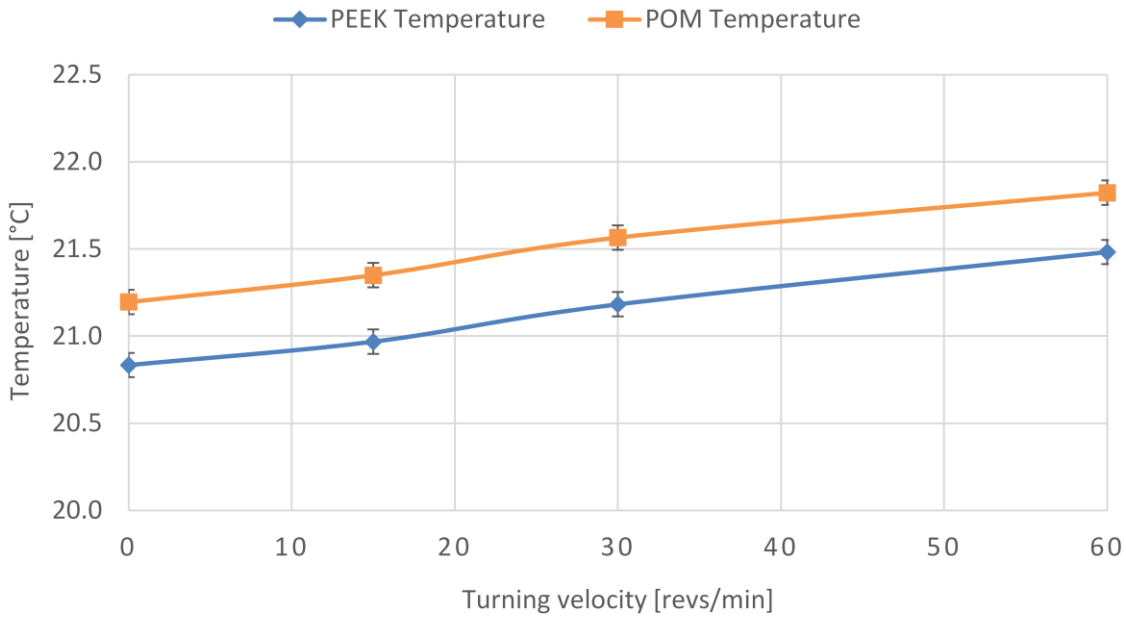

Figure 6-3: Tooth temperature at vacuum 20°C environment

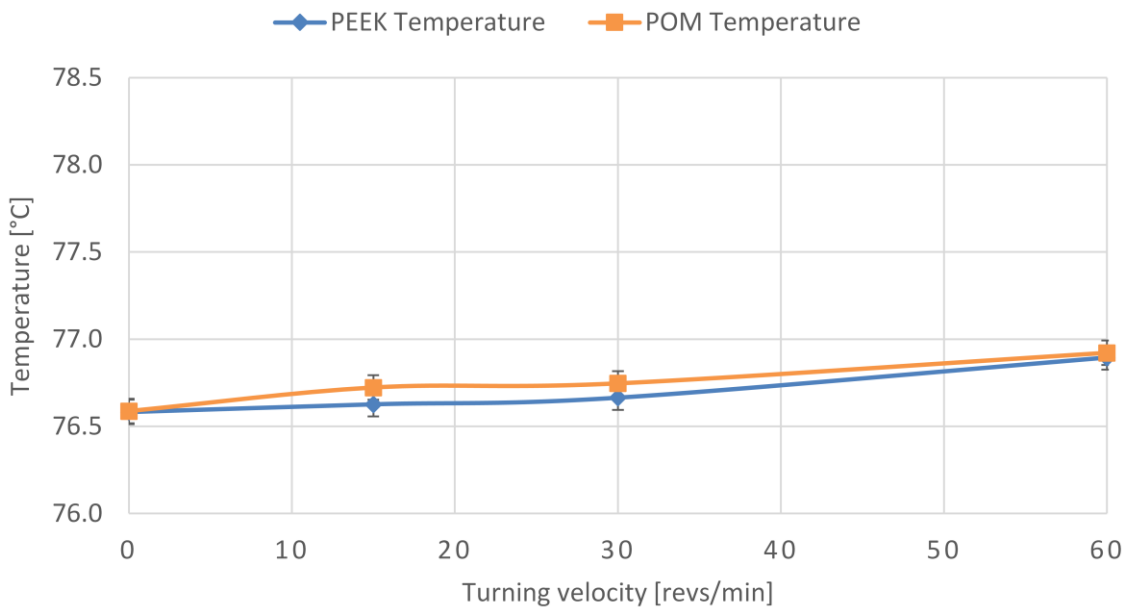

Figure 6-4: Tooth temperature at vacuum 80°C environment

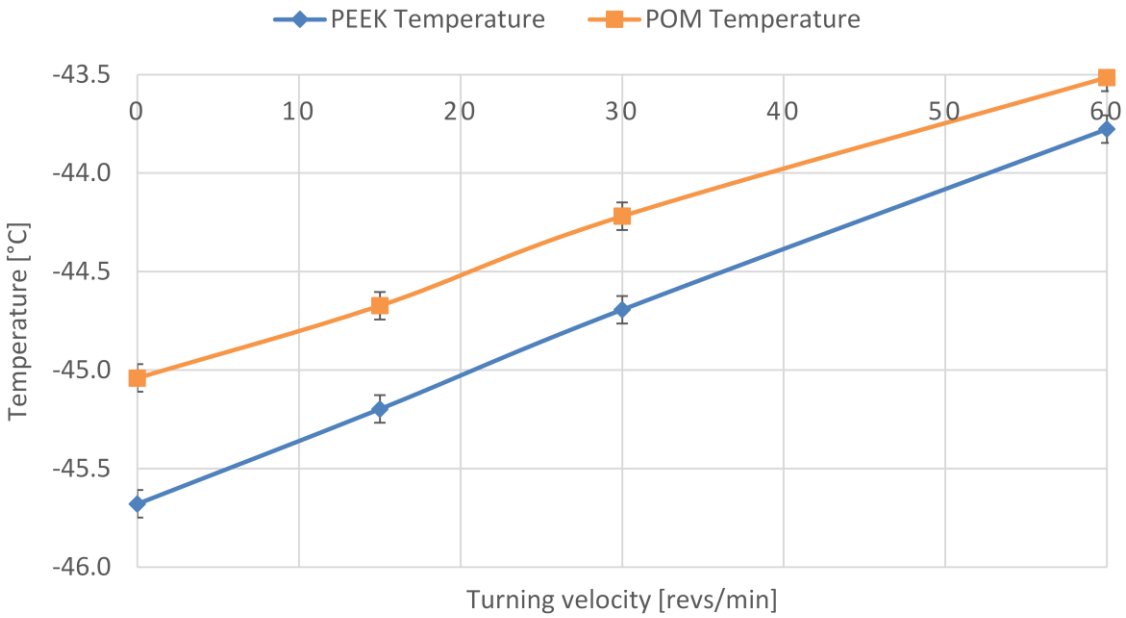

Figure 6-5: Tooth temperature at vacuum -55°C environment

In all plots four data points are given for each gear wheel. The data points describe the tooth temperature when standing still and at velocities of 15, 30, and 60 revolutions per minute. Therefore the average of the two thermo-elements was calculated. All charts show an increasing tooth temperature for increasing velocities. For the vacuum condition at -55°C

the change in temperature is largest. In average POM has a higher temperature level than PEEK.

For better illustration of the temperature change depending on the environment, Figure 6-6 is used. At a constant turning velocity of 60 revolutions per minute, the change in temperature compared with the starting temperature (still standing wheel) is shown. It can be seen, the largest temperature change happens at vacuum conditions at -55°C.

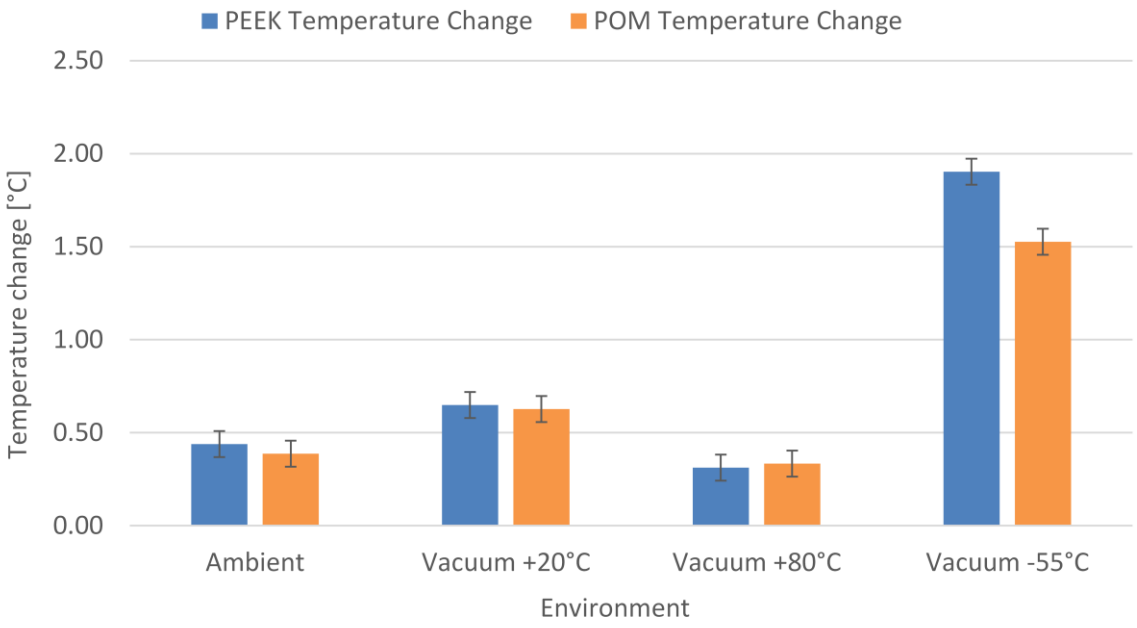

Figure 6-6: Temperature change as a function of environment

6.6 Discussion

The most important conclusion derived from the results of the test is that the critical temperature of neither PEEK nor POM is exceeded. This was a big concern for polymer gear wheels and the main motivation for conducting the tests. Even for the test series at environmental conditions of vacuum and 80°C the gear tooth temperature only rises by 0.4°C and is far away from the critical 152°C (PEEK) and 110°C (POM). But nevertheless one has to take into account that the temperature is measured at a distance of about 0.5 mm from the flank. That means that the actual temperature at the tooth flank might be larger than the measured temperature at the center of the tooth. For two reasons it is assumed that even at the tooth flank the critical temperature is not exceeded. First, the increase in temperature of only 0.4°C at the tooth is too small to expect an increase of more than 30°C at the flank. And second, a melting of the tooth flank happens according to [64] not before

a turning velocity of 5m/s, and that is not reached during the applications in the context of this work.

When having a first look at Figure 6-2 to Figure 6-5, one recognizes a deviation of the gear wheels starting temperature from the environment temperature. The reasons therefore are losses and inaccuracies at the thermal-vacuum chamber. When setting a certain temperature at the TV chamber only means that the temperature of the thermo fluid has that temperature. The actual temperature inside the chamber varies by up to 5°C depending on the heat transfer. But for these tests more important than the actual temperature inside the chamber is its constancy at the gear wheel. And this is accomplished with the mentioned steady-state criteria.

In general the temperatures of PEEK and POM show a quite similar pattern throughout the tests. This has to do with the steady-state criteria. With that, both materials is given enough time to reach a constant temperature. For ambient and vacuum 80°C environment the temperatures are even equal, aside from measurement inaccuracies. At vacuum 20°C and vacuum -55°C, there is a difference between the PEEK and POM temperatures, even at the beginning of the test series. This might be a results of the test setup. The POM gear wheel is located closer to the motor and might receive some radiation from the motor which results in a slightly increase of temperature. But since the objective of the test is to detect any critical temperature changes, the absolute temperature is secondary and consequently the reason for a difference in temperature between PEEK and POM is not of larger interest.

In Figure 6-6 the temperature change relative to the still standing gear wheel is plotted at a turning velocity of 60 revs/min. The largest of the three velocities was chosen on purpose because at 60 revs/min the change in temperature is largest and with that the results are more significant. The chart shows an increase of temperature change between ambient and vacuum conditions, both at 20°C. This is a consequence of vacuum. No heat can be exchanged with air, hence the temperature rises. But overall, with an increase in the range of 0.3°C, the difference between ambient and vacuum is rather low and should not have an impact on the design of a space mechanism. The temperature change at vacuum 80°C is smallest. This might have to do with the large temperature level of 80°C. This conclusion is supported by the results of the temperature change at -55°C. At that temperature the difference is largest. Probably because of the overall low temperature, the heating caused by the motion of the wheel has a larger effect and can be detected better than at larger temperatures. Also the difference in temperature change between PEEK and POM is only significant at -55°C vacuum environment. The reason for that might be the different thermal conductivity of PEEK and POM. PEEK has a thermal conductivity of 0.25 W/(m·K), POM of 1.5 W/(m·K). Hence, POM transfers heat from the tooth to the core faster than PEEK and consequently the tooth is not heated so much.

The linear trend of the temperature as a function of velocity means an equal heating of the gear wheel. With that the temperature development of higher velocities can be estimated carefully.

6.7 Summary

The idea of the test series was to measure the gear wheel tooth temperature as a function of turning velocity and environment in order to identify a possible exceeding of the critical temperature of the polymers PEEK and POM. PEEK is dimensional stable up to a temperature of 152°C, POM up to 110°C. Both limits were not reached during testing. Even at an environment of 80°C and vacuum the temperature at the gear wheel does not even come close to the limit temperature. Also the influence of vacuum on the temperature development is rather low. A dependency of the temperature on the turning velocity was detected, but with the pretty small rotational velocities in the application of most of the space mechanisms, problems should not occur.

The results of this test are definitely valid for velocities up to 60 revs/min (360°/s). Referring back to Table 1-3 where mechanism specifications are summarized, none of the listed mechanisms requires a turning velocity of more than 360°/s. Consequently one could state that exceeding the critical temperature is not an issue for PEEK and POM gear wheels during the application in common space mechanisms.

7 Gearing quality

Due to manufacturing inaccuracies, it is not possible to build gear wheels mathematically accurate. Therefore one has to allow tolerances in the manufacturing process and the gearing quality has to be specified for every gear wheel. Based on measurements at the wheels, individual and total variations can be described and the manufactured gear wheel can be classified in a certain accuracy (quality) group. Quality 1 stands for the highest, hardly to manufacture, accuracy. Quality 12 means lowest accuracy. Usually Quality 1 to 4 is rarely used because manufacturing is expensive. Only for high accuracy measuring instruments these qualities are applied. In general, Quality 7 to 10 are used in common engineering applications. The different quality groups are specified in DIN 3967. Several parameters play a role in describing gearing variations [34]:

- Flank variation
- Pitch variation
- Concentricity variation
- Axis variation
- Working variation

The flank variation describes the difference between actual and specified flank surface. It considers the profile of a tooth in transvers section plane. The pitch and concentricity variations are the most relevant parameters for this work and are therefore described later. The axis variation defines the slope between two axis and the working variation considers the axis distance between the wheels and other orientation parameters.

Pitch and concentricity variation are particular interesting in the context of this work because they consider pitch distance errors and radial position differences which might play a role in backlash evaluation. The relevant parameters are summarized in Table 7-1.

Name ***German translation***	**Symbol**	**Unit**
Individual pitch variation *Teilungs-Einzelabweichung*	f_p	µm
Total pitch variation *Teilungs-Gesamtabweichung*	F_p	µm
Pitch fluctuation *Teilungsschwankung*	R_p	µm
Pitch error *Teilungssprung*	f_u	µm
Concentricity variation *Rundlaufabweichung*	F_{rl}	µm

Table 7-1: Gearing quality parameters [34]

The individual pitch variation f_p defines the difference between the actual and specified circular pitch p_t measured at the reference diameter for one certain tooth. With measuring the individual pitch variation on all teeth of the gear wheel, the pitch fluctuation R_p can be calculated, which is the difference between the largest and smallest f_p value at a gear wheel. Furthermore, the pitch error f_u considers the absolute value of the difference between two consecutive individual pitch variations. With the total pitch variation F_p the largest possible rotation angle variation can be described. The concentricity variation F_{rl} considers eccentricity and center offset, as a consequence of pitch variation.

During the test program of this thesis a total of eight 30 mm pinions have been fabricated. Four made of PEEK and four made of POM. All wheels were fabricated at the same company with the same tools. Prior to each test series their quality parameters were determined with the 3D measurement unit. The pitch and concentricity variations of these measurements are summarized in Table 7-2 for PEEK and Table 7-3 for POM:

Symbol	Unit	PEEK 1		PEEK 2		PEEK 3		PEEK 4	
		left	right	left	right	left	right	left	right
f_p	µm	9.2	9.1	12.8	10.4	12.4	11.1	6.9	8.2
F_p	µm	49.5	52.1	73.0	72.3	77.3	76.7	47.5	50.5
R_p	µm	17	14.4	23.1	19.9	24.4	21.4	13.3	15.2
f_u	µm	6.6	8.2	7.1	6.4	7.1	5.1	5.5	6.8
F_{rl}	µm	39.0		63.2		66.4		35.5	

Table 7-2: Pitch and concentricity variation for PEEK pinion

Symbol	Unit	POM 1		POM 2		POM 3		POM 4	
		left	right	left	right	left	right	left	right
f_p	µm	10.4	8.7	10.7	9.8	11.6	10.6	8.4	8.6
F_p	µm	79.9	78.9	82.4	85.5	89.4	90.1	55.5	56.7
R_p	µm	20.2	17.3	20.6	18.9	21.8	20.8	13.8	14.8
f_u	µm	11.8	3.6	3.3	3.4	5.3	6.8	3.6	4.6
F_{rl}	µm	71.0		73.6		80.5		47.6	

Table 7-3: Pitch and concentricity variation for POM pinion

With these measurements one has the possibility to decide whether the fabrication accuracy is good enough for the application as space gear wheels and what repeatability in fabrication is possible. From the results of the measurement, three different aspects of synthetic gear wheel machinability can be considered:

(1) Quality difference in the fabrication between PEEK and POM

One important question comes up, when fabricating PEEK and POM gear wheels: Is the fabrication quality the same or can one material be machined better than the other one. This can be answered by comparing the different variation parameters and there is no sign that one material has better fabrication properties (better quality) than the other one. This can be shown by comparing the mean values and standard deviations of the specific parameters (Figure 7-1). Although the mean values show a small difference, their standard deviation is quite large and consequently no significant variation can be identified.

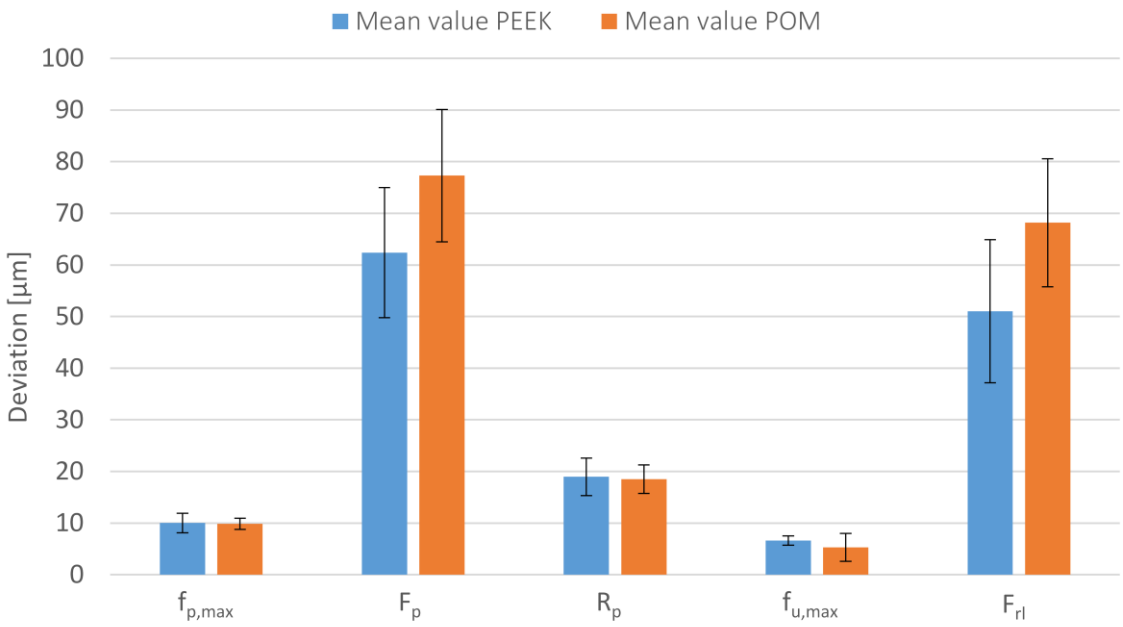

Figure 7-1: Quality difference in the manufacturing of PEEK and POM pinions

(2) Concentricity fluctuation of the synthetic gear wheels

When evaluating the accuracy of synthetic gear wheels it has to be determined what variation the gaps between the teeth have depending on the position of the wheel. Because a variation in the gap results in a change in backlash which is a critical parameter in space mechanisms. A variation in gap may result from eccentricity and center offset of the gear wheel due to manufacturing errors. This offset is described with the concentricity variation factor F_{rl}. The mean values of F_{rl} are already given in Table 7-2 and Table 7-3, but to make a statement about backlash change the positive and negative variations from the theoretically fabricated value are required. These numbers are given in Table 7-4 and Table 7-5. From these numbers the corresponding quality class can be derived which is also shown in the table. In the same table the change in backlash due to the concentricity variation is listed.

	PEEK 1	PEEK 2	PEEK 3	PEEK 4
Positive concentricity variation $F_{rl,pos}$ [mm]	17.7	33.9	33.3	19.2
Negative concentricity variation $F_{rl,neg}$ [mm]	21.3	29.4	33.1	16.3
Corresponding quality	9	11	11	9
Positive backlash change [°] due to $F_{rl,pos}$	0.05	0.09	0.09	0.05
Negative backlash change [°] due to $F_{rl,neg}$	0.06	0.08	0.09	0.05

Table 7-4: Backlash change due to concentricity variation for PEEK pinion

	POM 1	POM 2	POM 3	POM 4
Positive concentricity variation $F_{rl,pos}$ [mm]	36.4	35.0	38.4	19.2
Negative concentricity variation $F_{rl,neg}$ [mm]	34.6	38.6	42.1	28.3
Corresponding quality	11	11	12	10
Positive backlash change [°]due to $F_{rl,pos}$	0.10	0.10	0.11	0.05
Negative backlash change [°] due to $F_{rl,neg}$	0.10	0.11	0.12	0.08

Table 7-5: Backlash change due to concentricity variation for POM pinion

The numbers from Table 7-4 and Table 7-5 show a gearing quality for concentricity of the gear wheels in the range between 9 and 12. This is at the lower end of the quality classification and means a loss in accuracy. The low accuracy results in backlash changes of up to 0.12° compared to the theoretical value. Considering the difference between maximum positive and maximum negative backlash change, in the worst case even a backlash change of 0.23° is possible. And this is no longer acceptable for high accuracy space mechanisms. Consequently the milling method applied in the manufacturing process for the gear wheel for this thesis has to be improved in order to get more accurate pinions. That this is possible is described in [34] where quality classes up to 8 or 9 are stated for synthetic gear wheels.

For the tests described in this work, the low accuracy of the gear wheels is no issue. The wear test, for example, compares one specific tooth before and after operation and consequently any variation which depends on the circumferential position of the gear wheel is irrelevant. Also the gear tooth temperature test only considers one specific tooth. With the geometry test a relative change at different environments is measured and thus any absolute variations cancel each other out.

(3) Overall quality of the synthetic gear wheels

Beside the quality class for concentricity fluctuation, also the quality classes for the other pitch parameters can be calculated with the numbers from Table 7-2 and Table 7-3. They are summarized in Table 7-6 and Table 7-7 for the different PEEK and POM gear wheels.

	PEEK 1		**PEEK 2**		**PEEK 3**		**PEEK 4**	
	left	right	left	right	left	right	left	right
f_p – Quality class	8	8	8	8	8	8	6	7
F_p – Quality class	9	10	10	10	10	10	9	10
f_u – Quality class	6	7	6	6	6	5	5	6

Table 7-6: Overall quality of PEEK gear wheel

	POM 1		**POM 2**		**POM 3**		**POM 4**	
	left	right	left	right	left	right	left	right
f_p – Quality class	8	7	8	8	8	8	7	7
F_p – Quality class	10	10	11	11	11	11	10	10
f_u – Quality class	8	4	4	4	5	6	4	5

Table 7-7: Overall quality of POM gear wheel

The results show a moderate quality for individual pitch variation f_p, a low quality for total pitch variation F_p, and a good quality for pitch error f_u. Similar as stated before, these numbers can be improved by better fabrications methods but do not influence the tests described in this thesis.

8 Concluding Discussion, Summary, and Future Work

8.1 Concluding discussion

After reaching the objective of this work to test the most important gearing parameters of polymer gear wheels in space environment, it is now possible to evaluate their applicability in space mechanisms. In chapter 1.3.1, three different categories of mechanisms were described, each with different requirements. Deployment mechanisms with large loads but a cycle number of one, rotating mechanisms with moderate accuracy but large cycle numbers, and pointing mechanisms with high accuracy requirements but medium cycle numbers. In the following for each mechanism group, the applicability of the PEEK and POM gear wheels shall be discussed.

8.1.1 Backlash

The two main gear wheel characteristics evaluated in this thesis are backlash and strength. Backlash is influenced by wear, environmental impact, deformation of teeth, and gearing quality. All of these parameters have been tested in this work and been described in the last chapters. It turned out that deformation of teeth does not play a critical role at rather low loads which occur at space mechanisms. The gearing quality is a very important parameter and has to be considered when manufacturing gear wheels. As the tests showed, a gearing quality of nine or worse is not sufficient for the high accuracy demands in space mechanisms. Therefore gearing qualities in the range of five to six is recommended regarding the specific requirements of the mission.

Leaving wear and environmental impact on the geometry as the parameters to be discussed in order to find appropriate application fields of polymer gear wheels. In terms of backlash, deployment mechanisms are rather uncritical. Often accuracies of 1° is enough and since cycle number is one, no wear has to be considered over mission duration. The maximum backlash change due to environmental impact on the geometry of the pinions is in the range of 0.05° for POM and 0.025° for PEEK. Consequently, regarding backlash, both materials work for deployment mechanisms.

For rotating mechanisms the requirements change completely. The cycle numbers go up to 90 000 000 and loads of 10 N·m can occur. Although this is the worst case scenario, one has consider these numbers. In Figure 8-1 the change in backlash as a function of number of revolutions is shown for PEEK and POM in vacuum 20°C environment and a load of 1 N·m.

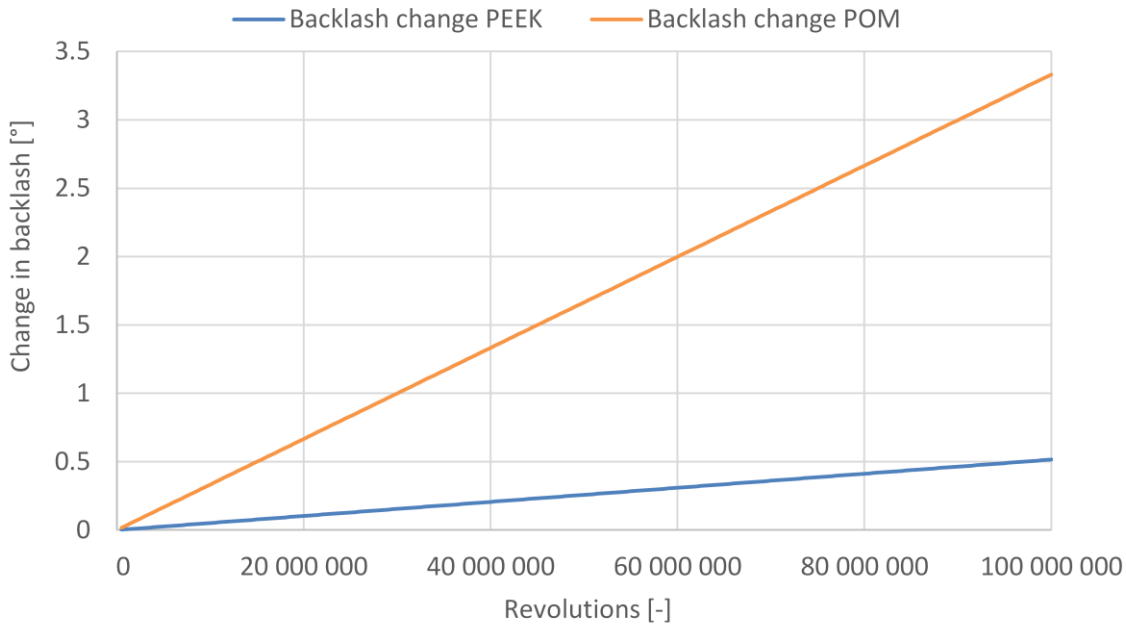

Figure 8-1: Change in backlash as a function of revolutions for a load of 1 N·m

It is getting obvious that for high cycle applications polymer gear wheels have shortcomings. After 100 000 000 revolutions, the increase of backlash for a POM pinion goes up to 3° which basically means gear wheel failure. PEEK would have an increase of backlash of 0.5° which might still be tolerable for some applications. Things look even worse when an applied load of 10 N·m is assumed (backlash rises by a factor of 10 compared to 1 N·m). In that case POM is not appropriate at all anymore and the backlash increase of PEEK would exceed 1° after 200 000 revolutions. And for extreme temperatures the numbers would even get worse since the wear coefficient at 20°C is the best compared with 80°C and -55°C. The effect of environmental caused geometry change can be neglected compared to the influence of wear.

Overall it can be concluded that for high-cycle rotating mechanisms at loads larger than 1 N·m, polymer gear wheels are not the best choice. POM cannot be recommended at all, and PEEK might be applicable as long as accuracy requirements are not too strong (<0.3°) and cycle number stays in the range of 50 000 000 or lower.

Pointing mechanisms differ from rotating mechanisms in higher accuracy requirements but typically lower loads and fewer cycle numbers. For pointing mechanisms both components that influence backlash have to be taken into account: wear as well as temperature caused geometry change. This makes discussing the results difficult because both effects have to be evaluated at once. Therefore we look at two possible scenarios and make some simplifications in order to be able to display the behavior of the backlash clearly.

In the first scenario we assume a low Earth orbit application where temperatures vary between -55°C and 80°C. The wear coefficient is chosen to be an average of the wear coefficients at -55°C, 20°C, and 80°C, however the 20°C coefficient is counted twice since transition from hot to cold environment and cold to hot has to be considered during one orbit. Consequently the average wear coefficient for PEEK is calculated as followed:

$$k_{w,PEEK,ave} = \frac{2 \cdot k_{w,PEEK,20} + k_{w,PEEK,80} + k_{w,PEEK,-55}}{4} = 15.6 \cdot 10^{-6} \frac{N \cdot m}{mm^3} \quad (41)$$

For the POM gear wheel:

$$k_{w,POM,ave} = \frac{2 \cdot k_{w,POM,20} + k_{w,POM,80} + k_{w,POM,-55}}{4} = 75.6 \cdot 10^{-6} \frac{N \cdot m}{mm^3} \quad (42)$$

It is understood that the temperature at the gear wheel would not change that fast, but assumptions have to be made and since the wear coefficient is worse at the extreme temperatures, this can be considered as worst case scenario.

In the mentioned Earth orbit the backlash of the gearing system depends on two things. First, the temperature at the gear wheel and the so caused change in geometry. And second, the number of revolutions the gear has been running and the so caused wear. The change in backlash at the three gear wheel temperatures 20°C, 80°C, and -55°C is shown for PEEK in Figure 8-2 and for POM in Figure 8-3. Assuming the calculated average wear coefficients and a constant torque at the wheel of 0.3 N·m, which is a quite realistic number for pointing mechanisms (see requirements overview in chapter 1.3.1).

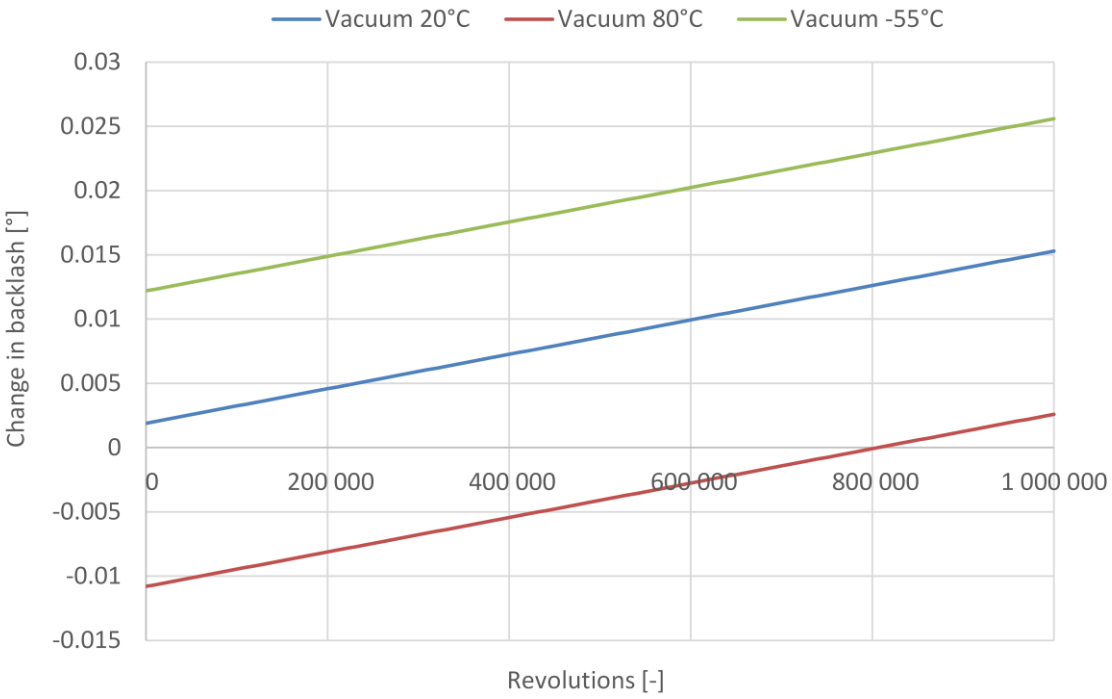

Figure 8-2: Change in backlash at different temperatures for the PEEK pinion and a load of 0.3 N·m

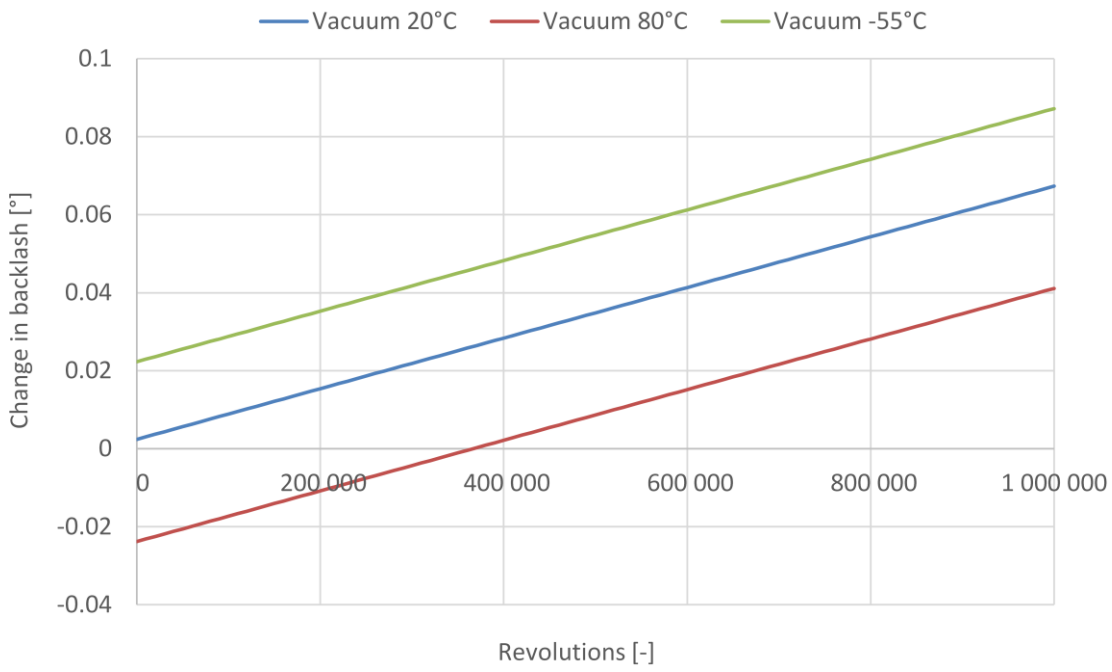

Figure 8-3: Change in backlash at different temperatures for the PEEK pinion and a load of 0.3 N·m

The numbers show the change in backlash relative to an unused gear wheel in ambient environment. At a cycle number of zero, only the influence of the environment caused geometry change is relevant. As the gear wheel is in operation and the cycle number increases, also the backlash increases. Therefore the relative difference between the hot and cold case stays constant but the absolute numbers change. Is, for example, the backlash at the beginning at 20°C around zero, after 1 000 000 revolutions and -55°C gear wheel temperature the backlash is 0.025° for PEEK pinion and 0.08° for the POM pinion.

From this one has to conclude that for missions where the gear wheels are exposed to a large change in temperature polymer gear wheels have limited accuracy potentials. Assuming a required cycle number of 350 000 and a load of 0.3 N·m (as it has been assumed throughout the thesis due to literature research in chapter 1.3.1) the PEEK gear wheel can provide an accuracy in the range of 0.02° and the POM pinion in the range of 0.05°.

But from a more application-oriented standpoint, the question arises what is the maximum allowable temperature change in order to still fulfill a certain accuracy requirement. This question shall be answered with Figure 8-4. Assuming a maximum tolerable backlash of 0.01° and a load torque of 0.3 N·m, the maximum allowable temperature difference is shown as a function of revolutions.

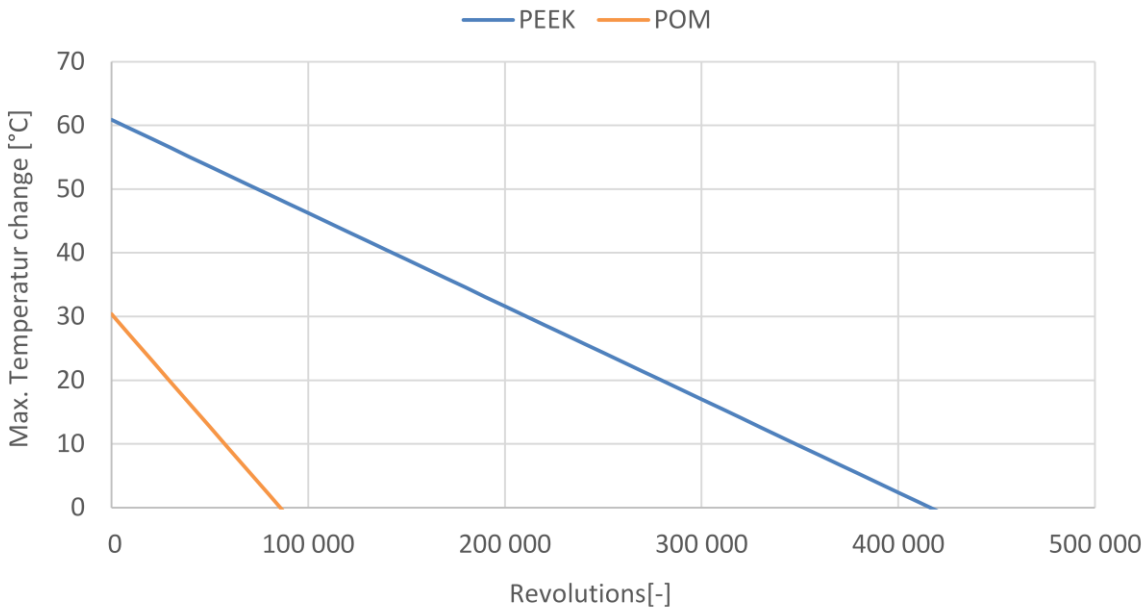

Figure 8-4: Maximum allowable temperature change as a function of revolutions for a maximum allowable backlash of 0.01° at a load torque of 0.3 N·m

The plot shows again that the potential of the POM gear wheel is quite limited. Already after 50 000 revolutions only a temperature change of 10°C is allowed to still fulfill the 0.01° backlash requirement. The main problem in the case of POM, is its large coefficient of thermal expansion which makes the gear wheel quite sensitive to temperature changes. But also the rather large wear rate, especially at extreme temperatures, makes POM not the best choice for the application in the mentioned scenario.

PEEK however looks more promising. After 200 000 cycles a temperature change of ±30°C is still acceptable. That would make an application from -10°C up to 50°C possible. These a quite realistic numbers for space mechanisms. But when approaching cycle numbers of more than 300 000 the 0.01° backlash requirement is hard to fulfill if temperature variations occur.

In the second scenario we chose a mechanism which is placed somewhere inside the spacecraft where temperature changes are small. To make calculation easier it is assumed temperatures stay constant around 20°C. For a first rough estimation, such strong simplification have to be made. This time we fix the requirement of a maximum backlash of 0.01° and calculate what maximum torque is allowed as a function of cycle numbers (Figure 8-5). In that scenario, since temperatures are staying around 20°C, the environmental caused change in geometry does not have to be considered.

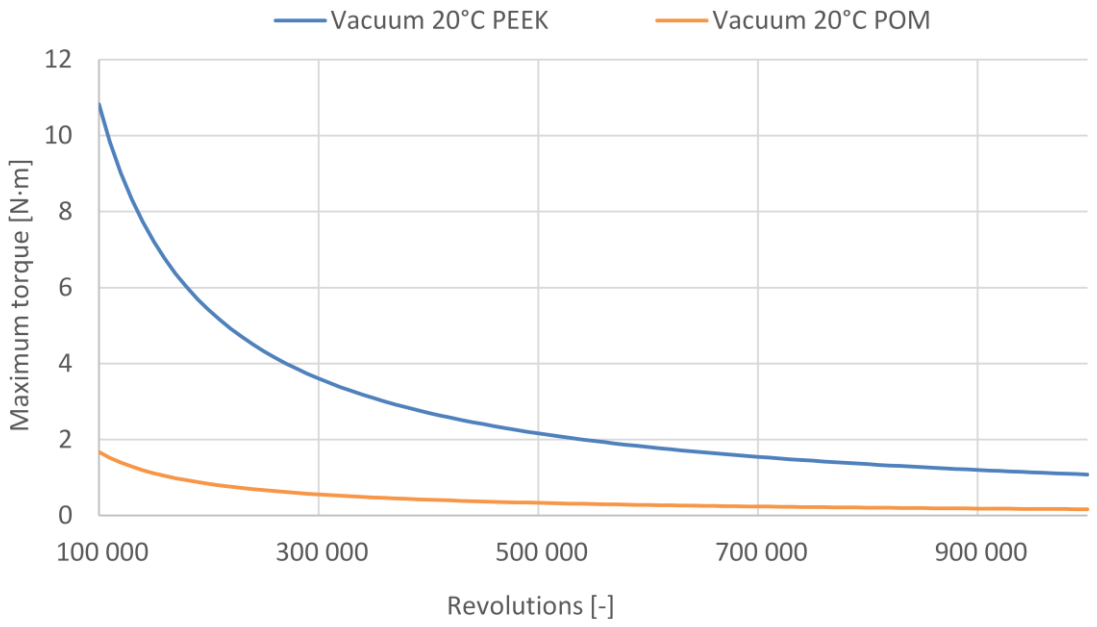

Figure 8-5: Maximum allowable torque as a function of revolutions for a maximum backlash of 0.01°

This consideration shows that for small cycle numbers, the torque at the wheel can go up to 10 N·m for PEEK and 2 N·m for POM and it still meets the requirement of a maximum backlash of 0.01°. For our 350 000 revolutions for PEEK still a torque of 3 N·m is allowed and for POM of 0.5 N·m. At very large cycle numbers around 1 000 000 revolutions, the maximum allowable torque to fulfill the 0.01° backlash requirement goes back to about 1 N·m for PEEK and 0.15 N·m for POM.

From this follows, if temperature changes are small, both PEEK and POM are appropriate materials for space gear wheels even when accuracies around 0.01° are required. Especially PEEK shall be used if the expected loads are above 1 N·m. But as soon as temperature changes have to be taken into account polymer gear wheels lose their accuracy due to their large coefficient of thermal expansion.

To make a long backlash discussion short, one could summarize the findings as follows: When temperature changes of more than 10°C are expected, POM can only be used if number of revolutions are lower than 50 000 or if accuracy requirements are in the range of 1°. PEEK, on the other hand, has a much wider field of application. When the required accuracies are in the range of 0.01°, for missions with temperatures from -10°C to 50°C PEEK can be recommended as long as number of revolutions do not exceed 200 000, or the torque increases above 0.3 N·m. For applications with more or less no temperature changes, PEEK works even for 500 000 cycles and 2 N·m load.

8.1.2 Strength

Beside wear, the strength (or load capacity) is one of the key parameters for gear wheels. To evaluate the strength of synthetic gear wheels, the tooth root load carrying capacity was evaluated in the context of this thesis. As described, the test rig limitation influenced the tests in two ways. First the tests could not be conducted in the desired environment and second, the gear wheel geometry which was used for all the other tests could not be used in that test. Consequently trade-offs in the conduction of the tests had to be made. The first one was not to conduct the tests in the space-like environment but to expose the gear wheels to the space condition first, and to run the tests afterwards. The second compromise was not to use the 30 mm pinion, but instead a 120 mm gear wheel which is standard for that test. These trade-offs have to be taken into account when analyzing the results.

The load carrying capacity Pulsator tests show that, as expected, PEEK performs much better in terms of strength as POM. Although PEEK loses strength when exposed to thermal-vacuum conditions, it is still stronger than POM in its initial state. For POM on the other hand, thermal-vacuum environment seems to have a positive influence on its strength behavior. And since the exposure to radiation does neither influence the strength of PEEK

nor of POM, the most critical situation which has to be evaluated in more detail, is the POM gear wheel in its initial state. Therefore the bending stress at the 30 mm gear wheel, which results from an acting torque of 0.3 N·m, was calculated. And even with a safety factor of two, the load carrying capacity is still a factor of 2.3 over the critical value. This means the maximum allowable load for the gear wheel, assuming a safety factor of one, would be 1.4 N·m for POM. For PEEK even more. From this it follows, that regarding strength, the PEEK as well as the POM pinion is applicable in typical space mechanisms.

8.1.3 Roundup conclusion

With referring back to chapter 1.3.1, where the requirements on space mechanisms were studied, suggestions for the application of PEEK and POM wheels can now be made. Based on the requirements, three different mechanism categories were formed, each with specific requirements: deployment mechanisms, rotating mechanisms, and pointing mechanisms. For deployment mechanisms, with its low cycle numbers basically both materials work as long as the load is in the range of 0.3 N·m. Deployment mechanisms usually have low accuracy demands and therefore even for large temperatures variations PEEK as well as POM might be an appropriate material for gear wheels. Only possible locking of the gear wheel has to be considered when temperatures increase and not enough room was left during the design to allow the gear wheel to expand. Rotating mechanisms have very large revolution numbers, which generally states a problem for synthetic gear wheels because of their larger wear compared to metallic gear wheels. Assuming an accuracy requirement in the range of 0.1° and a torque of 0.3 N·m, for large temperature fluctuation, POM wheels could be applied for up to 1 000 000 revolutions and PEEK for up to 3 000 000 revolutions. But that might still be not enough for many rotating mechanisms. For pointing mechanisms POM gear wheels shall not really be considered. Pointing mechanisms require high accuracies and assuming temperature changes of 10°C and 50 000 required cycles, a POM gear wheel cannot even fulfill an accuracy of 0.01° anymore. PEEK wheels on the other hand might be an option. Pointing mechanisms do not require these large cycle numbers like pointing mechanisms. And for lower cycles, like 200 000 for example, a PEEK gear wheels even fulfills a 0.01° accuracy requirements for a temperature range from -10° up to 50°C.

At the beginning of this thesis the hypothesis was formulated that gear wheels made out of the polymers PEEK and POM are appropriate for the application in space mechanisms. Now, one could state that synthetic gear wheels absolutely have the potential for an application in space mechanisms. But it strongly depends on the requirements. Due to their large coefficient of thermal expansion, it generally makes polymers for applications with large temperature differences problematic. But since gear wheels in space mechanisms are often mounted inside the spacecraft where the temperature range is rather small, fields of

application increase. Especially PEEK is a high performance polymer with good wear behavior, which is in vacuum even better than in air. Consequently it is recommended to definitely take PEEK as gear wheel material into account when designing a new space mechanism. And as soon as requirements for the design are known, this thesis can guide one through the decision whether to use the PEEK wheel or not. In terms of strength, the situation is less critical compared to wear. PEEK and POM gear wheels both provide enough load carrying capacity to be used in the typical space mechanisms, even under the extreme conditions of space environment.

8.2 Summary

The goal of this work was to answer the question of how the space environment influences the behavior of gear wheels made out of the polymers PEEK and POM and whether these materials are suitable for space mechanisms. From this question the overall objective of the thesis was derived, to evaluate the behavior of PEEK and POM gear wheels in a simulated space environment and discuss their applicability in space mechanisms. This objective was divided into seven sub-objectives. In the following, it is explained how these sub-objectives were fulfilled and what the outcome of each objective is.

Objective 1: **Study of space mechanism requirements as applicable for gear wheels:**

Studying the requirements for space mechanisms as they applied to the study of gear wheels was important to this thesis for two reasons. First, the requirements on the polymer gear wheels were derived based on the space mechanism requirements. And second, the test environment that would be utilized was defined after evaluating the environmental requirements of the different mechanisms. This assured that the tests were carried out as close to real applications as possible.

To identify the space mechanism requirements, a broad literature review was conducted. A total of 24 mechanisms were reviewed and their requirements were summarized. The mechanisms were categorized in three groups: (1) deployment mechanisms, (2) rotating mechanisms, and (3) pointing mechanisms. The pointing mechanisms were of particular interest because they require the highest accuracy and, if all testing was successful, a polymer gear wheel might be integrated into an antenna pointing mechanism currently being developed at the Institute of Astronautics at TUM.

Six performance parameters were reviewed in the literature research: (1) cycle number, (2) accuracy, (3) turning velocity, (4) minimum and (5) maximum temperature, and (6) turning torque. By definition, the cycle number for deployment mechanisms is one. This is because antennas, solar arrays, and instruments are typically deployed only once. The largest cycle number, 90 000 000, occurs with pointing mechanisms which often rotate continuously throughout the mission. With 20 000 to 300 000 cycles, pointing mechanisms, on average, move less than rotating mechanisms. But, in return, pointing mechanisms have to fulfill higher accuracy requirements. On average a pointing error of less than 0.01° is tolerable for pointing mechanisms. For deployment mechanisms, accuracy usually is not relevant. Highest turning velocities occur in rotating mechanisms with up to 200°/s. Turning velocities of pointing mechanisms are in the range of 0.1 to 10°/s. The required torque for pointing mechanisms is in general lower than 1 N·m. For rotating mechanisms not much information

was found about required torque and for deployment mechanisms, torque is rather large but is applied only once.

From these numbers the average test conditions were derived: cycle number of 350 000, a velocity of 360°/s, and a load torque of 0.3 N·m. There were also additional reasons for these chosen test conditions, such as those due to test rig constraints and test procedure itself, but all in all it was emphasized to test as close as possible to the real numbers. The minimum and maximum temperatures where most of the reviewed mechanisms are operated is between -40°C and 80°C. These are also roughly the temperatures where most of the tests were conducted.

Objective 1 was fulfilled by reviewing a total of 24 space mechanisms in order to identify all the requirements. From the mechanism requirements, the requirements on the polymer gear wheels were derived and the test conditions were defined.

Objective 2**:** **Preselecting promising polymers for space and gear wheel application**:

Many different polymers are available nowadays. Some have great mechanical properties but undesirable temperature behavior, others low outgassing rates but large wear rates. Therefore, before starting testing, it was important to preselect promising material candidates for gear wheels applied in space. Thus the material had to provide excellent performance in two areas: (1) in gear wheel tribology and (2) in space environment behavior. The gear wheel tribology includes good wear properties, high strength, and low friction. For space application material outgassing rates must be within the ESA standards and exhibit good behavioral characteristics at temperatures between -55°C and 80°C. After comparing various polymers such as Polyamide, Polyethylene, Polyvinylchloride, or Polyimide, Polyetheretherketone (PEEK) and Polyoxymethylene (POM) were selected for testing. PEEK is a high performance polymer which has already been used in space. It has excellent outgassing rates, great mechanical properties, and shows good behavior over a large temperature range. POM is the less expensive alternative to PEEK. It also fulfills all the requirements but with respect to mechanical and temperature behavior it cannot compete with PEEK. However, it was decided that a low cost solution should also be tested.

Objective 2 was fulfilled by comparing various polymers regarding their mechanical behavior and their applicability and performance in a space environment. As a result of this comparison the polymers Polyetheretherketone (PEEK) and Polyoxymethylene (POM) were selected for further investigation.

Objective 3**:** **Wear characterization of PEEK and POM gear wheels in a simulated space environment:**

Wear being one of the critical parameters for polymer gear wheels, its characteristics in the space environment had to be evaluated. For an accurate and realistic evaluation it was necessary to conduct a test series with the polymer gear wheels in a space-like environment. Therefore, as a first challenge, a test method had to be found and a test rig had to be designed which allowed testing in a thermal-vacuum environment. As an appropriate test method, the tactile method was chosen where the loss of material of a gear wheel tooth is determined by scanning the contour of the tooth before and after operation. With knowing the cycle number, the acting torque at the wheel, as well as the gear wheel parameters, the wear coefficient of the polymer pinion could be calculated. For this test method the gear wheel had to be operated to generate wear. The operation of the wheel had to take place under thermal-vacuum conditions in order to study the wheel's behavior in a space environment. Therefore a test rig was designed which allowed the operation of the wheel in a space-similar environment. This was one of the main challenges in the context of the wear characterization because all the bearings, the motor, and the measurement unit had to be designed for reliable and long-term operation in thermal-vacuum environment. With the design, manufacturing, and assembly of the thermal-vacuum compatible back-to-back test rig, an appropriate test setup for wear testing under space conditions was developed which is now available at the Institute of Astronautics, also for future tests.

In order to determine the wear behavior of PEEK and POM gear wheels as a function of the space environment, four main test series were conducted under different conditions: (1) under ambient environment, defined as a pressure of 1 bar and a temperature of 20°C, (2) at vacuum and 20°C, (3) at vacuum and 80°C, and (4) at vacuum and -55°C. In general, four conclusions could be drawn from these tests. First, there exists an environmental dependency of the wear behavior. Second, the results confirm the superior properties of PEEK compared to POM. In all conditions, PEEK exhibited better wear performance than POM. Third, the influence of vacuum on the wear behavior is marginal. And fourth, at 80°C and vacuum, POM shows a tremendous increase in wear.

Objective 3 was fulfilled by choosing the tactile test method and by designing a thermal-vacuum compatible back-to-back test rig for wear testing. The tests were conducted in space-like conditions and the influence of the test environment on the wear behavior of PEEK and POM gear wheels was determined.

Objective 4: **Strength characterization of PEEK and POM gear wheels in a simulated space environment:**

Beside wear, strength is an important parameter for the evaluation of gear wheels. Consequently in the context of a gear wheel evaluation for space application, the dependency of the performance of the gear wheel load capacity on the space environment had to be investigated. For polymer gear wheels the tooth root load carrying capacity is the crucial strength parameter and for determining its performance in a space environment an appropriate test method had to be found. It was decided to use the Pulsator test rig, which is operated by the Institute of Machine Elements at TUM. For the simulated space environments, thermal-vacuum and radiation were chosen. Since the Pulsator test rig could not be operated inside a thermal-vacuum chamber or a radiation facility it was decided to expose the gear wheels to the space environment first, and then conduct the strength test under laboratory conditions. Consequently, for each material, three test series were conducted. The first was conducted with gear wheels which were not exposed to any space-like environment conditions. The second test was performed with wheels which were cycled 50 times in a thermal-vacuum chamber between -55°C and 80°C for the duration of 17 days, and the third test with gear wheels which were exposed to 100 krad gamma radiation.

The results showed PEEK had higher strength values when compared to POM. This was not surprising given the excellent mechanical properties of PEEK. For both materials the exposure to 100 krad gamma radiation did not influence the load capacity. The thermal-vacuum environment, however, decreased the strength of PEEK, but increased the load capacity of POM.

Objective 4 was fulfilled by exposing the gear wheels to a space-like environment and measuring their load capacity afterwards. With that test the dependency of the performance of the wheels on the space environment could be determined.

Objective 5: **Characterization of the environmental impact on the geometry of PEEK and POM gear wheels:**

One drawback of polymers compared to metallic materials is their greater dependency on the environment, in particular on temperature but also on pressure. Polymers have larger coefficients of thermal expansion and also their outgassing rates are higher, although still within ESA limitations. Nevertheless it is important to describe the impact of the space environment on the geometry of the PEEK and POM gear wheels, especially with respect to any possible backlash changes. Therefore a test method was developed that determined the surface area of a pinion as well as the gap between the teeth as a function of exposure to a space-like environment. This was accomplished by taking high resolution photos of the

pinion. From these photos the area and the tooth gap could be calculated. A test setup was chosen where the pinion was mounted inside a thermal-vacuum chamber and a camera placed outside to take photos through a window. Each pinion (PEEK and POM) was observed at four different environments: (1) ambient, (2) vacuum 20°C, (3) vacuum 80°C, and (4) vacuum -55°C.

As expected, the results showed an increase of surface area at 80°C and a decrease at -55°C. A small decrease in area was also observed due to vacuum exposure. With the measurement of the gap between the teeth, a conclusion on the backlash change as a function of the environment could be drawn. This backlash change was up to 0.023° for PEEK and 0.046° for POM when comparing the geometries at 80°C and -55°C.

Objective 5 was fulfilled by measuring the geometry of the pinions with a high resolution photo test setup. With that the change of backlash of the pinions as a function of the space-like environment could be determined.

Objective 6: **Temperature characterization of PEEK and POM gear wheels in a simulated space environment:**

Polymers are not as temperature resistant as metallic materials. Consequently it had to be assured that the temperature of a synthetic gear wheel would not exceed the critical temperature of the polymer during operation. Since there are no state of the art calculation methods for temperature development in synthetic gear wheels in a space environment, a test series was conducted to determine maximum temperature tolerance of the gear wheel in thermal-vacuum conditions. The idea of the test was to measure the temperature inside the tooth of the wheel as a function of turning velocity and environment. The same test rig was used as for the wear test, with some modifications.

The results showed that even at the highest tested surrounding temperature of 80°C and at the highest tested turning velocity of 60 revs/min, the tooth temperatures of the PEEK and POM pinion did not come close to any critical temperature of the material. With actual space mechanisms turning velocities of more than 60 revs/min (which corresponds to 360°/s) do not happen very often, therefore it could be concluded that critical temperature should not become an issue.

Objective 6 was fulfilled by measuring the temperature inside the tooth of the PEEK and POM pinions during operation. With that the tooth temperature as a function of turning velocity and environment could be determined and it could be tested whether the critical temperature of the material would ever be exceeded or not.

Objective 7: **Evaluation of the applicability of PEEK and POM gear wheels in space mechanisms:**

After testing the relevant gear wheel parameters of PEEK and POM wheels in a space-like environment, one has to evaluate what requirements can be fulfilled by them and in what space mechanisms their application makes sense. For this purpose the results of all the tests were considered in combination. This led to many different application scenarios, depending on boundary conditions such as applied load, number of revolutions, and accuracy or operational requirements. This also made it difficult to formulate a clear statement whether the wheels are applicable or not. The answer always depends on the boundary conditions.

Nevertheless, certain fields of applications for utilizing the two gear wheel materials could be defined. POM shall mainly be applied when temperature changes are in the range of ±10°C or when accuracy does not have to be better than 1°. PEEK on the other hand, provides a good solution even when accuracy has to be in the range of 0.01°. But in that case temperature changes should not exceed ±30°C and number of revolutions shall stay under 200 000, assuming a torque of 0.3 N·m. For applications with basically no temperature changes, PEEK works even for 500 000 cycles and 2 N·m load. Based on these numbers and on the definition of space mechanism requirements from objective one, possible applications could be recommended.

Objective 7 was fulfilled by considering all the outcomes from the tests in combination and considered along with the space mechanism requirements.

8.3 Future Work

In the presented thesis the gearing parameters of standard, straight toothed gear wheels made out of PEEK and POM were evaluated. This leaves room for much more research in that field in the future. In particular because with this work the required test setups were manufactured and are now available and functioning, and also personal contacts to other departments exist now. Consequently with relatively low effort, many more studies could be conducted. Either with the existing materials or with other polymers. Taking the existing materials it might be worthwhile to measure the wear coefficient at different temperatures and not only at -55°C, 20°C, and 80°C. For example in 5°C steps in order to evaluate the influence of the temperature on the wear behavior in more detail. Our results show that wear highly depends on the temperature and consequently more measuring points could lead to a better understanding of the temperature influence. But these tests would be quite expensive and complex because assuming testing a temperature range from -55°C up to 80°C in 5°C steps, 27 measurements would be required which means 27 gear wheels and 54 contour measurements (always before and after operation). Also evaluating the wear coefficient as a function of the revolution number might be a worthwhile study. Therefore the author would recommend to determine the wear coefficient in 200 000 revolutions steps. It would be interesting to find out if wear depends on how long the gear wheel has already been operated or if there is no influence at all. But that test takes a lot of time. With a turning velocity of 60 revs/min, not before two days and eight hours the 200 000 revolutions are reached. And if someone wants to test up to 1 000 000 revolutions it takes already more than eleven days testing time.

Besides testing the existing materials in more depth, one could also modify the material and measure the influence. PEEK, for example, would be an interesting candidate. Therefore, instead of the natural PEEK used in this work, one could modify the PEEK with fillers like graphite, molybdenum disulfide, or PTFE and determine their influence on the gearing parameters. There are several reasons for adding other materials to polymers to make composites: (1) to increase the polymers load carrying capacity, for example by adding fibers, (2) by including lubricating additives the friction coefficient and the wear rate can be lowered. (3) increase the composites thermal conductivity [9]. However, graphite as additive usually is not used for space application since it needs absorbed vapor to be a good lubricant. But molybdenum disulfide functions better in the absence of air, which makes it an excellent lubricant in vacuum. Therefore it would be interesting to learn more about additives and their influence on gearing properties.

Also materials which have not been tested in this work should be taken into account for further investigation. One candidate recommended by the author is Vespel. Vespel has already been used in many space applications and can also be modified with different fillers to increase its performance. Vespel shows excellent wear behavior and has good

mechanical properties. But Vespel is quite expensive and consequently possible tests should be prepared very well in order to avoid repeating any tests. Since 3D printing is getting more and more important in recent years one could also evaluate 3D printed gear wheels for the application in space mechanisms. Especially the manufacturing accuracy might become a problem and it would be really interesting to study it.

The gear wheels used for the tests in this thesis have standard geometry with standard toothing. This was done in purpose in order to provide a basic work other future studies can be compared with. But tribology provides many other gear wheel solutions. For example different modulus or gear wheel thickness. With a thicker wheel, for example, the wear might be decreased and strength could be increased. These effects would be worthwhile to study.

One result which was in particular interesting to the author, was the fact that POM gear wheels increase their strength when being exposed to thermal-vacuum environment. This finding could not be explained in detail. Consequently an extended test series to study that phenomena is recommended.

This work has shown that polymer gear wheels can be applied in certain space mechanisms. But nevertheless the work has also shown that polymer gear wheels have shortcomings. More research is required to understand these shortcomings in more detail and evaluate even better the fields of application for synthetic gear wheels. With that the synthetic gear wheels might have a promising future in space flight applications.

A Appendix

A.1 Datasheets

Werkstoffkennwerte/Technische Daten

KTK Kunststofftechnik

Produkt: **PEEK natur**

Allgemeine Eigenschaften	Wert	Maßeinheit	Testmethode /Norm
Dichte	1,32	g/cm³	DIN EN ISO 1183-1
Brennverhalten	V0/V0	3 mm / 6 mm	UL 94
Feuchtigkeitsaufnahme	0,20	%	DIN EN ISO 62
Mechanische Eigenschaften			
Streckspannung/Festigkeit	110	MPa	DIN EN ISO 527
Reißdehnung	20	%	DIN EN ISO 527
E-Modul/Steifigkeit (Zug)	4000	MPa	DIN EN ISO 527
Kerbschlagzähigkeit (Charpy)	5	kJ/m²	DIN EN ISO 179
Kugeldruckhärte	230	MPa	DIN EN ISO 2039-1
Shore-Härte	88	Skala D	DIN EN ISO 868
Thermische Eigenschaften			
Schmelztemperatur	343	°C	ISO 11357-3
Wärmeleitfähigkeit	0,25	W / (m · K)	DIN 52612-1
Spezifische Wärmekapazität	1,34	kJ / (kg · K)	DIN 52612
Linearer thermischer Ausdehnungskoeffizient (Ø 20 – 60°C)	50	10-6 K-1	DIN 53752
Dauergebrauchstemperatur min.	-60	°C	Richtwerte
Dauergebrauchstemperatur max.	250	°C	Richtwerte
Einsatztemperatur kurzzeitig (max.)	310	°C	Richtwerte
Wärmeformbeständigkeit	152	°C	DIN EN ISO 306 (Vicat B)
Elektrische Eigenschaften			
Dielektrizitätszahl 50 Hz	3,20		DIN IEC 60250
Dielektrischer Verlustfaktor 50 Hz	0,001		DIN IEC 60250
Spezifischer Durchgangswiderstand	$4,9X10^{16}$	Ω · cm	DIN IEC 60093
Oberflächenwiderstand	10^{18}	Ω	DIN VDE 0303-3
Durchschlagfestigkeit	20	kV/mm	DIN EN 60243

Die kurzzeitige maximale Einsatztemperatur gilt nur für Anwendungen mit sehr niedriger mechanischer Belastung über wenige Stunden. Die langfristige maximale Einsatztemperatur basiert auf der Wärmealterung der Kunststoffe durch Oxidation, die eine Abnahme der mechanischen Eigenschaften zur Folge hat. Angegeben sind die Temperaturen, die nach einer Zeit von mindestens 5.000 Stunden eine Abnahme der Zugfestigkeit (gemessen bei Raumtemperatur) um 50% im Vergleich zum Ausgangswert verursachen. Dieser Wert liefert keine Aussage zur mechanischen Festigkeit des Werkstoffes bei hohen Anwendungstemperaturen. Bei dickwandigen Teilen ist von der Oxidation bei hohen Temperaturen nur die Oberflächenschicht betroffen, die durch den Zusatz von Antioxidantien besser geschützt werden kann. Der Kernbereich der Teile bleibt in jedem Fall ungeschädigt. Die minimale Einsatztemperatur wird maßgeblich bestimmt von einer möglichen Schlag- oder Stoßbelastung im Einsatz. Die angegebenen Werte beziehen sich auf geringe Schlagbeanspruchung.

Die elektrischen Kennwerte wurden an naturfarbenem, trockenem Material gemessen. Bei anderen Einfärbungen (insbesondere schwarz) oder feuchtem Material kann es zu deutlichen Veränderungen der elektrischen Kennwerte kommen.

Die mechanischen Eigenschaften von faserverstärkten Materialien wurden an spritzgegossenen Probekörpern in Faserrichtung ermittelt. Für die Auslegung von Konstruktionen und die Definition von Materialspezifikationen nennen wir Ihnen auf Anfrage gerne die für Ihre Anwendung zutreffenden Daten.

Die angegebenen Werte wurden aus vielen Einzelmessungen als Durchschnittswerte ermittelt und entsprechen dem Stand unserer heutigen Kenntnisse. Sie dienen lediglich als Information über unsere Produkte und sollen eine Hilfe zur Materialauswahl sein. Wir sichern damit nicht bestimmte Eigenschaften oder die Eignung für bestimmte Einsatzzwecke rechtlich verbindlich zu. Da die Eigenschaften auch von den Dimensionen der Halbzeuge und dem Kristallisationsgrad (z.B. Nukleierung durch Pigmente) abhängen, können die tatsächlichen Eigenschaftswerte eines bestimmten Produkts von den Angaben etwas abweichen.

Datenblatt 539-1

Werkstoffkennwerte/Technische Daten

Produkt: Polyacethalharz Copolymer | POM C extrudiert

Allgemeine Eigenschaften	Wert	Maßeinheit	Testmethode /Norm
Dichte	1,41	g/cm^3	DIN EN ISO 1183-1
Brennverhalten	HB/HB	3mm/6mm	UL 94
Feuchtigkeitsaufnahme	0,2	%	DIN EN ISO 62
Mechanische Eigenschaften			
Streckspannung/Festigkeit	67	MPa	DIN EN ISO 527
Reißdehnung	30	%	DIN EN ISO 527
E-Modul/Steifigkeit (Zug)	2800	MPa	DIN EN ISO 527
Kerbschlagzähigkeit (Charpy)	6	kJ/m^2	DIN EN ISO 179
Kugeldruckhärte	150	MPa	DIN EN ISO 2039-1
Shore-Härte	81	Skala D	DIN EN ISO 868
Thermische Eigenschaften			
Schmelztemperatur	165	°C	ISO 11357-3
Wärmeleitfähigkeit	0,31	W/(m*)	DIN 52612-1
Spezifische Wärmekapazität	1,5	kJ/(kg*)	DIN 52612
Linearer thermischer Ausdehnungskoeffizient	110	10^{-6} K^{-1}	DIN 53752
Einsatztemperatur langfristig	-50 bis +100	°C	
Einsatztemperatur kurzzeitig	140	°C	
Wärmeformbeständigkeit	110	°C	DIN EN ISO 75 Verf. A
Elektrische Eigenschaften			
Dielektrizitätszahl	3,8		DIN IEC 60250
Dielektrischer Verlustfaktor	0,002		DIN IEC 60250
Dielektrischer Durchgangswiderstand	10^{13}	Ω*m	DIN IEC 60093
Oberflächenwiderstand	10^{13}	Ω	DIN EN 60093
Durchschlagfestigkeit	40	kV/mm	DIN EN 60243
Vergleichszahl der Kriechwegbildung	600		DIN EN 60112 (Prüflösung A)

Die kurzzeitige maximale Einsatztemperatur gilt nur für Anwendungen mit sehr niedriger mechanischer Belastung über wenige Stunden. Die langfristige maximale Einsatztemperatur basiert auf der Wärmealterung der Kunststoffe durch Oxidation, die eine Abnahme der mechanischen Eigenschaften zur Folge hat. Angegeben sind die Temperaturen, die nach einer Zeit von mindestens 5.000 Stunden eine Abnahme der Zugfestigkeit (gemessen bei Raumtemperatur) um 50% im Vergleich zum Ausgangswert verursachen. Dieser Wert liefert keine Aussage zur mechanischen Festigkeit des Werkstoffes bei hohen Anwendungstemperaturen. Bei dickwandigen Teilen ist von der Oxidation bei hohen Temperaturen nur die Oberflächenschicht betroffen, die durch den Zusatz von Antioxidantien besser geschützt werden kann. Der Kernbereich der Teile bleibt in jedem Fall ungeschädigt. Die minimale Einsatztemperatur wird maßgeblich bestimmt von einer möglichen Schlag- oder Stoßbelastung im Einsatz. Die angegebenen Werte beziehen sich auf geringe Schlagbeanspruchung.

Die elektrischen Kennwerte wurden an naturfarbenem, trockenem Material gemessen. Bei anderen Einfärbungen (insbesondere schwarz) oder feuchtem Material kann es zu deutlichen Veränderungen der elektrischen Kennwerte kommen.

Die mechanischen Eigenschaften von faserverstärkten Materialien wurden an spritzgegossenen Probekörpern in Faserrichtung ermittelt. Für die Auslegung von Konstruktionen und die Definition von Materialspezifikationen nennen wir Ihnen auf Anfrage gerne die für Ihre Anwendung zutreffenden Daten.

Die angegebenen Werte wurden aus vielen Einzelmessungen als Durchschnittswerte ermittelt und entsprechen dem Stand unserer heutigen Kenntnisse. Sie dienen lediglich als Information über unsere Produkte und sollen eine Hilfe zur Materialauswahl sein. Wir sichern damit nicht bestimmte Eigenschaften oder die Eignung für bestimmte Einsatzzwecke rechtlich verbindlich zu. Da die Eigenschaften auch von den Dimensionen der Halbzeuge und dem Kristallisationsgrad (z.B. Nukleierung durch Pigmente) abhängen, können die tatsächlichen Eigenschaftswerte eines bestimmten Produkts von den Angaben etwas abweichen.

Datenblatt 548-2

Pulsatoren
Pulsators

Anwendung
Application

- Ermittlung von statischen und dynamischen Festigkeitskennwerten an Bauteilen und Bauteilproben durch Einstufenversuche und Lastkollektiv-Versuche

  Determination of static and dynamic strength values of components and component specimens by the use of single-stage and load spectrum tests
- Schwerpunkt: Ermittlung der Zahnfußfestigkeit bei geradverzahnten Stirnrädern abhängig von Werkstoff, Wärmebehandlung und Baugröße

  Main focus: determination of the strength at the root for spur gears depending on material, heat treatment and part size

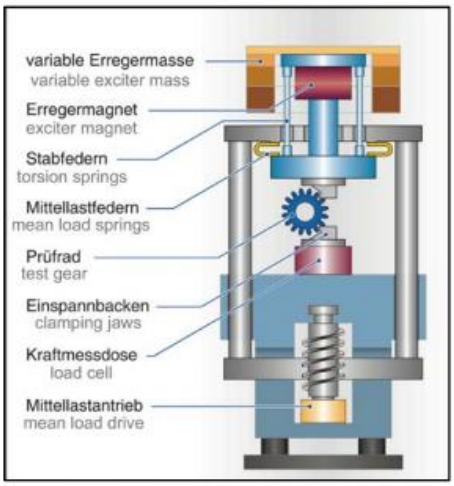

Schema eines Pulsators
diagrammatic plan of a pulsator

Technische Daten - Hydraulikpulsatoren, Resonanzpulsatoren (mech.), Resonanzpulsatoren (elektr.)
Technical data - hydraulic pulsators, resonance pulsators (mech.), resonance pulsators (electr.)

Frequenzbereich: frequency range	ca. 30 … 150 Hz
Modulbereich bei Zahnrädern: module range for gears	1 … 10 (20) mm
max. Mittelkraft: max. averaged force	± 60 ... ± 250 kN
max. dynamische Kraft: max. dynamic force	± 50 ... ± 250 kN
max. Probendurchmesser: max. sample diameter	200 … 700 mm
max. Probenlänge: max. sample length	200 … 1000 mm

Elektrischer Resonanzpulsator
electrical resonance pulsator

z. T. Lastkollektivsteuerung (Blockkollektive und Zufallskollektive), Statische Versuche (Aufzeichnung der Verformung), Aufzeichnung der Resonanzfrequenz
Partly load collective control, static tests (recording of deformation), recording of resonance frequency

Lehrstuhl für Maschinenelemente • Forschungsstelle für Zahnräder und Getriebebau
Technische Universität München, Boltzmannstr. 15, 85748 Garching
www.fzg.mw.tum.de

A.2 Technical Drawings

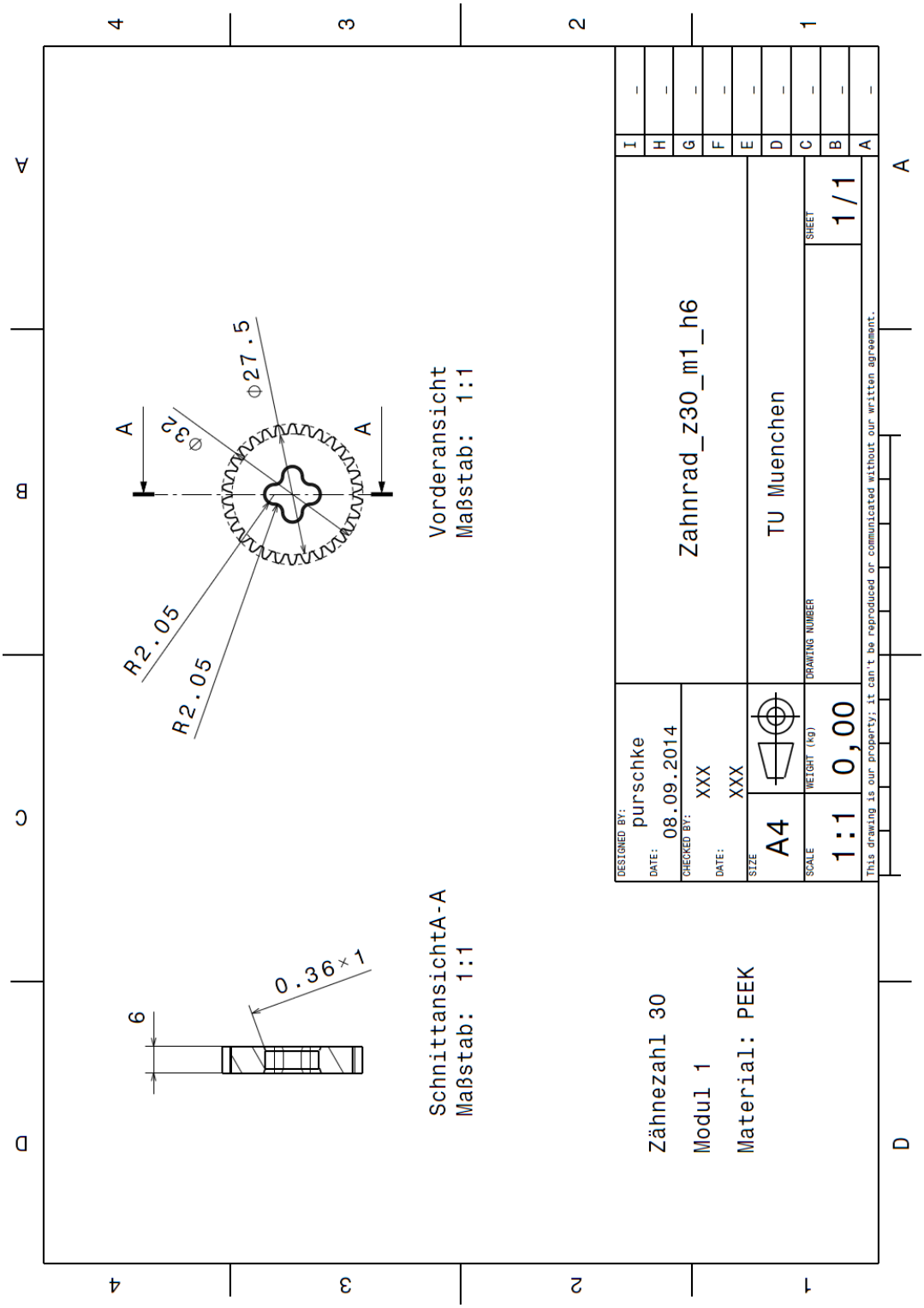

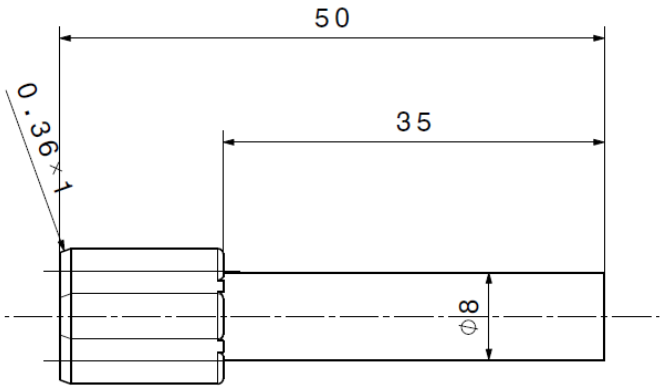

Seitenansicht rechts
Maßstab: 2:1

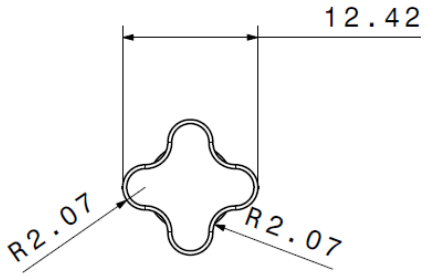

Vorderansicht
Maßstab: 2:1

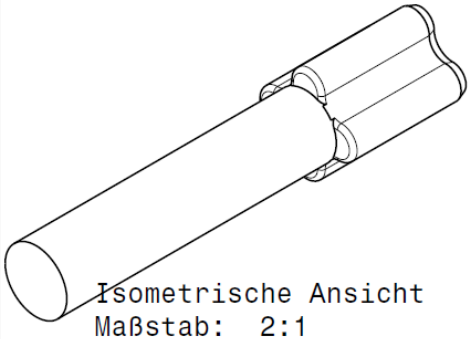

Isometrische Ansicht
Maßstab: 2:1

DESIGNED BY: rpurschke DATE: 2/18/2014		Zahnrad_Welle_v01	
CHECKED BY: XXX DATE: XXX			
SIZE A4			
SCALE 2:1	WEIGHT (kg) 0.00	DRAWING NUMBER	SHEET 1/1

This drawing is our property; it can't be reproduced or communicated without our written agreement.

I	_
H	_
G	_
F	_
E	_
D	_
C	_
B	_
A	_

A.3 References

[1] N. Takada, T. Amano, T. Ohhashi, and S. Wachi, “An Antenna-Pointing Mechanism for the ETS-VI K-Band Single Access (KSA) Antenna,” 1991.

[2] S. L. Zolnay, “An Acquisition and Tracking Receiver for Satellite-to-Satellite Relaying at 55 GHz,” 1971.

[3] N. Phillips, “Mechanisms for the Beagle2 Lander,” 2001.

[4] P. Campo, A. Barrio, N. Puente, and R. Kyle, “Development of a High Temperature Antenna Pointing Mechanisms for BepiColombo Planetary Orbiter,” *15th European Space Mechanisms & Tribology Symposium – ESMATS 2013*, 2013.

[5] M. Shmulevitz and A. Halsband, “The Design, Development and Qualification of a lightweight Antenna Pointing Mechanism,” *30th Aerospace Mechanisms Symposium*, 1996.

[6] T. p. Sarafin and W. J. Larson, *Spacecraft Structures and Mechanisms: From Concept to Launch*. Torrance, California: Microcosm, 1998.

[7] M. Ferris and N. Phillips, “The Use and Advancement of an Affordable, Adaptable Antenna Pointing Mechanism,” *14th European Space Mechanisms & Tribology Symposium – ESMATS 2011*, 2011.

[8] ESA, *Space Tribology Handbook*, 1997.

[9] R. L. Fusaro, “Self-Lubricating Polymer Composites and Polymer Transfer Film Lubrication for Space Application,” *NASA Technical Memorandum 102492*, 1990.

[10] T. Gradt and G. Theiler, “Influence of Solid Lubricant Fillers on the Tribological Behaviour of PEEK Composites in Vacuum,” *13th European Space Mechanisms and Tribology Symposium – ESMATS 2009*, 2009.

[11] P. L. Conley, D. Packard, and W. Purdy, *Space Verhicle Mechanisms: Elements of Successful Design*. New York: John Wiley & Sons, Inc, 1998.

[12] R. L. Fusaro, *NASA Space Mechanism Handbook*. Springfield, VA 22100: National Technical Information Service, 1999.

[13] W. J. Larson and J. R. Wertz, *Space Mission Analysis and Design*. El Segundo, California: Microcosm Press, 2006.

[14] Andion, J, A, R. Lopez, and G. Ybarra, “Rosetta Deployment Booms,” *10th European Space Mechanisms and Tribology Symposium – ESMATS 2003*, 2003.

[15] K. Koski, “Deployment Mechanism for Thermal Pointing System,” *Proceedings of the 42nd Aerospace Mechanisms Symposium, NASA Goddard Space Flight Center, May 14-16, 2014*, 2014.

[16] S. Steg, W. Vermeer, S. Tucker, and H. Passe, “An Innovative Aperture Cover Mechanism used on SDO/EVE and MMS/SDP,” *Proceedings of the 42nd Aerospace Mechanisms Symposium, NASA Goddard Space Flight Center, May 14-16, 2014*, 2014.

[17] M. Kubitschek, S. Woolaway, L. Guy, C. Dayton, B. Berdanier, D. Newell, and J. Pellicciotti, “Global Micromave Imager Spin Mechanism Assembly

Design, Development and Performance Test Result," *14th European Space Mechanisms & Tribology Symposium – ESMATS 2011*, 2011.

[18] C. Körner, D. Kampf, A. Poglitsch, J. Schubert, U. Ruppert, and M. Schoele, "Development of Cryogenic Filter Wheels for the HERSCHEL Photodetector Array Camera & Spectrometer (PACS)," *Proceedings of the 42nd Aerospace Mechanisms Symposium, NASA Goddard Space Flight Center, May 14-16, 2014*, 2014.

[19] M. Schmid, M. Jun, and Y. Shuang, "In-Orbit Performance of the MWRI Scanning Mechanisms," 2014.

[20] N. Scheidegger, M. Ferris, and N. Phillips, "Bi-Axial Solar Array Drive Mechanism - Design, Build and Environmental Testing," *Proceedings of the 42nd Aerospace Mechanisms Symposium, NASA Goddard Space Flight Center, May 14-16, 2014*, 2014.

[21] D. Sucher, D. Chassoulier, X. Francois, and F. Champandard, "SWIM RMA - High Antenna Lifetime Mechanism," 2013.

[22] J. Serrano, J. San Millan, and R. Santiago, "Antenna Pointing Mechanism for ESA ENVISAT Polar Platform," *30th Aerospace Mechanisms Symposium*, 1996.

[23] M. Schmid, S. Y. Yong, and S. G. Lee, "Extremely Compact Two-Axis X-Band Antenna Assembly," *13th European Space Mechanisms and Tribology Symposium – ESMATS 2009*, 2009.

[24] G. Szekely, D. Blum, M. Humphries, A. Koller, D. Mussett, S. Schuler, and P. Vogt, "A Coarse Pointing Assembly for Optical Communication," *Proceedings of the 40th Aerospace Mechanisms Symposium, NASA Kennedy Space Center, May 12-14, 2010*, 2010.

[25] P.-A. Mäusli, M.-T. Ivorra, V. Gass, and J.-F. Berthoud, "Coarse Pointing Mechanism Assembly for Satemte Interlink Experiment," *30th Aerospace Mechanisms Symposium*, 1996.

[26] M. Herald and L. C. Wai, "Two-Axis Antenna Positioning Mechanism," 1994.

[27] J. I. Bueno, J. Vazquez, J. Gavira, and G. Migliorero, "Regulated Deployment Mechanism for a Panel Like Appendage," *9th European Space Mechanisms and Tribology Symposium – ESMATS 2001*, 2001.

[28] D. Givios, J. Sicre, and T. Mazoyer, "A Low Cost Hinge for Appendices Deployment: Design, Test and Application," *9th European Space Mechanisms and Tribology Symposium – ESMATS 2001*, 2001.

[29] M. Eigenmann, M. Schmalbach, M. Schiller, T. Schmidt, and L. Scolamiero, "Ultra-Light Deployment Mechanism (UDM) for Sectioned Large Deployable Antenna Reflectors," *14th European Space Mechanisms & Tribology Symposium – ESMATS 2011*, 2011.

[30] B. Wood, G. Sutter, and N. Hamze, "The Development of a Low Power Solar Array Drive Mechanism," 2003.

[31] Heinrich B, Zemann J, and Rottmeier F, "Development of the Bepi Colombo MPO Solar Array Drive Assembly," *14th European Space Mechanisms & Tribology Symposium – ESMATS 2011*, 2011.

[32] V. Costabile, F. Lumaca, P. Marsili, G. Noni, and C. Portelli, “New Antenna Deployment, Pointing and Supporting Mechamsm,” *30th Aerospace Mechanisms Symposium*, 1996.

[33] A. Skullestad, “Pointing Mechanism for Optical Communication,” 1999.

[34] B. Schlecht, “Maschinenelemente 2,” 2010.

[35] DIN 867, “Bezugsprofil für Stirnräder mit Evolventenverzahnung,” *VDI-Richtlinien, Verein Deutscher Ingenieure*, 1989.

[36] DIN 780, “Modulreihe für Zahnräder,” *VDI-Richtlinien, Verein Deutscher Ingenieure*, 1977.

[37] VDI 2736, “Thermoplastic gear wheels - Cylindrical gears - Calculation of the load-carrying capacity,” *VDI-Richtlinien, Verein Deutscher Ingenieure*, 2013.

[38] DIN 3990, “Tragfähigkeitsberechnung von Stirnräder,” *VDI-Richtlinien, Verein Deutscher Ingenieure*, 1987.

[39] G. Niemann and H. Winter, Eds, *Maschinenelemente Band 2*. Berlin: Springer, 2003.

[40] R. L. Mott, *Mechanical Elements in Mechanical Design*, 2004.

[41] R. Slatter and R. Degen, “Miniature Zero-Backlash Gears and Actuators for Precision Positioning Applications,” *ESMATS*, 2005.

[42] D. DiBiase, “A Zoom Lens for the MSL Mast Cameras: Mechanical Design and Developmen,” *Proceedings of the 41st Aerospace Mechanisms Symposium, Jet Propulsion Laboratory, May 16-18, 2012*, 2012.

[43] K. Koski, “Focus Mechanism for Kepler Mission,” *Proceedings of the 39th Aerospace Mechanisms Symposium, NASA Marshall Space Flight Center, May 7-9, 2008*, 2008.

[44] R. F. ONeill, "Anti-Backlash Gears", April 7, 1964

[45] KTK Kunststofftechnik, “Werkstoffkennwerte/Technische Daten - PEEK natur,” 2014.

[46] Licharz, “Konstruieren mit technischen Kunststoffen,”

[47] I. Bostan, V. Dulgheru, and I. Bodnariuc, “Safety Aspects of Kinematic Planetary Precessional Transmission with Plastic Wheels,” *Mechanical Testing and Diagnosis ISSN 2247 – 9635, 2012 (II), Volume 4, 5-11*, 2012.

[48] G. Erhard and E. Strickle, *Maschinenelemente aus thermoplastischen Kunststoffen*. Düsseldorf, 1985.

[49] R. Weidig, “Metall substituieren,” *KU Kunstoffe Online-Archiv Jahrgang 91 (2001)*, 2001.

[50] P. B. Willis and C.-H. Hsieh, “Space Application of Polymeric Materials,” 1999.

[51] M. Dobrowolski and J. Grygorczuk, “Lock & Release Mechanism for the CHOMIK Penetrating Device and its Tribological Properties,” *Proceedings of the 41st Aerospace Mechanisms Symposium, Jet Propulsion Laboratory, May 16-18, 2012*, 2012.

[52] J. A. V. Vilan, M. L. Estevez, and F. A. Agelet, “Antenna Deployment Mechanism for the Cubesat Xatcobeo. Lessons, Evolution and Final Design,” 2012.

[53] R. Hevner, “Lessons Learned Designing a Spherical Satellite Release Mechanism,” *Proceedings of the 39th Aerospace Mechanisms Symposium, NASA Marshall Space Flight Center, May 7-9, 2008*, 2008.

[54] H. Arends, J. Gavira, B. Butler, K. Torkar, G. Fremuth, H. Jeszenszky, G. Coe, and M. Yorck, “The MIDAS Experiment for the Rosetta Mission,” 2001.

[55] L. Bernabe, N. Raynal, and Y. Michel, “3POD - A high Performance Parallel Antenna Pointing Mechanism,” *15th European Space Mechanisms & Tribology Symposium – ESMATS 2013*, 2013.

[56] J. M. Fernandez, M. Schenk, G. Prassinos, V. J. Lappas, and S. O. Erb, “Deployment Mechanisms of a Gossamer Satellite Deorbiter,” *15th European Space Mechanisms & Tribology Symposium – ESMATS 2013*, 2013.

[57] J. Grygorczuk and M. Dobrowolski, “Advanced Mechanisms and Tribological Tests of the Hammering Sampling Device CHOMIK,” *14th European Space Mechanisms & Tribology Symposium – ESMATS 2011*, 2011.

[58] G. Theiler and T. Gradt, “Tribological Behaviour of PEEK Composites in Vacuum Environment,” *Proc. 12th Euro. Space Mechanisms & Tribology Symp. (ESMATS)*, 2007.

[59] A. Murari, C. Vinante, and M. Monari, “Comparison of PEEK and VESPEL SP1 characteristics as vacuum seals for fusion applications,” *Vacuum 65 (2002) 137–145*, 2002.

[60] A. P. Povilus, C. J. Wurden, Z. Vendeiro, M. Baquero-Ruiz, and J. Fajans, “Vacuum Compatibility of 3D-Printed Materials,” 2013.

[61] M. Fürstenberger, “Betriebsverhalten verlustoptimierter Kunststoffzahnräder,” 2013.

[62] R. Feulner, “Kunststoffgetriebe für die Medizintechnik - Kennwertermittlung und Auslegung,” 2007.

[63] G. Erhard, *Konstruieren mit Kunststoffen*, 2004.

[64] E. Siedke, *Tragfähigkeitsuntersuchungen an ungeschmierten Zahnrädern aus thermoplastischen Kunststoffen*. Berlin, 1977.

[65] M. Pfeiffer, J. Harder, and U. Walter, “Development of a Compact Ka-Band Antenna Pointing Mechanism for Intersatellite Links on Small Satellites,” 2009.

[66] M. Thiel, J. Stöcker, and C. Rohe, “The Rosetta Lander Anchoring System,” 2003.

[67] FZG, “FZG back-to-back gear test rig,” Lehrstuhl für Maschinenelemente - Forschungsstelle für Zahnräder und Getriebebau, 2014.

[68] Phytron, “VSS 42.200.1,2 CR-HFUC-08-50-X documentation azimuth motor: Testreport,” 2010.

[69] J. Dever, B. Banks, K. K. deGroh, and S. Miller, “Degradation of Spacecraft Materials,” *Handbook of Environmental Degradation of Materials.*

[70] D. L. Burris and W. G. Sawyer, “A low friction and ultra low wear rate PEEK/PTFE composite,” *Wear 261 (2006) 410–418*, 2006.

[71] N. L. McCook, M. A. Hamilton, D. L. Burris, and W. G. Sawyer, “Tribological results of PEEK nanocomposites in dry sliding against 440C in various gas environments,” *Wear 262 (2007) 1511–1515*, 2007.

[72] H. Hachmann and E. Strickle, “Polyamide als Zahnradwerkstoffe,” *Konstruktion 18 (1966) 3, S. 81 - 94*, 1966.

[73] S. W. Zhang, “State-of-the-art of polymer,” *Tribology International Vol. 31, Nos 1–3, pp. 49–60, 1998*, 1998.

[74] R. Nalbandian, “Enhanced Pointing Gimbal Mechanisms for Next Generation Communication Antennas,” *15th European Space Mechanisms & Tribology Symposium – ESMATS 2013*, 2013.

[75] E. Haibach, *Betriebsfestigkeit*. Düsseldorf: VDI Verlag, 1989.

[76] B. Stawarczyk, C. Keul, F. Beuer, M. Roos, and P. Schmidlin, “Tensile bond strength of veneering resins to PEEK: Impact of different adhesives,” *Dental Materials Journal 2013; 32(3): 441-448.*

[77] VDI 2726, “Ausrichten von Getrieben,” *VDI-Richtlinien, Verein Deutscher Ingenieure*, 1982.

[78] R. Feulner, C. Dallner, G. Ehrenstein, and E. Schmachtenberg, *Maschinenelemente aus Kunststoff*. Erlangen, 2007.